


5-2019

Volumetric Muscle Loss: The Role of Physical Activity and Autologous Repair on Force Recovery and Signaling Pathways

Richard Perry

University of Arkansas, Fayetteville

Follow this and additional works at: <https://scholarworks.uark.edu/etd>

 Part of the [Biological Engineering Commons](#), [Biomechanics and Biotransport Commons](#), [Exercise Science Commons](#), [Kinesiotherapy Commons](#), and the [Physical Therapy Commons](#)

Recommended Citation

Perry, Richard, "Volumetric Muscle Loss: The Role of Physical Activity and Autologous Repair on Force Recovery and Signaling Pathways" (2019). *Theses and Dissertations*. 3274.

<https://scholarworks.uark.edu/etd/3274>

This Dissertation is brought to you for free and open access by ScholarWorks@UARK. It has been accepted for inclusion in Theses and Dissertations by an authorized administrator of ScholarWorks@UARK. For more information, please contact ccmiddle@uark.edu.

Volumetric Muscle Loss: The Role of Physical Activity and
Autologous Repair on Force Recovery and Signaling Pathways

A dissertation submitted in partial fulfillment
of the requirements for the degree of
Doctor of Philosophy in Kinesiology

by

Richard Perry
University of West Florida
Bachelor of Science in Exercise Physiology, 2011
University of West Florida
Master of Science in Exercise Physiology, 2014

May 2019
University of Arkansas

This dissertation is approved for recommendation to the Graduate Council.

Tyrone Washington, Ph.D.
Dissertation Director

Jeffrey Wolchok, Ph.D.
Committee Member

Nicholas Greene, Ph.D.
Committee Member

Sami Dridi, Ph.D.
Committee Member

ABSTRACT

Volumetric muscle loss affects both military and civilian persons. The hallmark of this injury is incomplete muscle regeneration, excessive fibrosis, and chronic inflammatory signaling resulting in permanent functional loss. Since permanent functional loss drastically reduces quality of life, many studies have been conducted to improve force recovery. Current scientific literature considers a repair strategy of either devitalized scaffolds infused with growth factors or viable tissue plus activating factors to be the more promising interventions for optimal force recovery. **PURPOSE** The purpose of this study is to incorporate autologous repair and physical activity and observe the effects of muscle force recovery and regeneration, fibrosis, and inflammatory signaling. **METHODS** 32 male Sprague-Dawley rats had 20% of their LTA removed then replaced to act as autologous repair. Half of the rats utilized wheel running, and at 2 and 8 weeks, the autologous tissue was excised from the LTA from both wheel running and sedentary rats. Electrophysiology measured peak tetanic force. Histology was used to measure CSA, centrally-located nuclei, percent of non-contractile tissue, and collagen deposition. qRT-PCR evaluated the gene expression of myogenic, ECM remodeling, and inflammatory signaling markers. **RESULTS** Wheel activity promoted force recovery at 2 weeks, but both groups had similar force output by 8 weeks. Myogenic gene expression did not differ in the LTA between groups at either time point. Wheel activity caused differential effects of collagen deposition in the defect and intact LTA tissue. Wheel activity differentially altered ECM remodeling markers at the 2 and 8 week time points in the wheel activity and sedentary groups. Wheel activity appeared to attenuate inflammatory signaling markers at 2 weeks, but showed evidence of a pro-inflammatory environment by 8 weeks. **DISCUSSION** Wheel activity promoted early beneficial responses in force recovery, ECM remodeling, and inflammatory signaling markers. These

responses were not evident by 8 weeks, however, the same early patterns of these markers were observed at 8 weeks in the sedentary group. Force recovery equalizes by 8 weeks with autologous repair but is expedited using wheel activity.

©2019 by Richard Perry
All Rights Reserved

TABLE OF CONTENTS

I.	Chapter 1 Introduction and Literature Review.....	1
a.	Satellite Cells.....	4
i.	Regulators of Satellite Cell Activation.....	4
ii.	Satellite Cells: From Quiescence to Activation.....	5
iii.	Skeletal Muscle Regeneration.....	7
iv.	Satellite Cells and Physical Activity.....	10
v.	Satellite Cells and VML.....	12
b.	Extracellular Matrix.....	13
i.	Extracellular Matrix and Activity.....	15
ii.	Extracellular Matrix and VML.....	16
c.	Immune Response.....	18
i.	Immune Response, Inflammation and VML.....	19
d.	Repair Strategies for VML.....	20
e.	VML and Physical Activity.....	22
f.	Conclusion.....	24
g.	Preliminary Data.....	25
i.	Wheel Running.....	25
ii.	Force Output.....	26
iii.	Cross-sectional Area.....	27
h.	Specific Aims.....	27
II.	Chapter 2: Methodology.....	29
a.	Animal Care and Use.....	29

b.	Tissue Harvest.....	31
c.	Histology.....	32
d.	Western Blot.....	33
e.	qRT-PCR.....	34
f.	Statistical Analysis.....	35
III.	Chapter 3: Muscle Regeneration and Satellite Cell Mechanics.....	36
a.	Abstract.....	36
b.	Introduction.....	37
c.	Methods.....	39
d.	Results.....	43
e.	Discussion.....	47
f.	Table 1.....	52
g.	Table 2.....	52
h.	Figures Legend.....	53
i.	Figures.....	54
IV.	Chapter 4: VML and ECM Remodeling.....	60
a.	Abstract.....	60
b.	Introduction.....	61
c.	Methods.....	64
d.	Results.....	69
e.	Discussion.....	72
f.	Figures Legend.....	75
g.	Figures.....	76

V.	Chapter 5: VML and Inflammatory Response.....	80
	a. Abstract.....	80
	b. Introduction.....	81
	c. Methods.....	82
	d. Results.....	85
	e. Discussion.....	88
	f. Figures Legend.....	91
	g. Figures.....	92
VI.	Overall Discussion.....	95
VII.	References.....	99
VIII.	Appendix.....	108

CHAPTER 1

INTRODUCTION

Skeletal muscle is a highly plastic and regenerative tissue able to overcome most minor damages and injuries sustained in daily living. Though post-mitotic, local muscle stem cells (satellite cells) provide much of the regenerative capacity for muscle to maintain size and function. However, this regenerative capacity cannot withstand large, traumatic loss of muscle tissue. “A frank loss of muscle tissue, or volumetric muscle loss (VML) injury, may result from primary or secondary injuries that are beyond the endogenous reparative and regenerative capacities of mammalian skeletal muscle” (Corona, Wenke & Ward, 2016).

Volumetric muscle loss (VML) was coined in 2011 by Grogan et al. and is defined as the traumatic or surgical loss of skeletal muscle with resultant functional impairment. The focal point of VML research has been to address the common type of injury inflicted on the modern-day battlefield. VML is not medically coded, so the rate and quantity of this injury is undeterminable. However, VML commonly occurs with severe, extremity wounds which account for >75% of all battlefield-inflicted wounds. VML is also witnessed within the confines of civilian life as well. Any severe accident may result in VML. Additionally, medical procedures, especially the removal of sarcomas, often result in major loss of skeletal muscle.

Currently, medical treatment does not focus on the recovery of force output in the VML-affected muscle/limb. Instead, the focus of regenerative and rehabilitative treatment is on closing of the wound and strengthening of unaffected tissue, respectively. Muscle flaps are the common regenerative treatment but often result in donor site morbidity in tissues in that area. Even when successfully incorporated, flaps lack the necessary factors (i.e. independent vasculature) for full incorporation into the VML site and regeneration of the affected tissue. Thus, muscle flaps are an

ineffective tissue for appropriate regeneration, and inadequate force recovery results from this treatment. When coupled with physical therapy, force is improved but still permanently diminished in the affected limb (Aurora et al., 2014). Regardless of current medicinal and rehabilitative treatment, the affected site does not recover the lost contractile tissue and, therefore, does not contribute as much force as the unaffected, contralateral limb. The resultant imbalance in force between limbs is followed by long-term detriments. Chronic conditions of VML include structural defects, reduced mobility and lower quality of life. VML is a common condition incurred by military and civilian persons alike. However, the lack of adequate medical techniques leaves these victims with permanent ramifications. Satisfactory recovery methods must be determined.

Current VML research is utilizing a variety of tissues such as biomedically engineered and synthetically-derived materials to determine the optimal tissue for regeneration and subsequent force recovery in VML patients (Wolf et al., 2015). Varying degrees of success have been accomplished, yet full force recovery has not yet been achieved. However, current literature suggests three major factors contribute to the overall obstacle of force recovery: satellite cell activation and migration, the inflammatory response, and collagen deposition. These three factors share a commonality in most VML studies in inhibiting proper regeneration and force recovery. Many recent studies incorporate varying tissue types and interventions to overcome these obstacles and mimic proper skeletal muscle regeneration in the affected area (Aurora et al., 2014; Corona et al., 2016). However, many of these studies lack thorough investigative research into the underlying cellular mechanisms involved with the degree and type of traumatic damage. Compounding the issue is the lack of observations made in autograph tissue which is arguably the most optimal, yet least clinically feasible material, to use for VML treatment. The purpose of

this study is to investigate the underlying cellular mechanisms of VML using autograph tissue. Of critical interest are the signaling pathways and resultant outcomes of satellite cell mechanics, inflammation and collagen deposition.

LITERATURE REVIEW

The focus of this literature review will be to discuss the three major obstacles that frequently present themselves during VML: 1) Satellite cell population, migration and activity; 2) dysfunctional extracellular matrix components; and 3) the dysregulated inflammatory response. Within each of these primary categories, there will be a discussion of how each respond within a healthy cell, to exercise-promoted signals, and within the confines of VML. Furthermore, additional sections, such as skeletal muscle regeneration and physical activity as an intervention to VML, will also be discussed as these topics are key to understanding the complex nature of repair and regeneration from VML.

Satellite Cells

Satellite cells are a population of heterogeneous, undifferentiated cells located between the basal lamina and sarcolemma of muscle cells and account for 2-7% of myofiber nuclei by adulthood (Fu et al., 2015). The cells are responsible for the growth, repair and regeneration of skeletal muscle tissue. In healthy, adult skeletal muscle, satellite cells remain in the G_0 phase and are inactive while in this phase (Schultz et al., 1978). While in this quiescent phase, satellite cells express Pax7 but not MyoD or MyoG (Cornelison & Wold, 1997). However, Myf5 has been detected on ~90% of quiescent satellite cells indicating their commitment to the myogenic lineage (Beuachamp et al., 2000).

Regulators of Satellite Cell Activation

Though satellite cells retain their quiescence in healthy tissue, activation of these cells is needed to maintain proper skeletal muscle health. Satellite cells become activated through various stimuli, most of which are associated with varying degrees of muscle stretch or injury. Regardless, a two-pronged approach to satellite cell activation is often needed: destruction of the

basal lamina and damage of the neighboring muscle fiber. The disruption or damage of the protective basal lamina allows for the satellite cell to anchor itself through integrins and to be exposed to ECM-derived hepatocyte growth factor (HGF), both of which play a role in activating the satellite cell (Tatsumi et al., 1998; Sanes, 2003). Even with the basal lamina intact in the presence of damaged skeletal muscle (as in the case of bupivacaine-induced damage), the muscle still releases factors such as calcium and nitric oxide (NO) which can also indirectly activate satellite cells (Wozniak & Anderson, 2007). Additionally, nitric oxide release has also been correlated with an increase in follistatin, a known myostatin antagonist (Pisconti et al., 2006). Myostatin has been shown to arrest cell cycle progression through the degradation of Cyclin D1 whose importance will be discussed in the following section (Yang et al., 2007). Additional upstream regulators include Wnt signaling, Notch signaling and sphingolipid signaling (Yin et al., 2013). Together, damage of the basal lamina and local skeletal muscle tissue set the mechanical and subsequent cellular stage for satellite cell activation.

Once muscle becomes damaged, the subsequent immune cell infiltration into the local area also plays a heavy role in satellite cell activation through the cytokines these inflammatory cells secrete (i.e. IL-6 and IFN γ) (Tidball & Villalta, 2010; Kurosaka & Machida, 2013). Through the intricate interaction of damage and locally secreted factors, satellite cells leave their quiescent state, become active and subsequently begin to proliferate.

Satellite Cells: From Quiescence to Activation

Once satellite cells become activated, proper skeletal muscle regeneration can only be fulfilled through proper proliferation, differentiation and incorporation of the myofibers/myoblasts. One of the key factors that releases the satellite cell from the G₁ phase into the S phase is Cyclin D1 (Resnitzky et al., 1994). Cyclin D1 is regulated in part by HGF

(discussed previously) as well as IL-6 (Allen et al., 1995; Serrano et al., 2008). Simply, Cyclin D1 is heavily expressed during proliferation of the satellite cell and suppresses the differentiation function of MyoD (Skapek et al., 1995). Coincidentally, the action of Cyclin D1 is arrested by a MyoD feedforward mechanism. Inflammatory cytokines initiate p38 activation which in turn activates MyoD transcription of Cyclin D1 inhibitors (Palacios et al., 2010). Therefore, unlike quiescent cells which express only Pax7 and Myf5, activated satellite cells express MyoD subsequently followed by Myogenin within 48 hours of leaving quiescence (Cornelison & Wold, 1997; Cooper et al., 1999; Rantanen et al., 1995). Of note, MyoD has been associated with the cell's commitment to differentiate without proliferation (Rantanen et al., 1995).

Once the cells undergo multiple cycles of proliferation, terminal differentiation of the satellite cells is initiated by Myogenin and Myf6/Mrf4 (Smith et al., 1994). The expression and suppression of various genes have been reported and hypothesized to play a role in the intricate signaling that regulates proliferation and differentiation; however, this mechanism needs to be more fully elucidated. It has been reported that Pax7, MyoD and Myogenin have an intricate association during myogenesis. Pax7 has been shown to repress the activity and expression of MyoD (Olguin et al., 2007), and It has been reported that the ratio of Pax7 to MyoD is associated with the satellite cell's fate determination (Olguin et al., 2007): high Pax7:MyoD is associated with quiescence, intermediate Pax7:MyoD with proliferation, and low Pax7:MyoD with differentiation. Myogenin's role is considered valuable in the cell's commitment due to its ability to suppress Pax7 subsequently allowing MyoD expression to increase (Olguin et al., 2007). In summary, quiescent satellite cells are Pax7⁺/MyoD⁻, proliferating cells are Pax7⁺/MyoD⁺, and differentiating daughter cells are Pax7⁻/MyoD⁺/Myogenin⁺ (Tidball, 2017). A small fraction of myoblasts will retain Pax7, downregulate myogenic factors (i.e. MyoD) and exit the cell cycle

thereby maintaining the satellite cell pool (Olguin & Olwin, 2004). As stated earlier, upstream regulation of these three key proteins still needs to be elucidated, but studies have shown to the importance of immune cell-derived factors (discussed in more detail in section III) such as $\text{TNF}\alpha$. $\text{TNF}\alpha$ has been shown to activate p38 MAPK which in turn regulates myogenic factors (Chen et al., 2007) as previously mentioned.

Once the satellite cells have differentiated into myoblasts, the process continues until the myoblasts have been incorporated into the myocyte or have been differentiated into myocytes and incorporated into the muscle fiber. It is important note that the satellite cell pool must be maintained by some of the proliferating satellite cells returning to the quiescent state and returning to the muscle niche. The satellite cell pool would become depleted over time if full differentiation were to occur.

Skeletal Muscle Regeneration

The previous sections have discussed the immediately acute role of satellite cell activation and incorporation of myoblasts into muscle upon injury. The following section will incorporate further details into the longer acute and chronic stages of skeletal muscle regeneration. Rather than focusing solely on the role of satellite cells, this section will incorporate a broader view of the local area including the muscle fibers itself and the role of the inflammatory response during skeletal muscle regeneration. The purpose of this section will be to briefly outline the stages of muscle regeneration as detailed discussion of the inflammatory response will be presented later.

Though varying sources describe the phases of skeletal muscle regeneration differently, there are effectively three phases to regeneration: 1) The destruction/inflammatory phase, 2) The repair/myogenic phase, and 3) the remodeling phase (Turner & Badylak, 2012; Ciciliot &

Schiaffino, 2010). During the initial injury to muscle, tearing or shearing of the myofibers occurs releasing intracellular components into the local area. Of importance is the release of intracellular calcium thereby activating calcium-dependent proteases that subsequently disintegrate myofibrils (Ciciliot & Schiaffino, 2010). Additionally, release of intracellular components initiate the complement cascade and chemotactic recruitment of neutrophils (followed by macrophages) (Ciciliot & Schiaffino, 2010). The first subset of macrophages to be identified at this stage of the inflammatory phase are the CD68+, M1 macrophages (Chazaud et al., 2009). This subset has been labeled the pro-inflammatory macrophage and has a role in clearing necrotic tissue in addition to promoting muscle regeneration through the release of factors such as IL-6 and TNF α (Tidball, 2008). The population of this subset reaches its peak 24 hour post-injury and is slowly replaced by the anti-inflammatory CD163+, M2 macrophage within 2-4 days post-injury (Chazaud et al., 2009).

The second phase of regeneration, the repair/myogenic phase, usually begins by the second day post-injury and is characterized by rapid proliferation of satellite cells. The activation of satellite cells has already been discussed in previous sections. However, it is important to note the timing of Notch and Wnt signaling during this phase. Notch signaling has been credited for regulating satellite cell proliferation whereas Wnt signaling is associated with differentiation (Brack et al., 2008). A large population of satellite cells is needed for sufficient regeneration; therefore, if Wnt signaling is activated too soon, the number of differentiating cells may be inadequate for proper repair (Brack et al., 2008).

Finally, the remodeling phase is characterized by a number of processes as the injured tissue reverts to its healthy status. During this phase, incorporation of the newly formed myotubes takes place within the intact basal lamina, typically three days post-injury depending

on the type and severity of injury (Ciciliot & Schiaffino, 2010). Once the myoblasts fuse with the existing myofiber, the myoblast nuclei migrate to the center of the cell (centrally located nuclei) and often acts as a sign of a regenerated muscle fiber (Cadot et al., 2015). Also during this time, muscle fibers reengage innervation and express myosin heavy chain (MyHC) which also act as signs of healthy regeneration and growth of muscle (Slater & Schiaffino, 2008; Whalen et al., 1990).

In addition to reinnervation and incorporation of the newly formed myofibers, the remodeling muscle fiber is highly active with several key signaling pathways important for survival and growth of the cell. Specifically, the IGF-1/Insulin activation of the PI3K/Akt/Mtor pathway is regarded as the predominant pathway of growth and protein synthesis within the cell (Bodine et al., 2001). Additional pathways important for proper genetic transcription during this time are the Calcineurin/NFAT, PKC-theta (type II fibers), PGC-1 α (Type I fibers), Ras/MAPK, and calcium/calmodulin pathways (Akimoto et al., 2005; Goodyear et al., 1996; McKinsey et al., 2000; Chin et al., 1998) .

Skeletal muscle regeneration in VML does not follow the canonical muscle regeneration that is more appropriately associated with less severe injuries. In addition to the traumatic loss of muscle mass and resident cells, regeneration of VML injury is also inhibited through the major loss of neuromuscular junctions, blood vessels and the extreme accumulation of scar tissue (Turner & Badylak, 2012). With VML, activated fibroblasts quickly deposit scar tissue which acts as a deterrent to regeneration subsequently hindering *de novo* formation of new fibers (Turner & Badylak, 2012).

Repair of VML injuries also differs from canonical regeneration due to a severe and prolonged inflammatory response. As discussed earlier, proper regeneration depends on a

sensitive time course of pro- and anti-inflammatory phases. However, the pro-inflammatory phase is prolonged, and proper regulation of myogenic factors is not mimicked (Turner & Badylak). Due to the alterations in the inflammatory response, the loss of muscle tissue and resident cells, and the damage to neuromuscular junctions and the local vasculature, VML regeneration responds to the injury differently than canonical, less-severe injuries. The assortment of added obstacles to an already complex repair mechanism results in permanent loss of force output in the affected muscle and usually limb.

In summary, VML regeneration and repair does not follow the same time course or have similar results as canonical skeletal muscle regeneration. Furthermore, the current body of literature lacks in-depth knowledge of the signaling pathways occurring in either the acute or chronic stage of remodeling. To date, most studies that focus on cellular signaling in VML models focus on either inflammatory or fibrotic-related pathways. Though these studies have greatly enhanced the understanding of how these mechanics differ from canonical regeneration, a necessity has grown for this knowledge to be extended to cellular signaling of the skeletal muscle as well.

Satellite Cells and Physical Activity

Satellite cells have been shown to respond to a number of exercise types and intensities. For the purposes of this literature review, however, focus will be placed on the effect of aerobic exercise and physical activity (particularly wheel running) on satellite cell mechanics in hindlimb muscles.

Since satellite cells respond to damage of the skeletal muscle and surrounding tissue, endurance training has to be of a sufficient time and intensity in order to induce appropriate levels of damage. It has been reported that 40-155 minutes of mid-to-high intensity exercise

increased satellite cell content whereas 30 minutes of low-intensity exercise did not (Bazqir et al., 2017). Though rats typically run for short bursts separated by longer durations of non-activity (Eikelboom & Mills., 1988), voluntary wheel running is still sufficient to promote satellite cell activation as will be discussed later in this section.

In addition to time and intensity, the observed muscle is also important when considering the effect of exercise on satellite cell mechanics. Muscles that are predominately Type II fibers do not respond to the same degree as muscles that are predominately Type I (Bazqir et al., 2017). It has been shown that the plantaris, a mixed fiber-type muscle, increases the amount of satellite cells without an increase in CSA after 8 weeks of voluntary wheel running (Kurosaka et al., 2009). Studies have also been conducted on the effects of wheel running on predominately Type II muscles such as the tibialis anterior (TA). Overall, wheel running does not appear to affect the muscle mass (Legerlotz et al., 2008), however, muscle fiber type was altered as evidenced by a reduction in Type Iib and an increase in Type Iia in mice (Allen et al., 2001). Concerning satellite cells, it has been shown that an increase in apoptotic myofibers and satellite cells are observed immediately following 16h of access to a running wheel, but this number decreases to normal levels at 96h post access in mice (Podhorska-Okolow et al., 1998).

Using two exercise-simulated models of exercise-induced damage (electrostimulation and bupivacaine injection), Hill et al. (2003) showed that, following expected damage to the tibialis anterior, satellite cell activation (observed through RNA and protein expression of M-cadherin) peaked at 5 days and was subsequently followed by muscle regeneration (morphological assessment and measurement of MyHC). The repair process was associated with highly expressed levels of MGF and IGF-1 (Hill et al., 2003).

Wheel running specifically affects satellite cell mechanics in rodents via Wnt signaling (Fujimaki et al., 2014) which has been shown to upregulate proliferation (Otto et al., 2008). Though the TA is not a prime contributor of force to the action of wheel running, it still receives the necessary exercise-induced damage for appropriate alterations to occur (Irintchev & Wernig, 1987).

Satellite Cells and VML

VML results in a complete reduction of satellite cells as well as other resident muscle cells. As a result, regeneration is greatly inhibited even when compared to other injury models such as cryoinjury (Nuutila et al., 2017). The intact skeletal muscle tissue and associated cells are not able to fully regenerate the defect area, and, as the definition of VML states, resultant functional deficits occur. Since proper regeneration is a key factor in recovering this functional loss, many studies have focused on satellite cell mechanics, especially satellite cell activation and migration in the defect area. This following section will discuss the findings of current literature as it pertains to this topic.

Early and recent investigations into VML tissue provide consistent histological hallmarks of the defect site: abundant fibrosis with increased immune cell infiltration but little myofiber formation or satellite cell migration/activation. Even with the use of tissue-engineered muscle repair (TEMR) constructs, desmin-positive cells (myofibers) account for only 30% of all cells in the implant and surrounding tissue (Machingal et al., 2011). It should be noted, however, the use of TEMR constructs has been shown to increase the genetic expression of Pax7 (Corona et al., 2012) and increase *de novo* muscle fiber regeneration (Corona et al., 2013; Sicari et al., 2014) compared to VML without repair. In addition to VML resulting in less myofibers, the CSA of these myofibers is also smaller compared to uninjured muscle 8 weeks post-injury (Corona et al.,

2013). These resulting factors indicate that VML causes an insufficient number or inadequate activity of satellite cells to properly repair the affected area.

Overall, VML results in complete removal of satellite cells in the defect area, and only minimal satellite cell migration into the defect site from nearby intact muscle is observable (Corona et al., 2012). Due to the lack of proper regeneration from resident muscle stem cells, perivascular progenitor cells will infiltrate the defect area (when an ECM scaffold is provided) as a compensatory alternative (Sicari et al., 2014), but regeneration is still limited. Consequently, VML injury, without proper repair interventions, results in a high percentage of fibrosis of the defect area due to minimal satellite cell population, migration and activation.

Extracellular Matrix

Skeletal muscle is a tissue comprised primarily of contractile material but is also comprised of neural, vasculature and connective tissue. The tissue that embeds many of the primary and secondary tissues in skeletal muscle and is responsible for providing structural and biochemical support is known as the extracellular matrix (ECM). The major component of the ECM is collagen which also accounts for roughly ~1-10% of muscle dry weight (Gillies & Lieber, 2011). Many ECM resident cells can contribute to collagen production, but fibroblasts are the primary cell of collagen production during periods of normal, healthy muscle functioning (Archile-Contreras et al., 2010). Other studies provide support that other cells, such as satellite cells and myogenic cells, may also contribute to the ECM especially during times of myogenesis and regeneration (Beach et al., 1985; Kuhl et al., 1982). Though various collagen types exist in the ECM of skeletal muscle, types I and III contribute the largest percentage and are primarily produced and secreted by fibroblasts (Light & Champion, 1984).

Proper turnover of the ECM is necessary to maintain tissue health, allow for adequate cell migration and myotube formation, and reorganization during muscle adaptation (Gillies & Lieber, 2011). The proteins responsible for regulating ECM turnover are matrix metalloproteinases (MMP) and tissue inhibitors of matrix metalloproteinases (TIMP). Common skeletal muscle MMPs are the gelatinases MMP-2 and -9 which degrade the type IV collagen (Kherif et al., 1999) and the collagenases MMP-1 and -13 that degrade collagen types I and III (Singh et al., 2000; Wu et al., 2003). MMP-1 has been particularly targeted as an important enzyme needed for satellite cell migration and differentiation as it is associated with increasing migration-related marker proteins (N-cadherin, β -catenin) as well as pre-MMP-2 and TIMP (Wang et al., 2009). Also, MMP-1 has been shown to degrade collagen thus reducing fibrosis. MMP-2, -7 and -9 have been associated with myotube formation to their combined effect of ECM breakdown and elimination of cell surface components that hinder fusion between myocytes and myotubes (El Fahime et al., 2000). During times of injury and repair of skeletal muscle, satellite cells must be able to migrate to places of injury. Thus, proper turnover of the ECM is essential to proper muscle regeneration. MMP-2 and -9 appear to have a significant role in the acute phases of muscle repair from injury (Kherif et al., 1999). These MMPs are needed to degrade the basement membrane to allow for satellite cell migration but have also been shown to help activate satellite cells (Fukushima et al., 2007).

Not only is healthy ECM required for proper cell migration, but dysregulation of the factors that contribute to normal ECM (fibroblasts, MMPs, TIMPs) often leads to fibrosis. Severe fibrosis can reduce force output due to dysregulating the ECM which is known to play a key role in proper mechanotransduction of skeletal muscle (Humphrey et al., 2014). TGF- β has been established as a leading upstream regulator that activates fibroblasts to upregulate the

production of collagen I (Leask & Abraham, 2004). The subsequent result of TGF- β activation in muscle is reduced isometric force, increased fibrosis and muscle muscle atrophy via activation of fibroblasts/collagen production and atrogen-1 (Mendias et al., 2012).

Extracellular Matrix and Activity

Exercise induces damage to skeletal muscle and subsequent alterations to the surrounding ECM. For satellite cell migration and muscle adaptations to occur as a result of exercise, adaptation to the ECM are also required. The following section will discuss the current understanding of exercise-induced alterations to the ECM as a result of aerobic-type exercises.

Eccentric exercise (cycle training) has been shown to upregulate the expression of many ECM-related genes at acute (immediately after and 2h post-exercise) and chronic (12 weeks) time points (Hjorth et al., 2015). Acutely, exercise affects expression of mainly proteases and protease inhibitors (i.e. MMPs, TIMPs) whereas chronic adaptations were observed with structural components of the ECM (i.e. collagen and proteoglycans) (Hjorth et al., 2015). Specifically, pro-MMP 2 and 9 decrease and increase, respectively, following exercise, and these changes are reflected by the appropriate changes in their respective TIMPs (Koskinen et al., 2004).

Acutely following exercise, ECM-related growth factors (IGF-1, TGF- β , IL-6) as well as collagen turnover and net collagen synthesis (chronically) (Kjaer et al., 2006; Heinemeier et al., 2011). These changes in collagen have been associated with increases in viscoelasticity of skeletal muscle thereby reducing stiffness (Gosselin et al., 1998). Chronically, a regular endurance program increased ECM-related expression of genes known to promote vascular growth (angiopoietin, VEGF, VEGF-1R, VEGF-2R), an important facet of regeneration from VML (Timmons et al., 2005).

Activity-induced ECM regulation not only affects the ECM itself, but also has the propensity to alter the direct relationship between the ECM and skeletal muscle. Following mechanical stress, an increased genetic expression of tenascin-C, an important glycoprotein for cell adhesion, has been associated with increased force transmission (Sarasa-Renedo & Chiquet, 2005) which will be discussed later within the scope of VML.

Extracellular Matrix and VML

Due to the overwhelming importance and contribution the ECM has on both fibrosis and satellite cell mechanics, it is a focal point for many VML studies. The following section of this literature review will discuss the current understanding of the status, contribution and dysfunction of the ECM during VML and current interventions used to regulate the ECM.

The hallmark of VML injury is the extent of collagen deposition leading to fibrosis. Li et al. (2013) noted that excessive fibrosis in VML sites may play a causative role in functional loss of affected muscle 4 weeks post-injury. However, fibrosis has also been reasoned to have beneficial effects such as allowing greater force output via force transmission (Garg et al., 2014b; Aurora et al., 2014; Corona et al., 2013).

Within the confines of VML, an intact and functional ECM is important for cell activation, migration and infiltration into the affected area. However, when lacking a functional ECM, the defect area is mainly filled with a fibrotic mass rather than skeletal muscle tissue (Garg et al., 2015). Therefore, many recent VML studies have incorporated an ECM scaffold (typically decellularized) into the defect. Though results vary, many of these studies report an increase in maximal isometric torque, increased regeneration as evidenced by larger CSA, and increased migration of satellite cells into the defect site (Valentin et al., 2010; Corona et al., 2013). Though these types of scaffolds are more successful at muscle regeneration and force

recovery compared to not having a repair intervention, acellular scaffolds still do not mimic normal skeletal muscle regeneration. Garg et al. (2014) reported that although immune cell infiltration into the defect site is more than doubled (compared to muscle grafts), these cells were less active. Even when the scaffolds are derived from muscle tissue, fibrosis still occurs though it has been argued that this is functional fibrosis given that force output was still elevated compared to the no repair group (Corona et al., 2013). Furthermore, satellite cell migration was limited when using ECM scaffolds, and *de novo* muscle fiber regeneration was impaired. Consequently, force output was lower in ECM scaffold-treated groups compared to muscle graft-treated groups. In summary, ECM scaffolds are more beneficial to the regenerative process compared to not having a repair intervention, but they do not mimic canonical regeneration as has been shown with using muscle grafts.

Using a PCR array in a porcine model of VML, Corona et al. (2017) showed that the expression of numerous ECM-related genes was upregulated at 4 weeks post-VML surgery versus the sham-operated comparison. Specifically, collagen (1A1, 1A2, 3A1, 5A2, 5A3), MMP (2, 3, 9) and TGF- β (1, 2, 3, R3) were all significantly upregulated at 4 weeks; however, expression of these genes was back to control levels at the 16-week time point. Markers of ECM and fibrosis are upregulated following VML; however, interventions to reduce the expression of these markers have also been associated with further reduction in force output rather than advantageous changes (Garg et al., 2014). The authors of the study concluded that a certain level of collagen deposition/fibrosis is needed for proper force transmission in the muscle. This theory is further supported by similar findings in Aurora et al. (2014).

Immune Response

The previous two sections have interwoven the importance of immunomodulatory roles in skeletal muscle regeneration especially in regard to satellite cells and ECM. This section will discuss, in depth, the role of the immune response to skeletal muscle regeneration, the effect of exercise on this response, and current scientific observations of the immune response during repair from VML injury.

As previously discussed, skeletal muscle has a remarkable capacity for repair and regeneration in response to damage. Although satellite cells have a direct role in this process, immune cells play an indirect role by cleaning damaged tissue and releasing factors that, among other factors, activate satellite cells. Therefore, proper immunomodulation during skeletal muscle damage is vital for proper repair and regeneration.

Similar to satellite cells, leukocytes (primarily macrophages or monocytes) are detectable intramuscularly and reside in a quiescent state until activated by trauma or increased muscle use (Honda et al., 1990). Once this initial activation is recognized, a predictable time course of immune-related events occurs. Initially, neutrophils will respond immediately to the site of damage due to chemoattractants (CXCL1 and CCL2) released by the activated, resident macrophages (Brigitte et al., 2010). In addition to neutrophils' role in wound repair via phagocytosis, degranulation and/or NETs, they are also vital for releasing chemokines and proinflammatory cytokines such as $TNF\alpha$, IL-6, IL-1 β and IFN γ (Tecchio et al., 2014). Thus, neutrophils are able to recruit specific subpopulations of immune cells to the damaged area and are subsequently activated once they reach the proinflammatory-rich environment.

The key activation at this stage of early repair is that of monocytes into proinflammatory M1 macrophages. During this time, an increase in activated, MyoD-expressing satellite cells is

also observed with the possibility of IFN γ be a candidate for key regulation of both the inflammatory and myogenic response in the early stages of muscle repair (Cheng et al, 2008). Specifically, IFN γ has been shown to regulate the expression and activation of M1 macrophages as well as bind to myogenic precursor cells (MPCs) which initiates the JAK/STAT(1) pathway resulting in a proliferative, non-differentiating satellite cell. IL-6 also activates the JAK/STAT(3) pathway leading to subsequent transcription of Ccnd (Cyclin D1) whose role in satellite cell activation and proliferation was discussed previously (Serrano et al., 2008).

In addition to IFN γ , TNF α has also been heavily implicated in its role for regulating myogenesis. Monocytes and macrophages release the biggest percentage of TNF α in the muscle microenvironment acutely following injury. As mentioned earlier, TNF α plays a role in silencing Pax7 via MAPK p38 signaling resulting in more prominent differentiation of the satellite cells. Also, TNF α has also been shown to repress Notch-1 signaling. Notch-1 suppresses MyoD and myogenin expression thereby reducing differentiation and increasing proliferation of satellite cells. Therefore, TNF-induced silencing of the Notch-1 gene results in increased differentiation of satellite cells during the early timepoint of muscle repair (Acharyya et al., 2010).

Immune Response, Inflammation and VML

As has already been discussed, the immune response is a key regulatory factor in skeletal muscle regeneration. Accordingly, many VML studies have focused on revealing how inflammation and the immune response modulate fibrosis and satellite cell activation. The following section will discuss the current literature on inflammatory factors during VML at early (2 weeks) to late (16 weeks) time points.

Due to the severity of damage to skeletal muscle, VML has been shown to have a prolonged inflammatory response compared to other injury models such as cryoinjury (Nuutila et

al., 2017). Though the adaptive immune system is involved in normal regeneration, some data would show that it does not provide a significant contribution to force recovery in a VML model (Corona et al., 2017). Conversely, the nude strain (deficient in T-cells) demonstrated a main effect of higher, maximal isometric torque compared to the wild type strain when force was normalized to muscle mass. In summary, the innate immune response has been the focal point of many studies. Since most studies do not observe the acute effects (<5 days post-surgery) of VML, neutrophil response and activity is poorly understood. Instead, the M1 and M2 macrophage have been studied more thoroughly concerning their role and response in VML models.

Although the cellular and molecular biology of VML-affected skeletal muscle is still poorly understood, many inflammatory markers have been examined at different time points and models of VML. Corona et al. (2017), showed an increase in the gene expression of cyclooxygenase (COX) 1 and 2, IL-6 and STAT2 in a porcine model of VML at 4 weeks post-surgery (compared to the sham-operated control).

Repair interventions (i.e. scaffolds, grafts) have been shown to modulate the immune response in VML models. Garg et al. (2014) showed that devitalized ECM scaffolds increase the number of pro-inflammatory CD68+ macrophages compared to vital grafts even though gene expression of CD68 was similar in both interventions. Furthermore, the same study showed that only anti-inflammatory markers (CD163, IL-4, TGF- β 1, VEGF, Fizz1, IL-10) were elevated in the vital graft group.

Repair Strategies for VML

Currently, ECM devices are FDA approved for soft tissue reinforcement. ECM devices are more highly used in comparison to autologous grafts due to their more abundant availability

and low donor tissue burden (Greising et al., 2017). However, the benefits of such interventions within the context of VML injury has been met with mixed reviews in the current literature. Earlier studies examined the effects of ECM scaffolds vs no repair on VML regeneration and found it to be advantageous for force recovery in subjects (Corona et al., 2013; Mase et al., 2010; Dziki et al., 2016) whereas further contributions are associated with cellular infusion (muscle-derived cells) into the scaffold (Corona et al., 2014, Quarta et al., 2017). However, recent developments in the field of VML has shifted away from the reliability of ECM scaffolds.

Although ECM scaffolds have proven to be more effective than no repair for VML (Sicari et al., 2012), several key dysfunctions have been associated with this intervention. First, a heightened pro-inflammatory response is noted in contrast to autologous muscle graft repair (Aurora et al., 2016; Griesing et al., 2017). This immune response appears to elicit the formation of a fibrotic scar rather than muscle fiber regeneration. In conjunction with the previous point, ECM scaffolds have been associated with limited *de novo* muscle fiber regeneration, in part, due to the lack of sufficient satellite cell migration into the scaffold-implanted defect site (Garg et al., 2014; Aurora et al., 2016). In summary, although the ECM scaffold is successful in recovering limited force output compared to no repair, current studies are shifting toward more effective strategies such as minced muscle and autologous muscle grafts.

Concerning satellite cell mechanics, the vital grafts have been shown to be more advantageous. For instance, ECM scaffolds offer limited satellite cell migration into the defect area (~0.5mm from intact muscle) (Garg et al., 2014a), and Pax7+ cells were not present at all according to another source (Garg et al., 2014b). This same study reported that protein expression of Pax7 was upregulated in vital grafts 2-weeks post-injury. This study further validated the findings of Corona et al. (2012) which also found Pax7 protein to be elevated in

muscle-derived constructs used as an intervention for VML. In addition to Pax7, gene expression of myogenic factors Pax7, Emhc and myogenin were also elevated in the vital grafts versus acellular grafts (Garg et al., 2014).

Overall, a wide and rapidly growing progression of interventions has been used in studies concerning VML in the last 10 years. Acellular and devitalized implants were first tested and proved to be more beneficial than unrepaired VML injuries. However, overall deficits in these models included lack of satellite cell migration and subsequent lack of de novo muscle regeneration leading to the area being filled in with fibrotic tissue. Common interventions then switched to vital tissue which generally resulted in lower collagen deposition, higher de novo muscle regeneration and immunomodulation compared to devitalized implants. However, force recovery was still limited in these models seemingly due to lack of a proper stimulus for satellite cell proliferation, differentiation and migration. Subsequent models focused on providing this stimulus through various means (i.e. growth factor injection/infusion, physical activity). At this point in the literature, it is understood that a proper scaffold containing vital cells/tissue and a proper myogenic stimulus is needed for improved force recovery in VML repair.

VML and Physical Activity

To this point, the discussion on VML has led to several convincing patterns: 1) Fibrosis and prolonged, severe inflammation are hallmarks of the VML model 2) Satellite cell migration and activation in the defect area, regardless of the repair intervention, are inhibited and 3) Limited muscle fiber regeneration results in force output detriments. Exercise and/or physical rehabilitation has been known to affect all three of the listed factors. Consequently, physical rehabilitation is being utilized more frequently in VML as will be discussed in full in the following paragraphs.

One of the first studies to investigate the role of exercise and VML used codelivery of muscle-derived cells with a matrix in a manner of “...simulating aspects of ‘exercise’ *in vitro*.” (Corona et al., 2012). Two months post-surgery, the “exercise” group exhibited higher force output recovery compared to the no repair and muscle-cell delivery control which did not mimic the effects of exercise.

Using a strict VML model (no repair), wheel running promoted a 17% increase in force recovery 8 weeks post-surgery despite no differences in morphological adaptations (CSA was not different from the sedentary group) and despite elevated fibrotic deposition (Aurora et al., 2014). The authors deduced that the improvement in force recovery was due to increased force transmission rather than force generation due to the increases in collagen deposition and absence of hypertrophy. Furthermore, this study noted an increase in gene expression of MyHC, collagen I and TGF- β and simultaneous reduction in metabolic markers (SIRT-1, PGC-1 α) in the injured muscle compared to non-injured sedentary control. These changes were the same regardless of

When incorporating both a repair intervention (muscle-derived cells infused into a bioconstruct) with rehabilitation (treadmill running), exercise promoted a 95% increase in functional recovery (gait pattern) 4 weeks post-surgery compared to the bioconstruct only group which exhibited a 75% recovery (Quarta et al., 2017). Furthermore, exercise resulted in reduced fibrosis, higher force output recovery, and better vasculogenesis than the non-exercised mice that only received a bioconstruct.

Following a multi-muscle VML injury to the posterior compartment (gastrocnemius, soleus, plantaris), adult mice underwent a rehabilitative protocol: ROM with electrostimulation, twice a week for 30 minutes each session for up to 14 days. Compared to the ROM only group, this mild form of rehabilitation resulted in lower inflammatory gene expression at 7 and 14 days

and rescued the depressed mitochondrial gene expression observed in the ROM only group (Greising et al., 2017).

Although there are no currently published studies on the effects of resistance training and VML, preliminary data shows that ladder climbing with increasing mechanical load resulted in 90% peak tetanic force of the affected muscle compared to the contralateral load (Song et al., 2015).

C57BL/6J mice underwent VML surgery of the TA and were shown to regain baseline wheel running distances 7 days post-injury (Quarta et al., 2017). Interestingly, when mice performed a treadmill running protocol for 7 days beginning immediately post-surgery, the defect site resulted in higher fibrosis, reduced regeneration as evidenced by smaller CSA, and had fewer mature NMJs compared to mice that waited one-week post-surgery to perform the same treadmill protocol. Therefore, there appears to be the necessity for sedentarism after VML injury occurrence before initiating a rehabilitative protocol.

CONCLUSION

Volumetric muscle loss is characterized by a loss of muscle that exceeds the normal regenerative capacity of skeletal muscle. Permanent functional loss results from the loss of contractile tissue and vascular, denervation, and the replacement of these functional components with fibrotic tissue. Interventions for promoting recovery from VML have included, among other treatments, ECM scaffolds (both acellular and infused), minced muscle and whole muscle grafts. These interventions have been used in conjunction with growth-promoting effects such as physical activity/exercise, infusion of growth factors (i.e. HGF) and anti-fibrotic treatments. Thus far, full force recovery has not been achieved.

The currently expanding body of literature has placed emphasis on inflammatory and fibrotic factors. Overall, VML is associated with a heightened inflammatory response and resultant fibrosis of the defect area regardless of intervention. These two factors severely impair proper activation and migration of satellite cells in the defect area leading to improper regeneration. With the use of stem cell-infused grafts or whole muscle grafts and growth stimuli enhanced *de novo* fiber formation is observed but with limited force recovery.

Studies that incorporate both physical activity and vitalized tissue have seen the greatest force recoveries within the VML model. However, these studies have not utilized whole muscle autographs which contain all resident cells important for adequate muscle regeneration. With the necessary resident cells, and proper growth factor to induce systemic alterations (i.e. physical activity), it is plausible to see a significant recovery from VML due to the modulations in the ECM, inflammatory response and satellite cell mechanics that physical activity provides.

PRELIMINARY DATA

Wheel Running

At the end of base line testing, rats averaged 698 m for the final 24-hour period. At 2 weeks post-surgery, the wheel running for the one week of wheel access was a non-significant 15% increase in (763 m/day) compared to the baseline distance. Therefore, rats did not run more or less at two weeks post-surgery than they did before undergoing VML surgery. Similarly, the 8 week time point wheel-running activity was a non-significant 19% increase from baseline distances (827 m/day), excluding outliers (one rat ran approximately 453% increased daily average compared to its baseline testing).

Force Output

At two weeks post-surgery, the force output of the WA LTA and RTA was 0.63 N and 0.94 N, respectively. When normalized to body weight, the force output of the WA LTA and RTA was 1.80 N/kg and 2.93 N/kg, respectively. Therefore, at two weeks post-surgery, the WA LTA force output was 67.4% of the RTA. The force output of the CA LTA and RTA was 0.40 N and 0.98 N, respectively. When normalized to body weight, the force output of the CA LTA and RTA was 1.10 N/kg and 2.98 N/kg, respectively. Therefore, at two weeks post-surgery the force output of the CA LTA was 41.6% of the RTA. In conclusion, the force output of the WA LTA was statistically higher than the CA LTA.

At eight weeks post-surgery, the force output of the WA LTA and RTA was 0.78 N and 1.12 N, respectively. When normalized to body weight, the force output of the WA LTA and RTA was 2.06 N/kg and 2.97 N/kg, respectively. Therefore, at two weeks post-surgery, the WA LTA force output was 69.5% of the RTA. The force output of the CA LTA and RTA was 0.86 N and 1.15 N, respectively. When normalized to body weight, the force output of the CA LTA and RTA was 2.15 N/kg and 2.85 N/kg, respectively. Therefore, at two weeks post-surgery the force output of the CA LTA was 75.6% of the RTA. In conclusion, the force output of the WA LTA was not statistically different than the CA LTA.

Overall, the WA LTA force output was higher than the CA LTA at two weeks post-surgery, but the force output was similar in the LTA between both groups at eight weeks post-surgery. The absolute and relative force output of the RTA was similar between both groups at both time points. The RTA absolute force output increased in both groups from two weeks to eight weeks, however, the relative force output was similar at two weeks and eight weeks within and between groups.

Cross-sectional Area

At two weeks post-surgery, CSA was similar between RTA and LTA of the CA and WA groups. Furthermore, CSA was similar between both groups. CSA of the CA LTA and RTA and of the WA LTA and RTA was 1135 ± 204 , 1092 ± 161 , 1012 ± 54 and 907 ± 124 , respectively. Similar to the two-week time point, CSA was similar between groups and between limbs at eight weeks post-surgery. CSA of the CA LTA and RTA and of the WA LTA and RTA was 1266 ± 58 , 1140 ± 21 , 1279 ± 18 and 1183 ± 43 , respectively.

SPECIFIC AIMS

AIM 1: Examine how VML recovery with an autograph and voluntary wheel running affect the muscle regeneration and satellite cell mechanics.

By using a whole muscle autograph, satellite cells will be present within the defect. The interest of this study will be to see how satellite cell proliferation and differentiation occur with and without exercise within the defect site. By immunostaining with Pax7, MyoD and Ki67 antibodies we will be able to analyze quiescent, proliferating and differentiating satellite cells. We will validate the histology measurements with Western Blot and/or PCR of major proteins associated with these processes (MuRFs, Cyclin proteins, etc.). Furthermore, upstream regulators of satellite cell activation (Ang II, Notch & Wnt signaling, etc.) will also be measured via western Blot in order to obtain further insight of key myogenic regulators in this VML model. Similarly, PCR analysis can be done on quiescent-specific gene expression (α 7-integrin, M-cadherin) to quantify quiescence.

AIM 2: Examine how VML recovery with an autograph and voluntary wheel running affect components of the extracellular matrix (ECM).

Excessive fibrosis is commonly observed in VML models, and dysregulated ECM often results in reduced force production as well as limited regeneration of muscle fibers. We will quantitatively and qualitatively analyze collagen deposition with IF collagen I and III staining and Masson's Trichrome staining, respectively. Key enzymes involved in the remodeling of the ECM are matrix metalloproteinases (MMPs) and their tissue inhibitors (TIMPs). These genetic expression of these enzymes and upstream regulators of MMPs, such as TGF β and EMMPRIN, will also be analyzed via PCR.

AIM 3: Examine how VML recovery with an autograph and voluntary wheel running affect immune cell infiltration and pro-, anti-inflammatory signaling.

Proper regeneration is dependent upon a tightly controlled time course of pro- and anti-inflammatory signaling which is concomitantly adherent to proper responses of specific immune cells. Exercise has been shown to modulate this immune response in the presence of regenerating muscle. In order to adequately detail the immune response in this VML model, we will utilize IF or IHC to observe the quantity and type of infiltrating immune cells. Of particular interest are M1 and M2 macrophages. To better understand the overall role of the immune response during these time courses, we will use PCR analysis to measure pro- and anti-inflammatory cytokines such as TNF, IL-6, IL-10, and IL-1B among others.

CHAPTER TWO

METHODS

Animal Care and Use

Animals

All animal care and use within this protocol was approved by the University of Arkansas Institution of Animal Care and Use Committee (protocol #17075) (see Appendix). Male, Sprague-Dawley rats (3-4 months old) will be used for this study. Rats will be allowed *ad libitum* access to normal chow and water throughout the duration of the study. Rats will be individually caged and kept in a climate-controlled room with automatic 12-12h light/dark cycle. Once rats reach the desired weight of 300g, running wheels will be unlocked, and rats will be allowed *ad libitum* wheel access for 72 hours to assess baseline running distance. At the conclusion of the 72 hours of wheel access, wheels will be locked and at least seven days will be allowed between this time and VML surgery to allow for any activity benefits to rescind. Baseline activity will be recorded as the average distance during the last 24 hours of the three-day period of wheel access.

At the end of the one-week wash-out following wheel lock, rats will undergo VML surgery. Immediately post-surgery, 24 hours after surgery, and 48 hours after surgery, rats will receive a .1 cc subcutaneous injection of .3g/1ml buprenorphine to reduce pain-associated distress as conducted in Wu et al. (2012). Additionally, rats will also be given Carprofen in the form of either Rodent MD'sTM Rimadyl tablets (2mg/tablet) (Bio Serv, MD150-2) or Medigel® CPF packs (ClearH₂O, 74-05-5022) for additional pain management post-surgery. One-week post-surgery, wheels will either remain locked (Cage Activity, CA) or unlocked (Wheel Activity, WA) for a period of either one week or seven weeks. Two-weeks post-surgery, tissue harvest

will be conducted on 16 rats (n=8 CA, n=8 WA). Eight-weeks post-surgery, tissue harvest will be conducted on 16 rats (n=8 CA, n=8 WA). Twenty-four hours before tissue harvest, wheels will be locked on the WA rats in order to avoid acute variations in exercise between rats.

VML Surgery

Rats will be anaesthetized by inhalation of isoflurane (2% in oxygen) during surgery. The lower left hindlimb will be shaved and sterilized using three rotations of alcohol and betadine. A 1-2 cm longitudinal incision will be made over the belly of the tibialis anterior (TA) cutting through the deep fascia to expose the belly of the TA. A surgical marker will be used to draw a line along the length of the medial 1/3 of the TA. Next, a muscle biopsy punch (approximately 8mm x 3mm) will be used to cause a defect equaling approximately 20% of the TA by weight. The weight of the defect will be determined using a regression equation based on the rat's body weight as defined by Wu et al. (2012). Once the defect is removed, it will be weighed and replaced in the defect site properly aligning with the line made from the surgical marker. Polypropylene sutures will be used to anchor the defect to the intact TA tissue using two sutures on both the distal and proximal ends of the defect. Vicryl thread will be used to suture the fascia and then the cutaneous layers together to completely close the wound.

Electrophysiology

The following protocol for electrophysiology was adopted from several sources (Conboy & Rando, 2005; Mintz et al., 2016; Kasukonis et al., 2016). Rats will be anaesthetized by inhalation of isoflurane (2% in oxygen) during tissue harvest. The legs will be shaved and sterilized with three rotations of betadine and alcohol wipes. The following protocol for force output measurement will be conducted on both legs. A transverse incision will be made on the proximal, anterior lower limb to expose the distal tendons of the TA, extensor digitalis longus

(EDL) and extensor hallucis longus (EHL). Tenotomy of the EDL and EHL tendons will be conducted leaving the TA tendon intact and isolated. The rat will be positioned so the knee is at a 90° angle, and the leg will be running parallel with the force platform. The ankle and pad of the foot will be secured onto the platform of the electrophysiology machine using surgical tape. Two probes will be inserted in the lateral border of the gastrocnemius and TA as well as the fibular head as described in Mintz et al. (2016) to adequately stimulate the peroneal nerve which innervates the TA. Once the leg and probes are secured, 100Hz at a 400ms pulse will be delivered to induce adequate peak tension. Five measurements will be taken with 60 seconds of rest allowed in between each measurement.

Tissue Harvest

The TA, EDL and gastrocnemius will be extracted from each leg and weighed. The EDL and gastrocnemius will be preserved in their entirety. The left TA (VML) will have a complete transverse cut effectively dividing the defect area into two equal halves and subsequently the TA will be sectioned into three parts: 1) The distal half of the TA containing half of the defect site (later used for histology), 2) the isolated defect site from the proximal TA, and 3) the remaining proximal TA tissue without the defect. The proximal half of the TA (including the proximal half of the defect) will be immediately flash frozen in liquid nitrogen and stored in -80°C. The distal half of the TA (used for histology) will be immediately flash frozen in liquid nitrogen-cooled isopentane the stored in -80°. The proximal, isolated defect and proximal TA will be used for protein, genetic and zymography analyses. Rats will be euthanized via either carbon-dioxide asphyxiation or exsanguination by removal of the heart. All collected tissue will be stored in -80°C until processed for analyses.

Histology

Tissues will be cut into 10µm sections using the Leica CM1859 cryostat (Leica Biosystems, Buffalo Grove, IL) set at -20°C. For this study, histology will be utilized to observe satellite cells, collagen deposition and infiltrating cells in all groups. The following portion of the methodology will describe the protocols used for Masson's Trichrome, Collagen I and III immunofluorescence, Pax7 immunohistochemistry, and M1 and M2 macrophage labeling.

Masson's Trichrome Staining

The following protocol is taken directly from the Chromaview™ Advanced Testing guidelines for their staining kit. Once the frozen slides are thawed at room temperature, they were placed in Boulin's Fluid at 56°C for 1 hour. After rinsing the slides in DI water for 3-5 minutes, slides will be placed in Weigert's Iron Hematoxylin Stain for 10 minutes. The slides will go through another DI rinse cycle before being placed in Biebrich Scarlet-Acid Fuchsin Solution for 5-10 minutes. After rinsing the slide for 30 seconds with DI water, slides will then be placed in Phosphotungstic-Phosphomolybdic Acid Solution for 5 minutes. Slides will then be incubated in Aniline Blue Stain Solution for 5-10 minutes before being placed in 1% Acetic Acid Solution for 1 minute. After another 30 second rinse in DI water, slide will be dehydrated in two changes of anhydrous alcohol. Afterward, sections will be mounted. The result will be nuclei stained as black, cytoplasm and muscle stained as red, and collagen stained as blue.

Masson's Trichrome will be used to analyze cross-sectional area of the muscle fibers. Each section will be imaged with a Nikon camera (Sight DS-Vi1) mounted on an Olympus CKX41 inverted microscope at 20X magnification (Olympus, Tokyo, Japan), and analyzed with Nikon NIS Elements BR software package (Nikon, Melville, NY). Cross-sectional area (CSA) will be performed as previously described (Washington et al., 2011). 150 fibers per sample will be

manually traced. Each traced fiber will be in the unaffected area of the muscle (away from the defect site).

Immunofluorescence of Collagen I and III

The following protocol is taken directly from Kim et al., 2016. Tissue immunoreactivity to collagen I will be calculated from fluorescent microscopic images (200X) using a custom algorithm developed for publicly available image analysis software (Image J, NIH). Using the algorithm, images will be converted to 8-bit gray scale, and uniformly threshold across all samples to isolate collagen type I and III positive tissue regions. From these images, the software will be used to determine the percent collagen type I and III positive tissue area for all tissue sections. Representative tissue sections collected from four animals per group will be used for all calculations. Within each section, three separate regions were imaged and analyzed to calculate the average collagen type I and III percent area. A total of twelve images were analyzed for each treatment group.

Western Blot

Protein quantification for satellite cell mechanics, fibrosis/collagen deposition, inflammation and ECM will be probed and analyzed via Western Blot. Tibialis Anterior homogenate will be fractionated in 8-12% SDS-polyacrylamide gels. Gels will then be transferred to low-fluorescing polyvinylidene difluoride (PVDF) membranes. Membranes will be stained with *Ponceau S* before blotting to verify equal loading of the gels. Membranes will be blocked in a 1:1 solution of LI-COR blocking buffer and 1x Tris-buffered saline (TBS) for two hours at room temperature. Primary antibodies will be diluted at 1:500 to 1:1000 in a 1:1 solution of LI-COR blocking buffer and 1x TBS and incubated at 4°C overnight. Anti-rabbit and anti-mouse monoclonal secondary antibodies (Cell Signaling Technologies, Danvers, MA) will be

diluted at 1:15000 to 1:20000 in a 1:1 solution of LI-COR blocking buffer and 1x TBS and incubated at room temperature for one hour. Fluorescence imaging will be performed using the LI-COR Fc to visualize antibody-antigen interaction. Blotting images will be quantified by densitometry using the Image Studio Lite v. 5.2 software. The Ponceau-stained membranes will be digitally scanned, and the 45-kDa actin bands will be quantified by densitometry and used as a protein loading correction factor for each lane.

qRT-PCR

RNA will be extracted with Trizol reagent (Thermo Fisher Scientific, Waltham, MA, USA). Total RNA will be isolated using the Purelink mRNA mini kit (Thermo Fisher Scientific, Waltham, MA, USA). Cdna will be reversed transcribed from 1 μ g of total RNA using the Superscript Vilo Cdna synthesis kit (Thermo Fisher Scientific, Waltham, MA, USA) for a final result of a 1:20 ratio of RNA to total volume. This final volume will then be brought to a 1:100 dilution factor. Real-time PCR will be performed, and results analyzed by using the StepOne Real-Time PCR system (Thermo Fisher Scientific, Waltham, MA, USA). Cdna will be amplified in a 25 μ L reaction containing appropriate probes and Taqman Gene Expression Mastermix (Thermo Fisher Scientific). Samples will be incubated at 95°C for 4 minutes, followed by 40 cycles of denaturation, annealing and extension at 95°C, 55°C and 72°C, respectively. TaqMan fluorescence will be measured at the end of the extension step each cycle. Cycle Threshold (Ct) will be determined, and the Δ Ct value will be calculated as the difference between the Ct value and the 18s Ct value. Final quantification of gene expression will be calculated using the $\Delta\Delta$ Ct method $Ct = [\Delta Ct(\text{calibrator}) - \Delta Ct(\text{sample})]$. Relative quantification will then be calculated as $2^{-\Delta\Delta Ct}$.

Statistical Analysis

All data will be analyzed using Statistical Package for the Social Sciences (SPSS version 22.0, Armonk, NY). Results will be reported as mean \pm SEM. A two-way ANOVA will be performed to analyze main effects of physical activity and injury and if there are any interactions between the dependent variables. When a significant interaction is detected, differences among individual means will be assessed using Fisher's LSD post-hoc analysis. Statistical significance will be set at $p \leq 0.05$.

CHAPTER THREE

AIM 1: Muscle Regeneration and Satellite Cell Mechanics

ABSTRACT

Volumetric muscle loss exceeds the normal regenerative capacity of skeletal muscle resulting in permanent functional loss. VML-centered research has focused on satellite cell mechanics (activation, migration, incorporation), but various repair strategies have not been successful in achieving optimal muscle regeneration and force recovery. **PURPOSE** The purpose of this study is to observe the effects of autologous repair and wheel activity on force recovery and satellite cell mechanics. **METHODS** 32 male Sprague-Dawley rats had 20% of their LTA removed then replaced to act as autologous repair. Half of the rats utilized wheel running, and at 2 and 8 weeks, the autologous tissue was excised from the LTA from both wheel running and sedentary rats. Force measurements were taken at 2- and 8-weeks post-injury. Histology was used to analyze CSA and centrally-located nuclei. qRT-PCR was used to measure gene expression of satellite cell mechanics. **RESULTS** At two weeks post-injury, LTA relative force was higher in the wheel active group vs sedentary group. By 8 weeks, LTA relative force was similar between both groups. There was a main effect of wheel activity to increase CSA. There were no differences in CLN in the LTA. There was a main effect of injury to increase gene expression of all markers except myostatin. **DISCUSSION** Though wheel activity improved force recovery at an early time point, further progression was not observed by 8 weeks, and both groups had similar force output by this late time point. Regardless of repair strategy or physical activity, gene expression of myogenic markers did not delineate differences in force output between groups at either time point. The various phases of satellite cell activation did not appear affected which may account for other key mechanisms (i.e. ECM remodeling) owing to changes in force recovery.

INTRODUCTION

Skeletal muscle is a highly plastic and regenerative tissue able to overcome most minor damages and injuries sustained in daily living. Local muscle stem cells (satellite cells) provide much of the regenerative capacity for muscle to maintain size and function (Relaix & Zammit, 2012). However, this regenerative capacity cannot withstand large, traumatic loss of muscle tissue. “A frank loss of muscle tissue, or volumetric muscle loss (VML) injury, may result from primary or secondary injuries that are beyond the endogenous reparative and regenerative capacities of mammalian skeletal muscle” (Corona, Wenke & Ward, 2016).

Volumetric muscle loss (VML) was coined in 2011 by Grogan et al. and is defined as the traumatic or surgical loss of skeletal muscle with resultant permanent functional impairment (Grogan et al., 2011). The focal point of VML research has been to address the common type of injury inflicted on the modern-day battlefield. VML is not medically coded, so the rate and quantity of this injury is undeterminable. However, VML commonly occurs with severe, extremity wounds which have accounted for 58% of battlefield-inflicted wounds in Operation Iraqi Freedom and Operation Enduring Freedom from 2001-2005 (Owens et al., 2008). VML is also witnessed within the confines of civilian life as well (Grogan et al., 2011). Any severe accident may result in VML. Additionally, medical procedures, especially the removal of sarcomas, often result in major loss of skeletal muscle.

Recent research has revealed atypical muscle regeneration to be one of the key factors of VML resulting in permanent loss of muscle force (Corona et al., 2013; Wu et al., 2012; Aurora et al., 2014). One of the hallmarks of VML is lack of mobility of satellite cells into the defect site resulting in major fibrosis in the tissue’s attempt to compensate for the loss of tissue (Corona et al., 2013). Therefore, implantation of an ECM scaffold, decellularized tissue and/or viable tissue

(autologous muscle) have been used to promote satellite cell migration into the defect site (Urciuolo & De Coppi, 2018). Still, some studies report a lack of regeneration possibly due to lack of a proper stimulus to promote necessary growth factors and cell migration (Garg et al., 2014). Therefore, recent studies have utilized physical activity as a necessary stimulus to promote and mediate proper regeneration within a VML model (Aurora et al., 2014; Quarta et al., 2017; Griesing et al., 2018). Specifically, voluntary wheel running has been observed to promote innervation, reduce fibrosis, and increase CSA in intact tissue near a VML site (Quarta et al., 2017) as early as 2 weeks after the injury had been induced.

In addition to phenotypic changes, the genotypic profile of myogenic markers is also of interest when understanding the response of the injured tissue in VML. Pax7, MyoD and myogenin are key proteins involved in the cell cycle regulation of satellite cells particularly the stages of quiescence, differentiation and proliferation, respectively (Cornelison & Wold, 1997). Ki67 is also a key marker of proliferation but is not specific to satellite cells (Scholzen & Gerdes, 2000). Upstream regulators of satellite cell activation are insulin-like growth factor (IGF-1) and myostatin (Bodine et al., 2001; Kurosaka & Machida, 2013). Whereas IGF-1 is a direct activator of satellite cell mechanics, myostatin has been shown to inhibit the activation of satellite cells (McCroskery et al., 2003).

At this point, the effect of a repair mechanism and physical activity at early and late time points (2 and 8 weeks post-injury, respectively) has not been researched. The purpose of this study was to observe the effect of an autologous repair strategy coupled with voluntary wheel running on muscle regeneration within a rat model of VML. Specifically, this study observed changes in tissue and body mass, force output of the injured and contralateral control muscles, regeneration (cross-sectional area and centrally-located nuclei), and the genetic profile of

myogenic markers and their regulators. We hypothesize that force recovery will be significantly greater in the wheel activity group vs the cage activity group.

METHODS

Animals and Experimental Design

All animal care and use within this protocol was approved by the University of Arkansas Institution of Animal Care and Use Committee (protocol #17075) (see Appendix). Male, Sprague-Dawley rats (3-4 months old) were used for this study. Rats were allowed *ad libitum* access to normal chow and water throughout the duration of the study. Rats were individually caged and kept in a climate-controlled room with automatic 12-12h light/dark cycle. Once rats reached the desired weight of 300 g, running wheels were unlocked, and rats were allowed *ad libitum* wheel access for 72 hours to assess baseline running distance. At the conclusion of the 72 hours of wheel access, wheels were locked, and at least seven days were allowed between this time and VML surgery to allow for any activity benefits to rescind. Baseline activity was recorded as the average distance during the last 24 hours of the three-day period of wheel access.

VML Surgery

Rats were anaesthetized by inhalation of isoflurane (2% in oxygen) during surgery. The lower left hindlimb was shaved and sterilized using three rotations of alcohol and betadine. A 1-2 cm longitudinal incision was made over the belly of the tibialis anterior (TA) cutting through the deep fascia to expose the belly of the TA. A surgical marker was used to draw a line along the length of the medial 1/3 of the TA. Next, a muscle biopsy punch (approximately 8mm x 3mm) was used to cause a defect equaling approximately 20% of the TA by weight. The weight of the defect was determined using a regression equation based on the rat's body weight as defined by Wu et al. (2012). Once the defect was removed, it was weighed and replaced in the defect site

properly aligning with the line made from the surgical marker. Polypropylene sutures were used to anchor the defect to the intact TA tissue using two sutures on both the distal and proximal ends of the defect. Vicryl thread was used to suture the fascia and then the cutaneous layers together to completely close the wound.

At the end of the one-week wash-out following wheel lock, rats underwent VML surgery. Immediately post-surgery, 24 hours after surgery, and 48 hours after surgery, rats received a .1 cc subcutaneous injection of .3g/1mL buprenorphine to reduce pain-associated distress as conducted in Wu et al. (2012). Additionally, rats were also given Carprofen in the form of either Rodent MD'sTM Rimadyl tablets (2mg/tablet) (Bio Serv, MD150-2) or Medigel® CPF packs (ClearH₂O, 74-05-5022) for additional pain management post-surgery. One-week post-surgery, wheels either remained locked (Cage Activity, CA) or unlocked (Wheel Activity, WA) for a period of either one week or seven weeks. Two-weeks post-surgery, tissue harvest was conducted on 16 rats (n=8 CA, n=8 WA). Eight-weeks post-surgery, tissue harvest was conducted on 16 rats (n=8 CA, n=8 WA). Twenty-four hours before tissue harvest, wheels were locked on the WA rats in order to avoid acute variations in exercise between rats.

Electrophysiology

The following protocol for electrophysiology was adopted from Kasukonis et al., 2016. Rats were anaesthetized by inhalation of isoflurane (2% in oxygen) during tissue harvest. The legs were shaved and sterilized with three rotations of betadine and alcohol wipes. The following protocol for force output measurement was conducted on both legs. A transverse incision was made on the distal, anterior lower limb to expose the distal tendons of the TA, extensor digitalis longus (EDL) and extensor hallucis longus (EHL). Tenotomy of the EDL and EHL tendons was conducted leaving the TA tendon intact and isolated. The rat was positioned so the knee was at a

90° angle, and the leg running parallel with the force platform. The ankle and pad of the foot were secured onto the platform of the electrophysiology machine using surgical tape. Two probes were inserted in the lateral border of the gastrocnemius and TA as well as the fibular head as described in Mintz et al. (2016) to adequately stimulate the peroneal nerve which innervates the TA. Once the leg and probes were secured, 100Hz at a 400ms pulse was delivered to induce adequate peak tension. Five measurements were taken with 60 seconds of rest allowed in between each measurement.

Tissue Harvest

The TA, EDL and gastrocnemius were extracted from each leg and weighed. The left TA (VML) had a complete transverse cut effectively dividing the defect area into two equal halves and subsequently the TA was sectioned into three parts: 1) The distal half of the TA containing half of the defect site (later used for histology), 2) the isolated defect site from the proximal TA, and 3) the remaining proximal TA tissue without the defect. The proximal half of the TA (including the proximal half of the defect) was immediately flash frozen in liquid nitrogen and stored in -80°C. The distal half of the TA (used for histology) was immediately flash frozen in liquid nitrogen-cooled isopentane the stored in -80°. The proximal, isolated defect and proximal TA was used for protein and gene expression. Rats were euthanized via either carbon-dioxide asphyxiation or exsanguination by removal of the heart. All collected tissue was stored in -80°C until processed for analysis.

Morphological Analysis

Tissues were cut into 10µm sections using the Leica CM1859 cryostat (Leica Biosystems, Buffalo Grove, IL) set at -20°C. For this study, histology was utilized to observe

cross-sectional area (CSA), centrally located nuclei (CLN) and percentage of non-contractile tissue (% NCT) in the defect site for all groups.

Collagen III Staining

The following protocol was taken from Kim et al., 2016. Tissue immunoreactivity to collagen III was calculated from fluorescent microscopic images (200X) using a custom algorithm developed for publicly available image analysis software (Image J, NIH). Using the algorithm, images were converted to 8-bit gray scale, and uniformly threshold across all samples to isolate collagen type III negative tissue regions. From these images, the software was used to determine the CSA for all tissue sections. Representative tissue sections collected from five animals per group were used for all calculations. Within each section, four separate regions (2 images of the defect site and 2 images of the area peripheral to the defect site) were imaged and analyzed to calculate the average collagen type I and III percent area. A total of twenty images were analyzed for each treatment group.

RNA Isolation, cDNA Synthesis, and Quantitative Real-Time PCR

RNA was extracted from the RTA and defect tissue of the LTA with Trizol reagent (Thermo Fisher Scientific, Waltham, MA, USA) as previously described (Perry et al., 2016). Total RNA was isolated using the Purelink mRNA mini kit (Thermo Fisher Scientific, Waltham, MA, USA). Cdna was reversed transcribed from 1 µg of total RNA using the Superscript Vilo Cdna synthesis kit (Thermo Fisher Scientific, Waltham, MA, USA) for a final result of a 1:20 ratio of RNA to total volume. This final volume was then brought to a 1:100 dilution factor. Real-time PCR was performed, and results analyzed by using the StepOne Real-Time PCR system (Thermo Fisher Scientific, Waltham, MA, USA). Cdna was amplified in a 25 µL reaction containing appropriate probes for Ki67, MyoD, Myogenin, CyclinD1, Pax7, IGF-1

and Myostatin and Taqman Gene Expression Mastermix (Thermo Fisher Scientific). Samples were incubated at 95°C for 4 minutes, followed by 40 cycles of denaturation, annealing and extension at 95°C, 55°C and 72°C, respectively. TaqMan fluorescence was measured at the end of the extension step of each cycle. Cycle Threshold (Ct) was determined, and the ΔCt value was calculated as the difference between the Ct value and the 18s Ct value. Final quantification of gene expression was calculated using the $\Delta\Delta\text{Ct}$ method $\text{Ct} = [\Delta\text{Ct}(\text{calibrator}) - \Delta\text{Ct}(\text{sample})]$. Relative quantification was calculated as $2^{-\Delta\Delta\text{Ct}}$.

Statistical Analysis

All data was analyzed using Statistical Package for the Social Sciences (SPSS version 22.0, Armonk, NY). Results were reported as mean \pm SEM. A two-way ANOVA was performed within each time point to analyze main effects of physical activity and injury and if there were any interactions between the dependent variables. When a significant interaction was detected, differences among individual means were assessed using Tukey's post-hoc analysis. A preplanned comparison between the 2-week and 8-week control group was done with a student's t-test. Statistical significance was set at $p \leq 0.05$.

RESULTS

Body and Tissue Mass

All body and tissue mass, along with force data, can be found in Table 1. Initial body mass of the rats was not significantly different among all four groups. The average initial body mass was approximately 339 grams. The 2-week WA group gained 1.4% body mass which was significantly lower than the 8.9% gain observed in the 2-week CA group ($p < 0.05$). The 8-week WA and CA groups had a significant 10% and 15% increase in body mass, respectively ($p <$

0.05) compared to the pre-injury weight, but this gain in mass was not significantly different between the two groups.

There were no significant differences in the defect tissue weight among all four groups. The defect tissue averaged ~103 mg and was approximately 18% of the LTA weight at time of harvest. For the 2-week time point, LTA mass was significantly lower than the RTA mass by 17% and 14% for the CA and WA groups, respectively, at the time of harvest ($p < 0.05$), however, the difference was not significantly different between the two groups. At 2 weeks, there was no significant differences of RTA mass between groups. At 8 weeks, LTA mass did not differ between the two groups but were 20 and 21% significantly lower than the RTA mass in the CA and WA groups, respectively ($p < 0.05$). RTA mass was not significantly different between groups. No significant differences were detected between all four groups for either LTA mass or percent differences of the RTA mass.

At two weeks, LEDL mass was significantly greater than the REDL mass of the CA and WA groups by 7% and 13%, respectively ($p < 0.05$). The gain in LEDL weight was not significantly different between the two groups. REDL mass was not significantly different between groups. At 8 weeks, LEDL mass was not significantly different between groups, and the LEDL was not significantly different than the respective REDL mass. There was a main effect of time to reduce LEDL mass. There were no significant differences in REDL between all four groups.

Wheel Running Data

Wheel running data can be found in Table 2. At the conclusion of the three-day baseline testing, rats averaged of 726 ± 73 meters/day. At two weeks post-injury, rats averaged of 763 ± 87 meters/day. At eight weeks post-injury, rats averaged a significantly higher distance of $1023 \pm$

104 meters/day ($p < 0.05$). Regardless of the time point, rats followed the typical nocturnal activity pattern observed in previous studies.

Force Data

At 2 weeks, there was a significant difference of 0.38 and 0.56 N of force produced in the CA and WA groups, respectively ($p < 0.05$) (Figure 1A). There was a significant difference in relative force (N/kg of body mass) of 1.03 and 1.63 between the CA and WA groups, respectively ($p < 0.05$) (Figure 1B). There was a significant difference in percentages of relative force output between the LTA and RTA of the CA and WA of 38% and 69%, respectively ($p < 0.05$) (Figure 1C). There were no significant differences in either force output or relative force output in RTA between the two groups. At 8 weeks, there were no significant differences in LTA force or relative force between the CA and WA groups. Relative force of the LTA as a percentage of the RTA was not different between both groups. Force output and relative force of the RTA was not different between the two groups. There was a main effect of time to increase force output in the LTA ($p < 0.05$). There was a main effect of time to increase relative force in the LTA ($p < 0.05$). There was a main effect of time to increase force output and relative force of the RTA ($p < 0.05$).

Cross Sectional Area and Centrally Located Nuclei

At 2 weeks, there was a main effect of injury and exercise to increase CSA by ~64% ($p < 0.05$) in the myocytes of the LTA outside of the defect area. At 8 weeks, there was a main effect of injury to increase CSA by ~33% ($p < 0.05$) in the cells of the LTA outside of the defect area. There were no differences between groups in the number of cells with centrally-located nuclei within the defect site of the LTA. Additionally, there were no differences in the number of cells with centrally-located nuclei between the RTA and cells of the LTA outside of the defect site.

The number of cells with centrally-located nuclei was ~8-fold higher in the defect site than either the RTA or the cells in the LTA outside of the defect site ($p < 0.05$).

Cell Cycle Regulators

There was a main effect of VML to increase mRNA abundance of IGF-1 at both 2- and 8-weeks post-injury ($p < 0.05$). There were no differences in the gene expression of IGF-1 between the 2-week and 8-week control groups. There was a main effect of VML to decrease mRNA abundance of Myostatin at both 2- and 8-weeks post-injury ($p < 0.05$). There were no differences in the gene expression of Myostatin between the 2-week and 8-week control groups. There was a main effect of VML to increase mRNA abundance of CyclinD1 at both 2- and 8-weeks post-injury ($p < 0.05$). There were no differences in the gene expression of CyclinD1 between the 2-week and 8-week control groups.

Satellite Cell Markers

There was a main effect of VML to increase mRNA abundance of Pax7 at both 2 and 8 weeks post-injury ($p < 0.05$). There were no differences in the gene expression of Pax7 between the 2-week and 8-week control groups. No significant differences in MyoD gene expression were observed between groups at either time point. Additionally, there were no differences in the gene expression of MyoD between the 2-week and 8-week control groups. There was a main effect of VML to increase mRNA abundance of Myogenin at both 2 and 8 weeks post-injury ($p < 0.05$). There were no differences in the gene expression of Myogenin between the 2-week and 8-week control groups. There was a main effect of VML to increase mRNA abundance of Ki67 2 weeks post-injury ($p < 0.05$). There were no differences in mRNA abundance of Ki67 between groups at 8 weeks. There were no differences in the gene expression of Ki67 between the 2-week and 8-week control groups.

DISCUSSION

This study is among the first to use complete autologous repair along with physical activity, in the form of voluntary wheel running, in promoting force recovery in a rat model of VML. Access to wheel running appeared to promote early-phase recovery of force production, but the effect of wheel running was lost by 8 weeks post-injury. Even though these differences in force production were observed, they occurred in spite of significant changes in satellite cell markers; therefore, force regeneration appears to occur despite significant contributions to satellite cell contributions in a VML model of autologous repair with voluntary wheel running.

Descriptive

Rats gained weight throughout the study as was expected since Sprague-Dawley rats do not taper in growth until 7-8 months of age (Sengupta 2013). The weight gain was dampened in the wheel running group as was also expected as this has been previously observed in a murine model (Moody 2015). This is also consistent with another rodent VML model that used wheel running (Aurora et al 2014). Average wheel running distance was not different pre- and post-surgery indicating that damage to the tibialis anterior did not affect physical activity. As the tibialis anterior is not a propulsive muscle in wheel running, wheel running was not expected to differ especially with one week of recovery time post-surgery.

Force Recovery

Aurora et al. (2014) has previously shown a benefit of voluntary wheel running at the 2-week time point in a similar TA VML model which did not utilize autologous repair. We also show the same effect of physical activity at this early time point. At 8 weeks, however, autologous repair normalized force recovery regardless of the exercise intervention. Therefore, exercise had an early-onset benefit to force recovery but was not effective in progressing force

recovery at a later time point. The tibialis anterior is not a propulsive muscle for wheel running, and morphological changes of skeletal muscle fibers (i.e. CSA) are usually not seen except in progressive loading models (Ishihara et al., 2001). Coinciding with Ishihara et al. (2001), no differences in CSA were detected in the wheel running group compared to the sedentary group (discussed in the next section), however, force recovery may have been a result of wheel running attenuating the inflammatory response and/or modulating fibrosis in the defect area (discussed in AIMS 2 and 3). Although voluntary wheel running has an acute effect on force recovery in a model of VML plus autologous repair, this same mode of physical activity appears insufficient to continually progress force recovery in this model of VML.

At 8 weeks post-surgery, when force of the muscle is made relative to the muscle's mass rather than body mass, force output is comparable to the contralateral, uninjured control TA (RTA). Despite the mass of the LTA remaining consistent between the 2-week and 8-week time points, relative force production was significantly increased. Again, physical activity had an acute effect at 2 weeks post-surgery to increase relative force of the LTA but was still significantly lower than the RTA. By 8 weeks, the autologous repair promoted a relative force recovery (N/T_{amg}) comparable to relative force of the RTA. Since the LTA mass was significantly lower than the RTA mass at 8 weeks, it is worth investigating if the force output would be similar between the two muscles if LTA mass were increased through a hypertrophic-centered exercise regimen.

CSA and CLN

At 2 weeks post-surgery, physical activity's effect to promote greater CSA may partially explain the larger force recovery compared to the sedentary group. It may be important to note the increase in CSA was independent of changes in muscle mass. The effect of physical

activity on CSA was no longer present at the 8-week time-point indicating that wheel activity may only afford an acute, beneficial effect.

Alternately, CLN was not different in the LTA defect site regardless of time or physical activity. The presence of centrally-located nuclei is regarded as a morphological marker of skeletal muscle regeneration as well as myopathy (Folker & Baylies, 2013). During development and regeneration, nuclei from fused myoblasts migrate to the center of the muscle fiber (Cadot et al., 2012); however, these nuclei eventually migrate to the periphery of the cell, and peripherally-located nuclei serve as a morphological cue of the completion of regeneration. With mild to moderate damage, regeneration is typically completed within 5-8 days. Given the extreme damaging nature of a VML injury, regeneration may take longer. Alternately, since CLN are still observed at 8 weeks, it is possible that these fibers have transitioned to a pathological state and may no longer have the capability for proper muscle regeneration (Cadot et al., 2012).

PCR Results

Changes in force output between sedentary and exercised groups and additionally between time points could not be explained by PCR results in either the upstream regulators or satellite cell markers typically involved in muscle regeneration. Though all markers, except Myostatin and MyoD, were upregulated in the VML limbs regardless of exercise or time point, none of the upregulated markers were different between the sedentary or exercised groups in either time point. Conversely, the upregulation of these markers may validate the hypertrophy of the LTA as being either compensatory in nature or as a byproduct of having growth factors upregulated in the neighboring defect site.

Voluntary physical activity does not promote a differential effect on these traditional satellite cell markers although it does appear to influence force recovery. This conclusion leads

to two hypotheses: 1) Physical activity's effect promotes force recovery in areas of the muscle outside of the defect area and/or 2) physical activity affects elements of force recovery inside the defect area other than satellite cell activity. Concerning the first hypothesis, it has been shown recently that wheel running, using the same model of VML, alters uninjured areas of the TA which results in increased force recovery. Regarding the second hypothesis, it has been well established that VML injuries impact not only the regenerative capability of the muscle but also several other key elements of normal muscle force recovery including fibrosis, the inflammatory response and innervation to the fibers.

As stated earlier, the TA is not the primary mover in wheel running; therefore, wheel running may not be the preferred method for satellite cell activation although it does promote force recovery from VML injury, especially in the early stages of recovery. It could be advantageous to use a form of physical activity that does not incorporate the injured muscle as the primary mover during the early stages of recovery as the exercise-induced damage may overload the recovery process. It may also be reasoned that physical activity should be transitioned into exercise to promote continual force recovery of the injured tissue at a later time point, but it is still unclear if this transition should be followed by an aerobic or resistance-trained regimen. By normalizing force to the muscle weight or CSA of the uninjured muscle fibers, it is clear that force production is present that is equivalent to the contralateral, uninjured muscle. Therefore, it is recommended that future research using this model of autologous repair and physical activity for VML injuries focus on advancing the rats to a hypertrophic form of exercise for the TA at a later time point.

CONCLUSION

This is the first study to investigate the effects of autologous repair with voluntary wheel running on the effects of muscle regeneration in a rat model of VML. Wheel running increased force recovery early-on, but autologous repair, regardless of activity, caused similar recovery of force by 8 weeks. Differences in CSA is the only factor within the parameter of this study that would explain why wheel activity caused an increase in force recovery but only at an early time point. Wheel running did not cause any differential effects in upstream regulators or myogenic targets of satellite cell activation, proliferation and differentiation. Thus, it is possible that wheel running promotes differences in other key factors (i.e. inflammation, fibrosis, innervation, etc.) beneficial for force recovery.

Table 1. Body Mass, Tissue Mass, Force Data

	2 Week		8 Week	
	Sedentary	Exercise	Sedentary	Exercise
TA Defect (mg)	103.5 ± 5.0	101.1 ± 6.2	104.1 ± 4.6	98.6 ± 3.2
% BW Diff ^{ME Time, Exercise}	8.9 ± 0.8	2.0 ± 0.6	15.5 ± 1.6	10.3 ± 2.5
LTA Mass (g)	0.54 ± 0.03	0.57 ± 0.03	0.57 ± 0.02	0.59 ± 0.05
RTA mass (g) ^{ME Time}	0.64 ± 0.01	0.61 ± 0.02	0.68 ± 0.03	0.71 ± 0.01
LTA Mass % RTA	83.5 ± 4.32	92.2 ± 5.3	85.9 ± 5.9	81.9 ± 4.9
LEDL Mass (g)	0.17 ± 0.01	0.15 ± 0.00	0.15 ± 0.01	0.14 ± 0.01
LEDL Mass % REDL ^{ME Time}	112.2 ± 2.9	106.6 ± 4.5	98.9 ± 7.0	94.9 ± 6.9
LTA Force (N/Kg)	1.03 ± 0.11	1.63 ± 0.17 †	2.02 ± 0.12 ‡	1.96 ± 0.08
RTA Force (N/Kg)	2.61 ± 0.08	2.6 ± 0.09	2.72 ± 0.09	2.81 ± 0.11
LTA Force % RTA	39.0 ± 5.1	67.4 ± 5.3 †	74.2 ± 3.2 ‡	70.9 ± 3.1

† = Significance between groups within time point (i.e. 2 Week Sed. Vs 2 Week Exer) ‡ = Significance between groups within activity group (i.e. 2 Week Sed. Vs 8 Week Sed.). ME = Main Effect. Significance set at P < 0.05

Table 2. Wheel Running Data

	Baseline (pre-surgery)	2-weeks post-surgery	8-weeks post-surgery
Distance (m/day)	726 ± 73	763 ± 87	1023 ± 104†

† = Significantly different from baseline distance. Significance set at P < 0.05.

Figure Legend

Figure 1 Force Data. Figure 1A) Raw force data of the left tibialis anterior in Newtons. Figure 1B) Force of left tibialis anterior relative to body mass in kilograms (N/Kg). Figure 1C) Relative force of the left tibialis anterior as a percentage of the relative force of the right tibialis anterior. † indicates significant difference from 2-week counterpart (i.e. 8-week sedentary vs 2-week sedentary). ‡ indicates significant difference from within time point (i.e. 2-week exercise vs 2-week sedentary). Significance was set at $p < 0.05$.

Figure 2 Cross-Sectional Area. Figure 2A) Cross-sectional area, in micrometers squared, of the left tibialis anterior peripheral to defect site and right tibialis anterior at 2 weeks. Figure 2B) Cross-sectional area, in micrometers squared, of the left tibialis anterior peripheral to defect site and right tibialis anterior at 8 weeks. Figure 2C) 10x representative immunofluorescence image of collagen 3 staining used for the 2-week CSA analysis. Figure 2D) 10x representative immunofluorescence image of collagen 3 staining used for the 8-week CSA analysis. ME = “main effect”. Significance was set at $p < 0.05$.

Figure 3 Centrally-Located Nuclei. Figure 3A) Percentage of fibers on the border of the defect area containing centrally-located nuclei at 2- and 8-week time points. Figure 3B) 10x H&E representative images of centrally-located nuclei.

Figure 4 Upstream Regulators of Satellite Cell Activation. mRNA abundance, normalized to 18S, of 4A) IGF-1 at 2 weeks, 4B) IGF-1 at 8 weeks, 4C) 2-week and 8-week IGF-1 comparison of control groups (right leg from sedentary groups). 4D) Myostatin at 2 weeks, 4E) Myostatin at 8 weeks, 4F) 2-week and 8-week Myostatin comparison of control groups (right leg from sedentary groups). 4G) Cyclin-D1 at 2 weeks, 4H) Cyclin-D1 at 8 weeks, 4I) 2-week and 8-week Cyclin-D1 comparison of control groups (right leg from sedentary groups). ME = Main Effect. VML = Volumetric Muscle Loss. † indicates significant difference from 2-week counterpart (i.e. 8-week sedentary vs 2-week sedentary). ‡ indicates significant difference from within time point (i.e. 2-week exercise vs 2-week sedentary). Significance was set at $p < 0.05$.

Figure 5 Satellite Cell Myogenic Regulators. mRNA abundance, normalized to 18S, of 5A) Pax7 at 2 weeks, 5B) Pax7 at 8 weeks, 5C) 2-week and 8-week Pax7 comparison of control groups (right leg from sedentary groups). 5D) MyoD at 2 weeks, 5E) MyoD at 8 weeks, 5F) 2-week and 8-week MyoD comparison of control groups (right leg from sedentary groups). 5G) Myogenin at 2 weeks, 5H) Myogenin at 8 weeks, 5I) 2-week and 8-week Myogenin comparison of control groups (right leg from sedentary groups). 5J) Ki67 at 2 weeks, 5K) Ki67 at 8 weeks, 5L) 2-week and 8-week Ki67 comparison of control groups (right leg from sedentary groups). ME = Main Effect. VML = Volumetric Muscle Loss. Significance was set at $p < 0.05$.

FIGURES

Figure 1

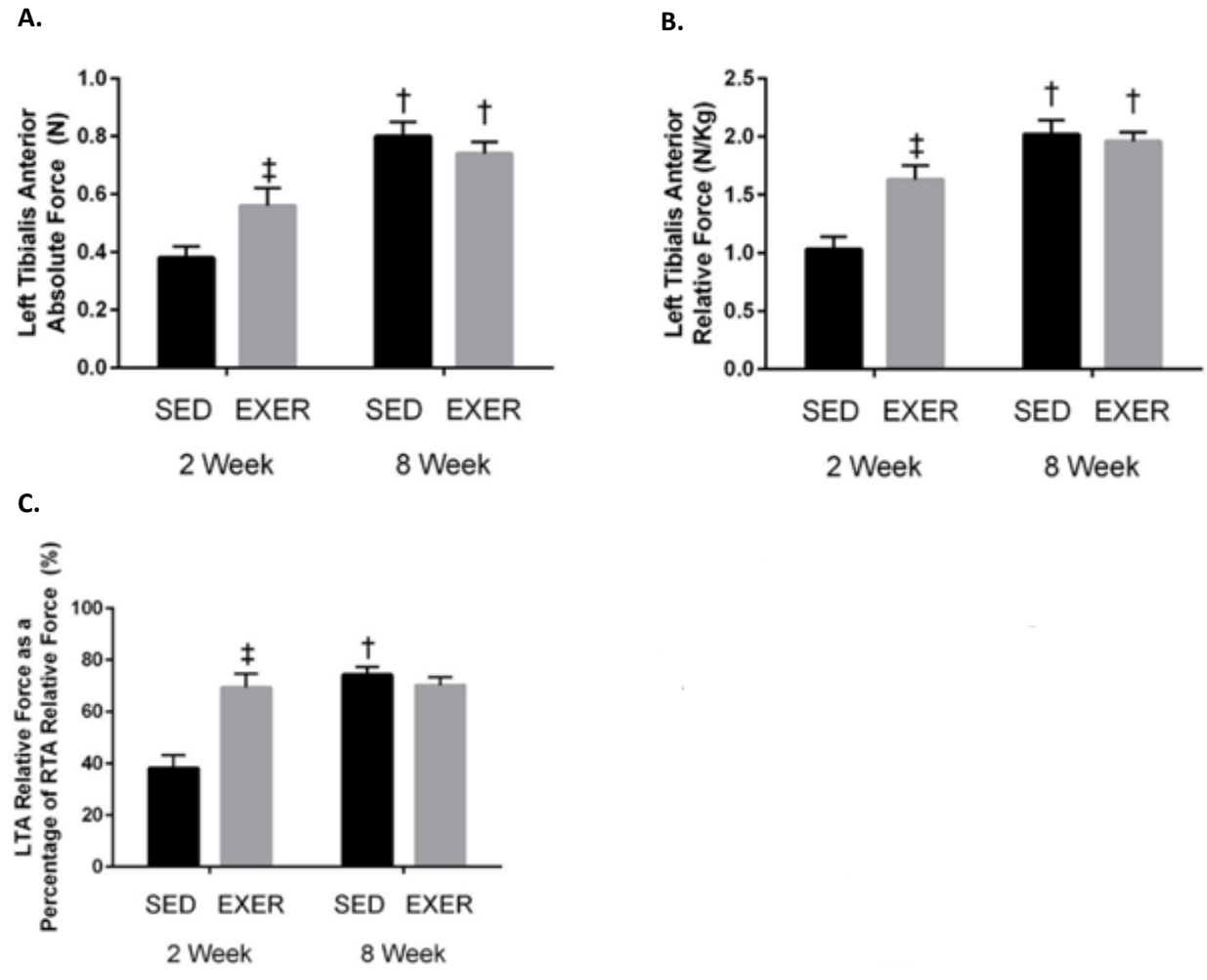


Figure 2

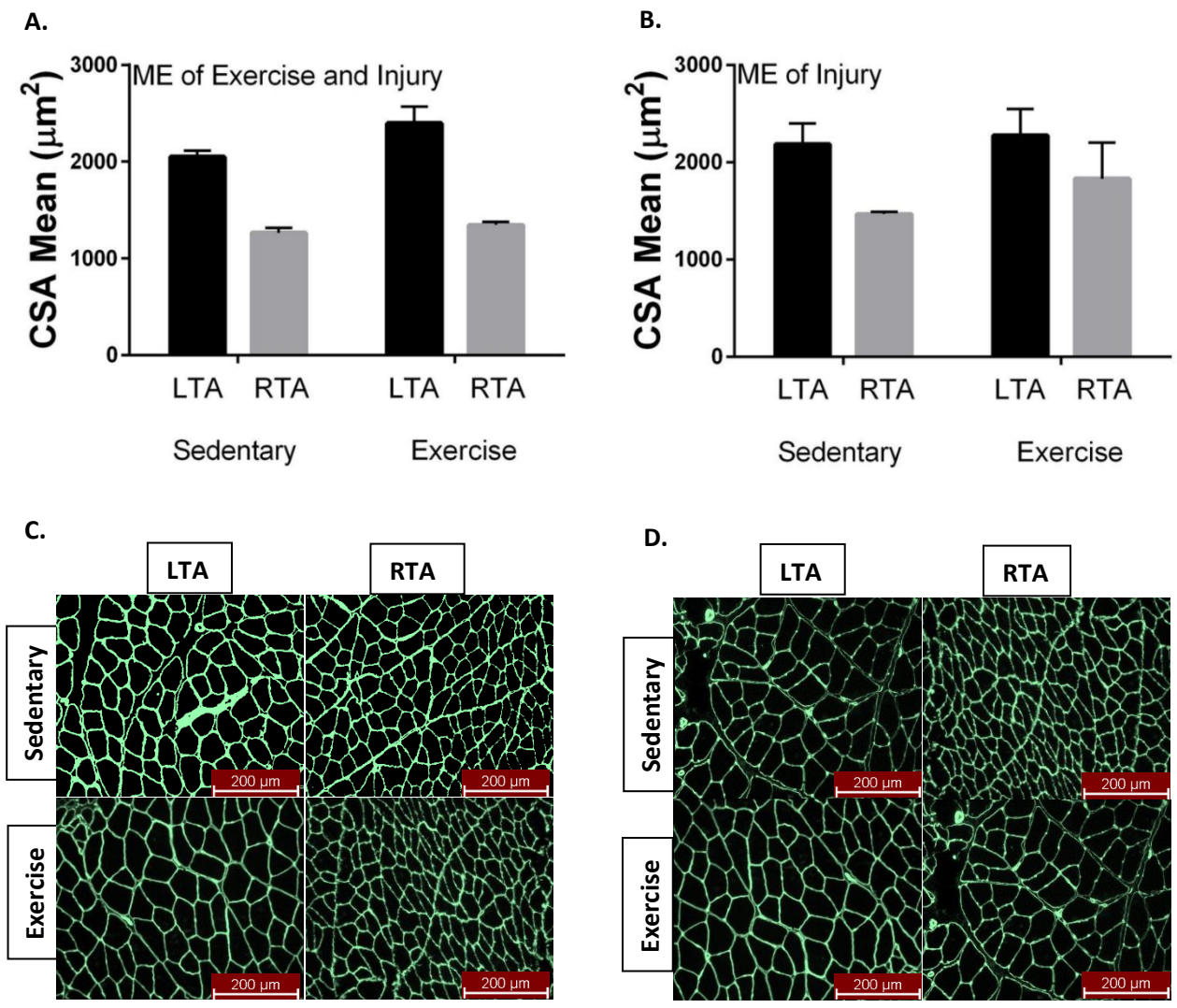


Figure 3

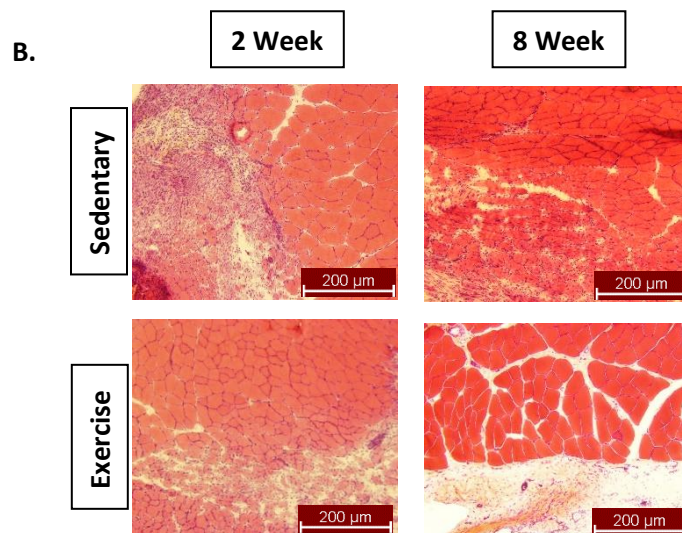
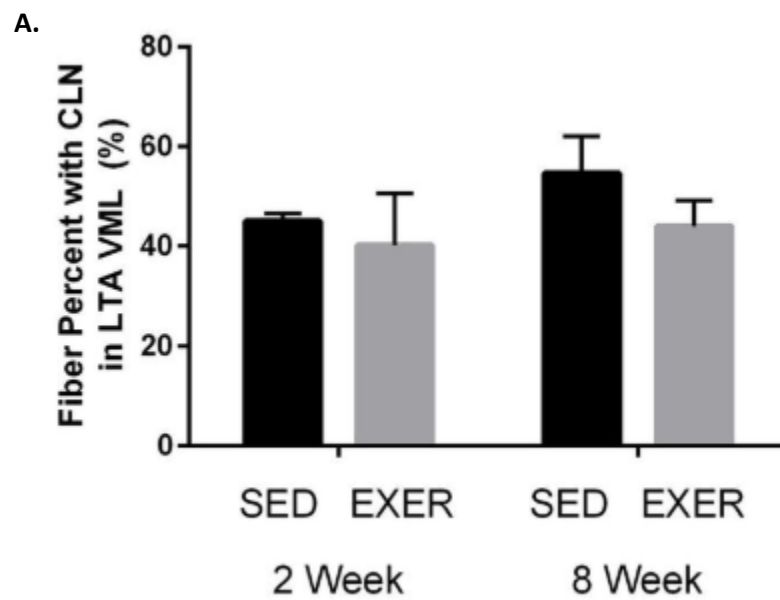


Figure 4

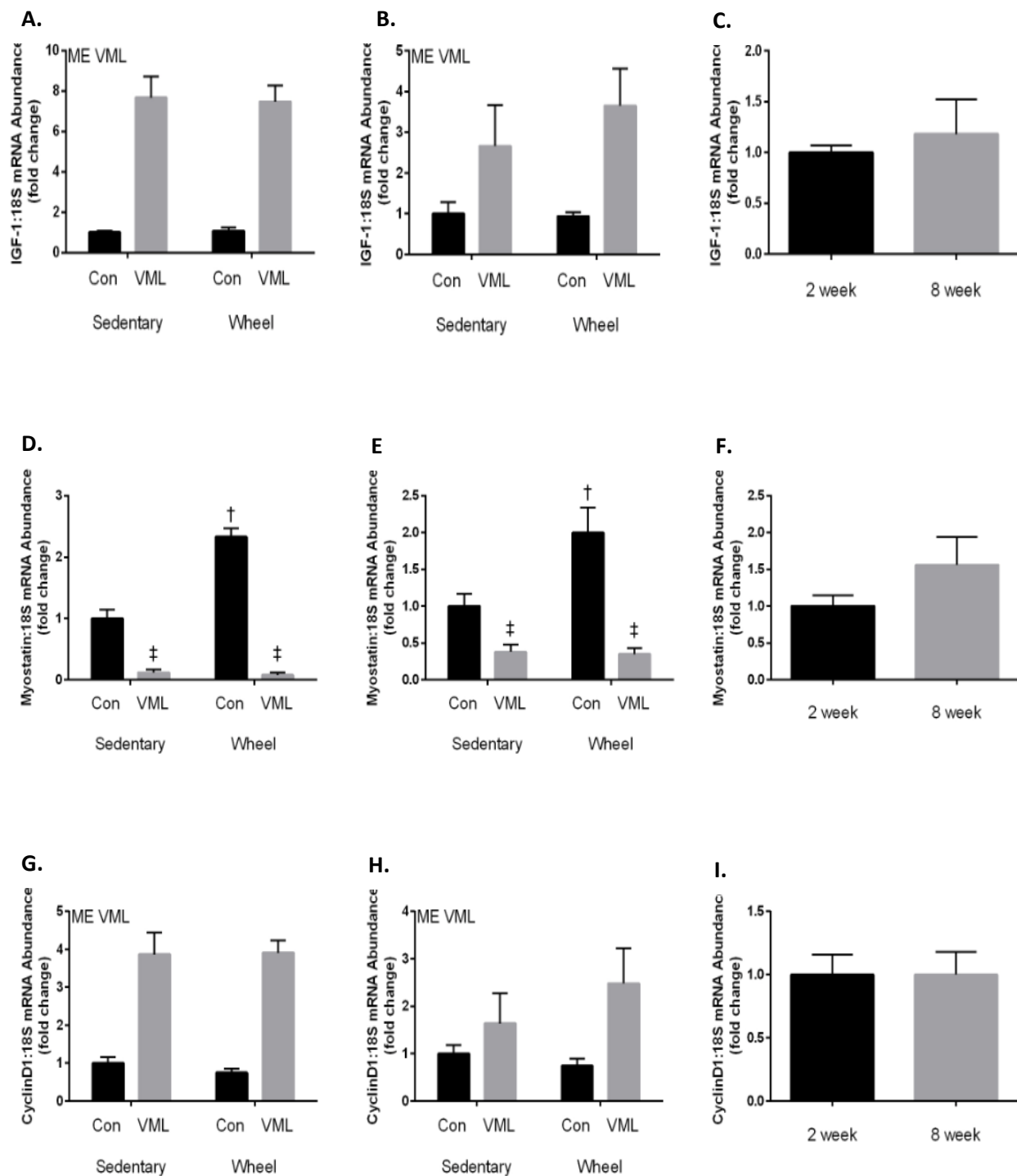
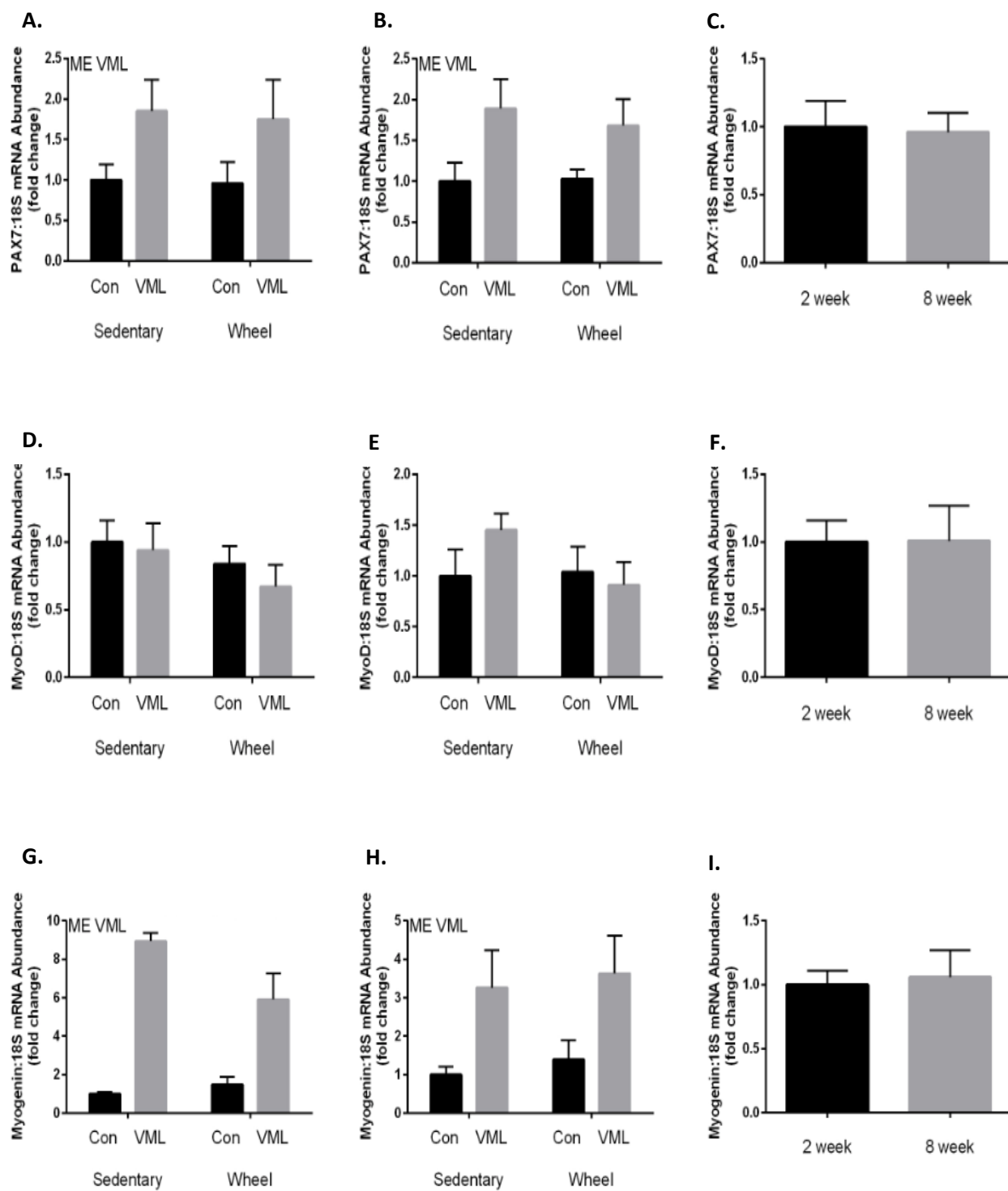
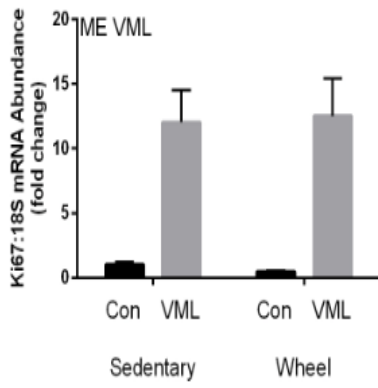


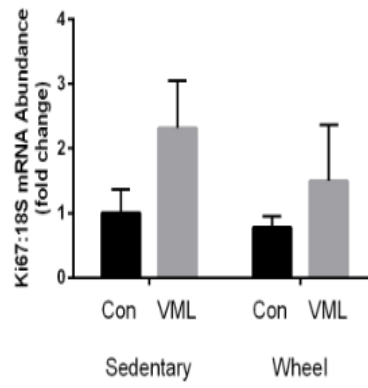
Figure 5



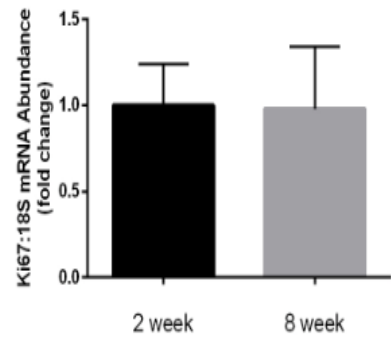
J.



K.



L.



CHAPTER FOUR

AIM 2: VML and ECM Remodeling

ABSTRACT

Volumetric muscle loss is characterized by permanent functional loss after traumatic injury to skeletal muscle. A key hallmark to impaired regeneration and subsequent inadequate force recovery is excessive fibrosis in the injured area. Several repair strategies and interventions have resulted in reduced scarring and/or functional fibrosis. Recent studies have shown promising consequences of early initiation of physical activity. **PURPOSE** The purpose of this study is to observe the effect of autologous repair and wheel activity on fibrosis in a VML model. **METHODS** 32 male Sprague-Dawley rats had 20% of their LTA removed then replaced to act as autologous repair. Half of the rats utilized wheel running, and at 2 and 8 weeks, the autologous tissue was excised from the LTA from both wheel running and sedentary rats. Histological analysis was used to measure collagen deposition and the percent of non-contractile tissue. qRT-PCR was used to measure gene expression of collagen and ECM-related markers. **RESULTS** Wheel activity caused differential responses in the collagen 3/1 ratio when observing the defect site and peripheral LTA tissue: the ratio was higher expressing in the LTA at 2 weeks but was reduced to sedentary levels by 8 weeks whereas there was a main effect of time and wheel activity to increase the ratio in the defect site. There was a main effect of time to decrease the percent of non-contractile tissue in the LTA. At 2 weeks, TGF β and MMP9 gene expression in the LTA was lower in the wheel active group vs sedentary group whereas TGF β , MMP2 and MMP9 were high expressing wheel activity group by 8 weeks post-surgery. **DISCUSSION** Wheel activity causes modulations in the ECM that may have benefits to early force recovery; however, these modulations are reversed between the wheel activity and sedentary groups at 8

weeks group, which may explain the stagnation of force recovery in the wheel activity and simultaneous progression of force recovery in the sedentary group.

INTRODUCTION

Skeletal muscle is a tissue comprised primarily of contractile material but is also comprised of neural, vasculature and connective tissue. The tissue that embeds many of the primary and secondary tissues in skeletal muscle and is responsible for providing structural and biochemical support is known as the extracellular matrix (ECM). The major component of the ECM is collagen which also accounts for roughly ~1-10% of muscle dry weight (Gillies & Lieber, 2011). Many ECM resident cells can contribute to collagen production, but fibroblasts are the primary cell of collagen production during periods of normal, healthy muscle functioning (Archile-Contreras et al., 2010). Though various collagen types exist in the ECM of skeletal muscle, types I and III contribute the largest percentage and are primarily produced and secreted by fibroblasts (Light & Champion, 1984).

Proper turnover of the ECM is necessary to maintain tissue health, allow for adequate cell migration and myotube formation, and reorganization during muscle adaptation (Gillies & Lieber, 2011). The proteins that regulate ECM turnover are matrix metalloproteinases (MMP) and tissue inhibitors of matrix metalloproteinases (TIMP). Common skeletal muscle MMPs are the gelatinases MMP-2 and -9 which degrade the type IV collagen (Kherif et al., 1999) and the collagenases MMP-1 and -13 that degrade collagen types I and III (Singh et al., 2000; Wu et al., 2003). MMP-1 has been particularly targeted as an important enzyme needed for satellite cell migration and differentiation as it is associated with increasing migration-related marker proteins (N-cadherin, β -catenin) as well as pre-MMP-2 and TIMP (Wang et al., 2009). Also, MMP-1 has been shown to degrade collagen thus reducing fibrosis. MMP-2, -7 and -9 have been associated

with myotube formation in their combined effect of ECM breakdown and elimination of cell surface components that hinder fusion between myocytes and myotubes (El Fahime et al., 2000). During times of injury and repair of skeletal muscle, satellite cells must be able to migrate to places of injury. Thus, proper turnover of the ECM is essential for proper muscle regeneration. MMP-2 and -9 appear to have a significant role in the acute phases of muscle repair from injury (Kherif et al., 1999). These MMPs are needed to degrade the basement membrane to allow for satellite cell migration but have also been shown to help activate satellite cells (Fukushima et al., 2007).

Not only is healthy ECM required for proper cell migration, but dysregulation of the factors that contribute to normal ECM (fibroblasts, MMPs, TIMPs) often leads to fibrosis. Severe fibrosis can reduce force output due to dysregulating the ECM which is known to play a key role in proper mechanotransduction of skeletal muscle (Humphrey et al., 2014). TGF- β has been established as a leading upstream regulator that activates fibroblasts to upregulate the production of collagen I (Leask & Abraham, 2004). The subsequent result of TGF- β activation in muscle is reduced isometric force, increased fibrosis and muscle atrophy via activation of fibroblasts/collagen production and atrogen-1 (Mendias et al., 2012).

Eccentric exercise (cycle training) has been shown to upregulate the expression of many ECM-related genes at acute (immediately after and 2h post-exercise) and chronic (12 weeks) time points (Hjorth et al., 2015). Acutely, exercise affects expression of proteases and protease inhibitors (i.e. MMPs, TIMPs) whereas chronic adaptations were observed with structural components of the ECM (i.e. collagen and proteoglycans) (Hjorth et al., 2015). Specifically, pro-MMP 2 and 9 decrease and increase, respectively, following exercise, and these changes are reflected by the appropriate changes in their respective TIMPs (Koskinen et al., 2004). Acutely

following exercise, ECM-related growth factors (IGF-1, TGF- β , IL-6) as well as collagen turnover and net collagen synthesis (chronically) increase (Kjaer et al., 2006; Heinemeier et al., 2011).

The hallmark of VML injury is the extent of collagen deposition leading to fibrosis. Li et al. (2013) noted that excessive fibrosis in VML sites may play a causative role in functional loss of affected muscle 4 weeks post-injury. However, fibrosis has also been reasoned to have beneficial effects such as allowing greater force output via force transmission (Garg et al., 2014b; Aurora et al., 2014; Corona et al., 2013).

Within the confines of VML, an intact and functional ECM is important for cell activation, migration and infiltration into the affected area. However, when lacking a functional ECM, the defect area is mainly filled with a fibrotic mass rather than skeletal muscle tissue (Garg et al., 2015). Therefore, many recent VML studies have incorporated an ECM scaffold (typically decellularized) into the defect. Though results vary, many of these studies report an increase in maximal isometric torque, increased regeneration as evidenced by larger CSA, and increased migration of satellite cells into the defect site (Valentin et al., 2010; Corona et al., 2013). Though these types of scaffolds are more successful at muscle regeneration and force recovery compared to not having a repair intervention, acellular scaffolds still do not mimic normal skeletal muscle regeneration. Garg et al. (2014) reported that although immune cell infiltration into the defect site is more than doubled (compared to muscle grafts), these cells were less active. Even when the scaffolds are derived from muscle tissue, fibrosis still occurs though it has been argued that this is functional fibrosis given that force output was still elevated compared to the no repair group (Corona et al., 2013). Consequently, force output was lower in ECM scaffold-treated groups compared to muscle graft-treated groups. In summary, ECM

scaffolds are more beneficial to the regenerative process compared to not having a repair intervention, but they do not mimic canonical regeneration as has been shown with using muscle grafts.

METHODS

Animal Care and Use

Animals

All animal care and use within this protocol was approved by the University of Arkansas Institution of Animal Care and Use Committee (protocol #17075) (see Appendix). Male, Sprague-Dawley rats (3-4 months old) were used for this study. Rats were allowed *ad libitum* access to normal chow and water throughout the duration of the study. Rats were individually caged and kept in a climate-controlled room with automatic 12-12h light/dark cycle. Once rats reached the desired weight of 300g, running wheels were unlocked, and rats were allowed *ad libitum* wheel access for 72 hours to assess baseline running distance. At the conclusion of the 72 hours of wheel access, wheels were locked, and at least seven days were allowed between this time and VML surgery to allow for any activity benefits to rescind. Baseline activity was recorded as the average distance during the last 24 hours of the three-day period of wheel access.

At the end of the one-week wash-out following wheel lock, rats underwent VML surgery. Immediately post-surgery, 24 hours after surgery, and 48 hours after surgery, rats received a .1 cc subcutaneous injection of .3g/1ml buprenorphine to reduce pain-associated distress as conducted in Wu et al. (2012). Additionally, rats were also given Carprofen in the form of either Rodent MD's™ Rimadyl tablets (2mg/tablet) (Bio Serv, MD150-2) or Medigel® CPF packs (ClearH₂O, 74-05-5022) for additional pain management post-surgery. One-week post-surgery, wheels either remained locked (Cage Activity, CA) or unlocked (Wheel Activity, WA) for a

period of either one week or seven weeks. Two-weeks post-surgery, tissue harvest was conducted on 16 rats (n=8 CA, n=8 WA). Eight-weeks post-surgery, tissue harvest was conducted on 16 rats (n=8 CA, n=8 WA). Twenty-four hours before tissue harvest, wheels were locked on the WA rats in order to avoid acute variations in exercise between rats.

VML Surgery

Rats were anaesthetized by inhalation of isoflurane (2% in oxygen) during surgery. The lower left hindlimb was shaved and sterilized using three rotations of alcohol and betadine. A 1-2 cm longitudinal incision was made over the belly of the tibialis anterior (TA) cutting through the deep fascia to expose the belly of the TA. A surgical marker was used to draw a line along the length of the medial 1/3 of the TA. Next, a muscle biopsy punch (approximately 8mm x 3mm) was used to cause a defect equaling approximately 20% of the TA by weight. The weight of the defect was determined using a regression equation based on the rat's body weight as defined by Wu et al. (2012). Once the defect was removed, it was weighed and replaced in the defect site properly aligning with the line made from the surgical marker. Polypropylene sutures were used to anchor the defect to the intact TA tissue using two sutures on both the distal and proximal ends of the defect. Vicryl thread was used to suture the fascia and then the cutaneous layers together to completely close the wound.

Electrophysiology

The following protocol for electrophysiology was adopted from several sources (Conboy & Rando, 2005; Mintz et al., 2016; Kasukonis et al., 2016). Rats were anaesthetized by inhalation of isoflurane (2% in oxygen) during tissue harvest. The legs were shaved and sterilized with three rotations of betadine and alcohol wipes. The following protocol for force output measurement was conducted on both legs. A transverse incision was made on the distal,

anterior lower limb to expose the distal tendons of the TA, extensor digialis longus (EDL) and extensor hallucis longus (EHL). Tenotomy of the EDL and EHL tendons was conducted leaving the TA tendon intact and isolated. The rat was positioned so the knee was at a 90° angle, and the leg running parallel with the force platform. The ankle and pad of the foot were secured onto the platform of the electrophysiology machine using surgical tape. Two probes were inserted in the lateral border of the gastrocnemius and TA as well as the fibular head as described in Mintz et al. (2016) to adequately stimulate the peroneal nerve which innervates the TA. Once the leg and probes were secured, 100Hz at a 400ms pulse was delivered to induce adequate peak tension. Five measurements were taken with 60 seconds of rest allowed in between each measurement.

Tissue Harvest

The TA, EDL and gastrocnemius were extracted from each leg and weighed. The EDL and gastrocnemius were preserved in their entirety. The left TA (VML) had a complete transverse cut effectively dividing the defect area into two equal halves and subsequently the TA was sectioned into three parts: 1) The distal half of the TA containing half of the defect site (later used for histology), 2) the isolated defect site from the proximal TA, and 3) the remaining proximal TA tissue without the defect. The proximal half of the TA (including the proximal half of the defect) was immediately flash frozen in liquid nitrogen and stored in -80°C. The distal half of the TA (used for histology) was immediately flash frozen in liquid nitrogen-cooled isopentane the stored in -80°. The proximal, isolated defect and proximal TA was used for protein and genetic analyses. Rats were euthanized via either carbon-dioxide asphyxiation or exsanguination by removal of the heart. All collected tissue was stored in -80°C until processed for analysis.

Histology

Tissues were cut into 10 μ m sections using the Leica CM1859 cryostat (Leica Biosystems, Buffalo Grove, IL) set at -20°C. For this study, histology was utilized to observe percentage of non-contractile tissue (% NCT) and collagen deposition in the defect site and tissue peripheral to the defect site for all groups. The following portion of the methodology will describe the protocols used for Hematoxylin and Eosin (H&E) staining and Collagen I and III immunofluorescent staining.

Collagen I & III Staining

The following protocol was taken from Kim et al., 2016. Tissue immunoreactivity to collagen I & III was calculated from fluorescent microscopic images (200X) using a custom algorithm developed for publicly available image analysis software (Image J, NIH). Using the algorithm, images were converted to 8-bit gray scale, and uniformly threshold across all samples to isolate collagen type I & III positive and negative tissue regions, respectively. From these images, the software was used to determine the percentage of collagen I and III for all tissue sections. Representative tissue sections collected from five animals per group were used for all calculations. Within each section, four separate regions (2 images of the defect site and 2 images of the area peripheral to the defect site) were imaged and analyzed to calculate the average collagen type I and III percent area. A total of twenty images were analyzed for each treatment group.

qRT-PCR

RNA was extracted with Trizol reagent (Thermo Fisher Scientific, Waltham, MA, USA). Total RNA was isolated using the Purelink mRNA mini kit (Thermo Fisher Scientific, Waltham, MA, USA). Cdna was reversed transcribed from 1 μ g of total RNA using the

Superscript Vilo Cdna synthesis kit (Thermo Fisher Scientific, Waltham, MA, USA) for a final result of a 1:20 ratio of RNA to total volume. This final volume was then brought to a 1:100 dilution factor. Real-time PCR was performed, and results analyzed by using the StepOne Real-Time PCR system (Thermo Fisher Scientific, Waltham, MA, USA). Cdna was amplified in a 25 μ L reaction containing appropriate probes for MMP-1, MMP-2, MMP-9, MMP-13, Collagen I, Collagen III, TGF- β and Taqman Gene Expression Mastermix (Thermo Fisher Scientific). Samples were incubated at 95°C for 4 minutes, followed by 40 cycles of denaturation, annealing and extension at 95°C, 55°C and 72°C, respectively. TaqMan fluorescence was measured at the end of the extension step of each cycle. Cycle Threshold (Ct) was determined, and the Δ Ct value was calculated as the difference between the Ct value and the 18s Ct value. Final quantification of gene expression was calculated using the $\Delta\Delta$ Ct method $Ct = [\Delta Ct(\text{calibrator}) - \Delta Ct(\text{sample})]$. Relative quantification was calculated as $2^{-\Delta\Delta Ct}$.

Statistical Analysis

All data was analyzed using Statistical Package for the Social Sciences (SPSS version 22.0, Armonk, NY). Results were reported as mean \pm SEM. A two-way ANOVA was performed to analyze main effects of physical activity and injury and if there were any interactions between the dependent variables. When a significant interaction was detected, differences among individual means were assessed using Tukey's post-hoc analysis. Student's t-test was used to confirm statistical differences of PCR targets between control groups when comparing the 2-week and 8-week time points. Student's t-test was also used for PCR targets when the control groups did not express those targets. Statistical significance was set at $p \leq 0.05$.

RESULTS

Collagen I and III Immunofluorescence

There was no significant difference in the percentage of area containing collagen I in the tissue peripheral to the defect area (Figure 1A). There were main effects of time and wheel access to increase the percentage of collagen III in the tissue peripheral to the defect site ($p < 0.05$) (Figure 1B). Similarly, there were main effects of time and wheel access to increase the collagen III/I ratio in the tissue peripheral to the defect site ($p < 0.05$) (Figure 1C). There were no significant differences between groups of the percentage of collagen I, collagen III or the collagen III/I ratio in the RTA (Figures 1G-I).

There was an interaction of wheel access and time to decrease the percentage of collagen I in the defect tissue in the exercise group at 8 weeks ($p < 0.05$). The percentage of area of collagen I in the defect area of the 8-week WA group was ~33% of the percentage of collagen observed in the defect tissue in either the 2-week WA or 8-week CA groups ($p < 0.05$) (Figure 1D). Similarly, there was an interaction of wheel access and time to decrease the percentage of collagen III in the defect tissue in the exercise group at 8 weeks ($p < 0.05$). The percentage of area of collagen III in the defect area of the 8-week WA group was ~75% of the 2-week WA and ~60% of the 8-week CA groups ($p < 0.05$) (Figure 1E). There was an interaction of wheel access and time to alter the Collagen III/I ratio. The collagen III/I ratio was ~2-fold higher in the 2-week WA vs the 2-week CA group ($p < 0.05$) (Figure 1F). At 8 weeks, the collagen III/I in the WA group was 40% of the III/I ratio of the 2-week WA group ($p < 0.05$) and was not significantly different from the 8-week CA group (Figure 1F).

Non-Contractile Tissue Percentage

There was a main effect of time to decrease the percentage of non-contractile tissue in the LTA from ~40% to ~27% ($p < 0.05$) (Figure 1A). There were no significant differences in %NCT in the RTA (Figure 2B).

Gene Expression of Collagen I and III, TGF- β

There was a main effect of VML to increase mRNA abundance of Collagen I at both 2 and 8 weeks post-injury ($p < 0.05$). Gene expression of Collagen I was ~2-fold higher in the 2-week control group vs the 8-week control group ($p < 0.05$). There was a main effect of VML to increase Collagen III at 2 weeks post-injury ($p < 0.05$). There was an interaction of VML and wheel access on the gene expression of Collagen III. In the sedentary group, gene expression of Collagen III was ~9-fold higher in the VML limb vs the control limb ($p < 0.05$). In the wheel access group, gene expression of Collagen III was ~9-fold higher in the VML limb vs the control limb ($p < 0.05$). In the control limbs, gene expression of Collagen III was 2-fold higher in the sedentary group vs the wheel access group ($p < 0.05$). In the VML limbs, gene expression of Collagen III was ~2-fold higher in the sedentary group vs the wheel access group ($p < 0.05$). There were no differences in the gene expression of Collagen III between the 2-week and 8-week control groups.

There was an interaction of VML and wheel access on the gene expression of TGF β at 2 weeks post-injury. In the sedentary group, gene expression of TGF β was 13-fold higher in the VML limb vs the control limb ($p < 0.05$). In the wheel access group, gene expression of TGF β was 7-fold higher in the VML limb vs the control limb ($p < 0.05$). Though no differences were detected between the control limbs, gene expression of TGF β was ~2-fold higher in the VML limb of the sedentary group vs the VML limb of the wheel access group ($p < 0.05$). There was an

interaction of VML and wheel access on the gene expression of TGF β at 8 weeks post-injury. Though no differences were detected within the sedentary group, gene expression of TGF β was ~4-fold higher in the VML limb vs the control limb of the wheel access group ($p < 0.05$). No differences were detected between the control groups but gene expression of TGF β was ~3.8-fold higher in the VML limb of the wheel access group vs the VML limb of the sedentary limb ($p < 0.05$). Gene expression of TGF β was 27% higher in the 8-week control group vs the 2-week control group.

MMP mRNA Abundance

MMP-1 mRNA abundance was not attainable due to insufficient expression. At 2 weeks post-surgery, there was a main effect of VML to increase MMP-2 by ~16-fold ($p < 0.05$) (Figure 4A). At 8 weeks post-surgery, there was an interaction of VML and wheel access on MMP-2. Though there were no differences in MMP-2 between the RTA and LTA defect tissue in the sedentary group, MMP-2 was ~2.5-fold higher in the LTA defect tissue vs the RTA of the wheel access group ($p < 0.05$) (Figure 4B). Similarly, at 8 weeks, MMP-2 was ~2.5-fold higher in the defect tissue of the WA group than the defect tissue of the CA group ($p < 0.05$) (Figure 4B). MMP-2 mRNA abundance was 2-fold higher in the 8-week control limb compared to the 2-week control limb ($p < 0.05$) (Figure 4C). At 2 weeks post-surgery, MMP-9 mRNA abundance within the defect site of the WA group was ~20% of MMP-9 in the defect site of the CA group ($p < 0.05$) (Figure 4D). At 8 weeks post-surgery, MMP-9 mRNA abundance within the defect site of the WA group was ~12-fold higher compared to the CA group ($p < 0.05$) (Figure 4E). For mRNA abundance of MMP-13, there were no significant differences between groups at either 2 weeks or 8 weeks post-surgery (Figures 4F and 4G).

DISCUSSION

This is the first study to measure fibrosis and ECM-related factors in a VML model using both physical activity and autologous repair and observing these factors at both an early and late time point (2 weeks and 8 weeks post-surgery, respectively). Though the percent area of non-contractile tissue was not different between groups at either time point, significant changes were observed in collagen deposition and key markers of ECM remodeling. These changes express patterns coinciding with the observations made with force measurements implying that ECM remodeling may have direct implications on force recovery from VML injury.

Collagen deposition is commonly used a marker of tissue fibrosis, but the absolute amount and ratio of the two primary collagens of muscle tissue, 1 and 3, grants insight to the functional role of the fibrosis. Following injury, the collagen III/I should decrease to normal but then is followed by an increase in this ratio as the repair process continues (Karalaki et al., 2009). This pattern was not observed in the LTA tissue peripheral to the defect site in either the sedentary or wheel-trained groups. Furthermore, an opposite pattern was observed with the wheel-trained group which may partially explain the stagnation in force recovery. Due to the limitations of this study, it is unclear if this pattern is expressed throughout the entire muscle or only in the tissue adjacent to the defect area; nevertheless, dysregulation of ECM remodeling, whether in the sedentary or wheel-trained groups, could implicate a root cause to dysfunction force recovery in a VML model using autologous repair.

Using a PCR array in a porcine model of VML, Corona et al. (2017) showed that the expression of numerous ECM-related genes was upregulated at 4 weeks post-VML surgery versus the sham-operated comparison. Specifically, collagen (1A1, 1A2, 3A1, 5A2, 5A3), MMP (2, 3, 9) and TGF- β (1, 2, 3, R3) were all significantly upregulated at 4 weeks; however,

expression of these genes was back to control levels at the 16-week time point. Markers of ECM and fibrosis are upregulated following VML; however, interventions to reduce the expression of these markers have also been associated with further reduction in force output rather than advantageous changes (Garg et al., 2014). The authors of the study concluded that a certain level of collagen deposition/fibrosis is needed for proper force transmission in the muscle. This theory is further supported by similar findings in Aurora et al. (2014).

In a rat model for crush injury, anti-MMP-9 and anti-MMP-2 antibodies were used to observe the effects on satellite activation and subsequent muscle regeneration (Zimowska et al., 2012). Though the anti-MMP-2 antibody had no effect, the anti-MMP-9 antibody ameliorated fibrosis and improved muscle regeneration in the soleus muscle. In our study, the lower expression of MMP-9 in the wheel training group at 2 weeks, coupled with the higher expression of MMP-9 in the same group at 8 weeks post-injury, implies a direct correlation of ECM remodeling to muscle force in the injured limbs. The upstream regulator of MMP-9, TGF- β , presents similar patterns and may contain contrasting implications. Gumucio et al. (2015) showed that following eccentric-based muscle damage, inhibiting TGF- β caused rapid, early onset strength improvements; however, observation at a later time point revealed incomplete muscle regeneration and resulting deficits in strength. Furthermore, overexpression of TGF- β has been shown to decrease muscle function (Kim et al., 2017). Thus, the inhibition of TGF- β and MMP-9 at the early time point in the wheel training group may result in rapid force recovery, but the high expression of both markers at the late time point may play a role in stagnating force recovery. Coincidentally, both of these markers, both of these markers have a lower expression in the sedentary group at 8 weeks post-injury, and force recovery in this group improved significantly from the 2-week to 8-week time point.

This study analyzed fibrosis and ECM-related markers in a VML model incorporating wheel activity and autologous repair. While the percentage of non-contractile tissue in the LTA did not differ between the sedentary and wheel-trained groups, wheel training did affect collagen deposition and certain ECM-related markers. TGF- β is a key upstream regulator of collagen deposition and MMP regulation. In this study, there was a correlation between TGF- β expression and MMP-9 mRNA abundance and the collagen 3/1 ratio in the unaffected LTA tissue suggesting that TGF- β modulation to be an important factor in regulating ECM remodeling with wheel training.

Figure Legend

Figure 1 Immunofluorescent analysis of Collagen 1 and Collagen 3 Staining. A) Percent area containing collagen 1 in LTA tissue peripheral to defect site. B) Percent area containing collagen 3 in LTA tissue peripheral to defect site. C) Collagen 3/1 ratio in LTA tissue peripheral to defect site. D) Percent area containing collagen 1 in LTA defect site. E) Percent area containing collagen 3 in LTA to defect site. F) Collagen 3/1 ratio in LTA defect site. G) Percent area containing collagen 1 in RTA H) Percent area containing collagen 3 in RTA. I) Collagen 3/1 ratio in RTA. J) 10x Representative immunofluorescence stacked images of collagen 3 and collagen 1. ME = Main Effect. † indicates significant difference from 2-week counterpart. ‡ indicates significant difference from group within same time point. Significance was set at $p < 0.05$.

Figure 2 Percent area containing non-contractile tissue. A) Percent area of non-contractile tissue of the LTA. B) Percent area of non-contractile tissue of the RTA. C) 10x representative H&E images of the LTA from the 1) 2 week CA group 2) 2 week WA group 3) 8 week CA group and 4) 8 week WA group. ME = Main Effect. Significance was set at $p < 0.05$.

Figure 3 mRNA abundance of TGF β , Collagen 1 and Collagen 3. A) mRNA abundance of TGF- β at 2 weeks. B) mRNA abundance of TGF- β at 8 weeks. C) Time point comparison of TGF- β MRNA abundance. D) MRNA abundance of collagen 1 at 2 weeks. E) mRNA abundance of collagen 1 at 8 weeks. F) Time point comparison of collagen 1 MRNA abundance. G) mRNA abundance of collagen 3 at 2 weeks. H) mRNA abundance of collagen 3 at 8 weeks. I) Time point comparison of collagen 3 MRNA abundance. ME = Main Effect. † indicates significant difference from sedentary counterpart. ‡ indicates significant difference from group within same time point. * indicates significant difference from 2-week counterpart. Significance was set at $p < 0.05$.

Figure 4 mRNA abundance of MMPs. A) mRNA abundance of MMP-2 at 2 weeks. B) mRNA abundance of MMP-2 at 8 weeks. C) Time point comparison of MMP-2 mRNA abundance. D) mRNA abundance of MMP-9 at 2 weeks. E) mRNA abundance of MMP-9 at 8 weeks. F) mRNA abundance of MMP-13 at 2 weeks. G) mRNA abundance of MMP-13 at 8 weeks. DNE = Did Not Express. ME = Main Effect. † indicates significant difference from sedentary counterpart. ‡ indicates significant difference from group within same time point. * indicates significant difference between groups.. Significance was set at $p < 0.05$.

Figure 1

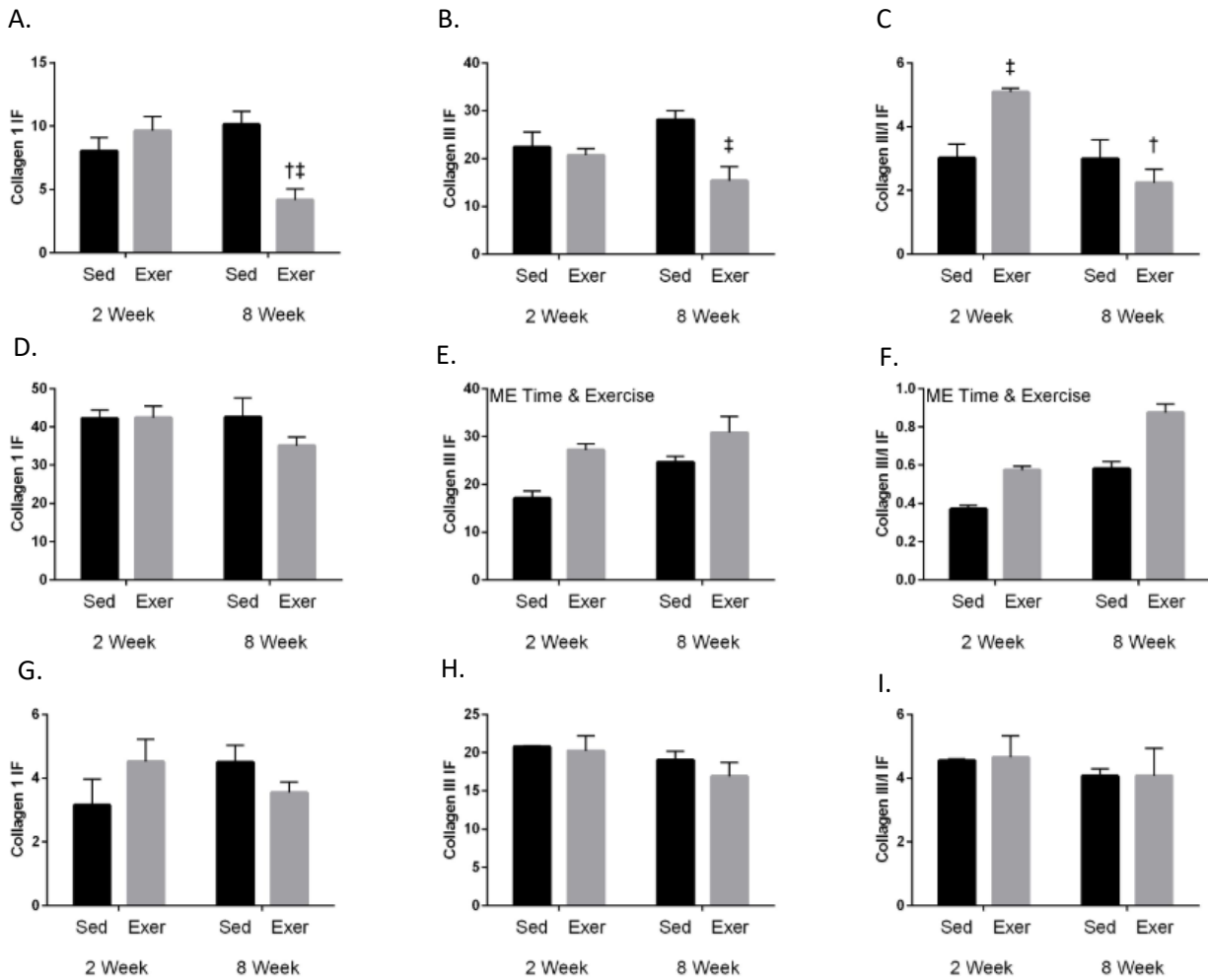


Figure 2

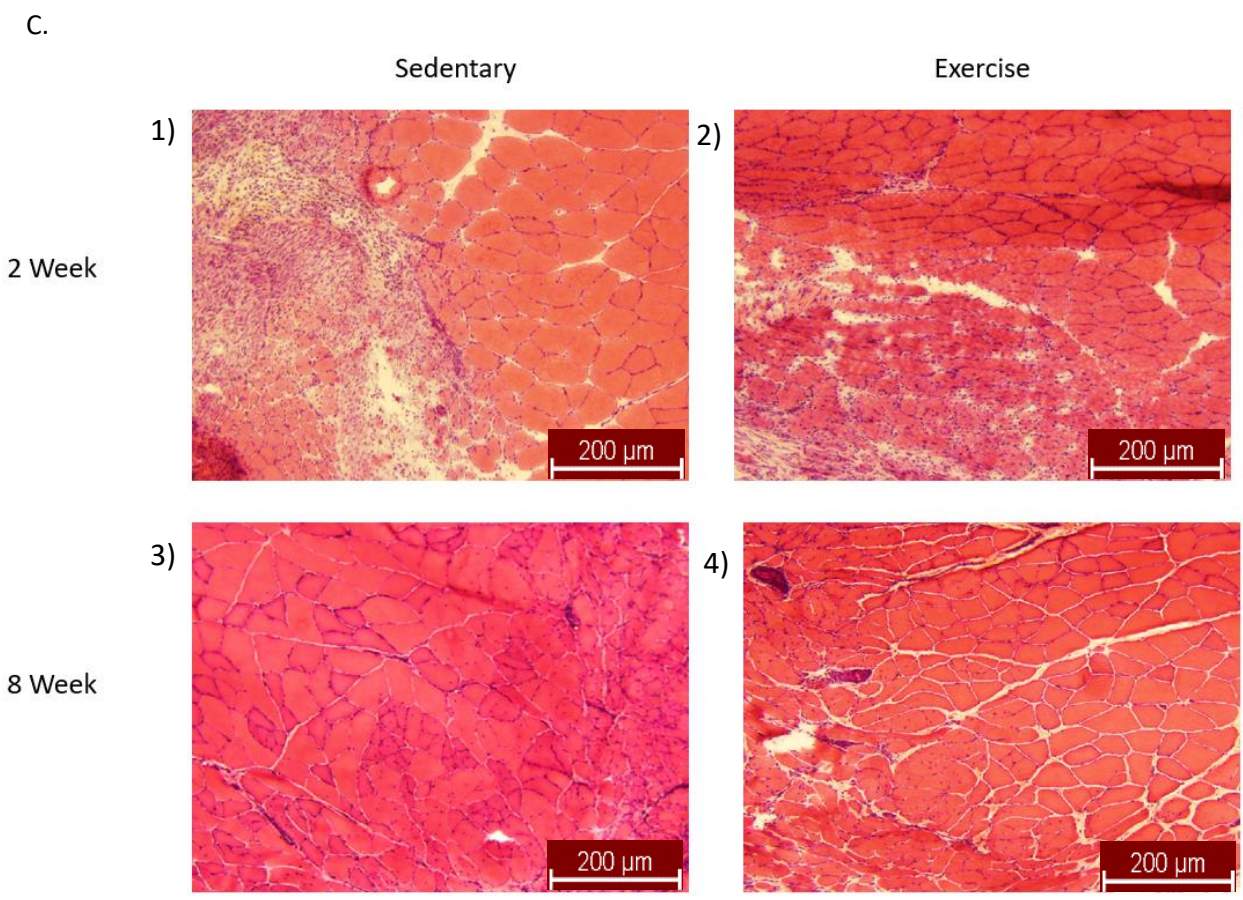
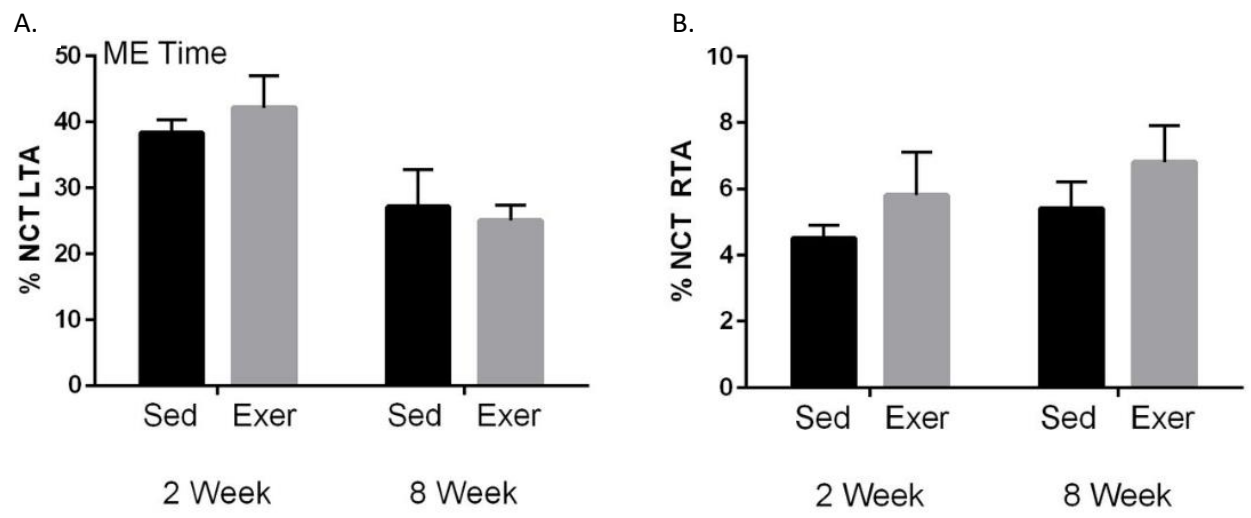


Figure 3

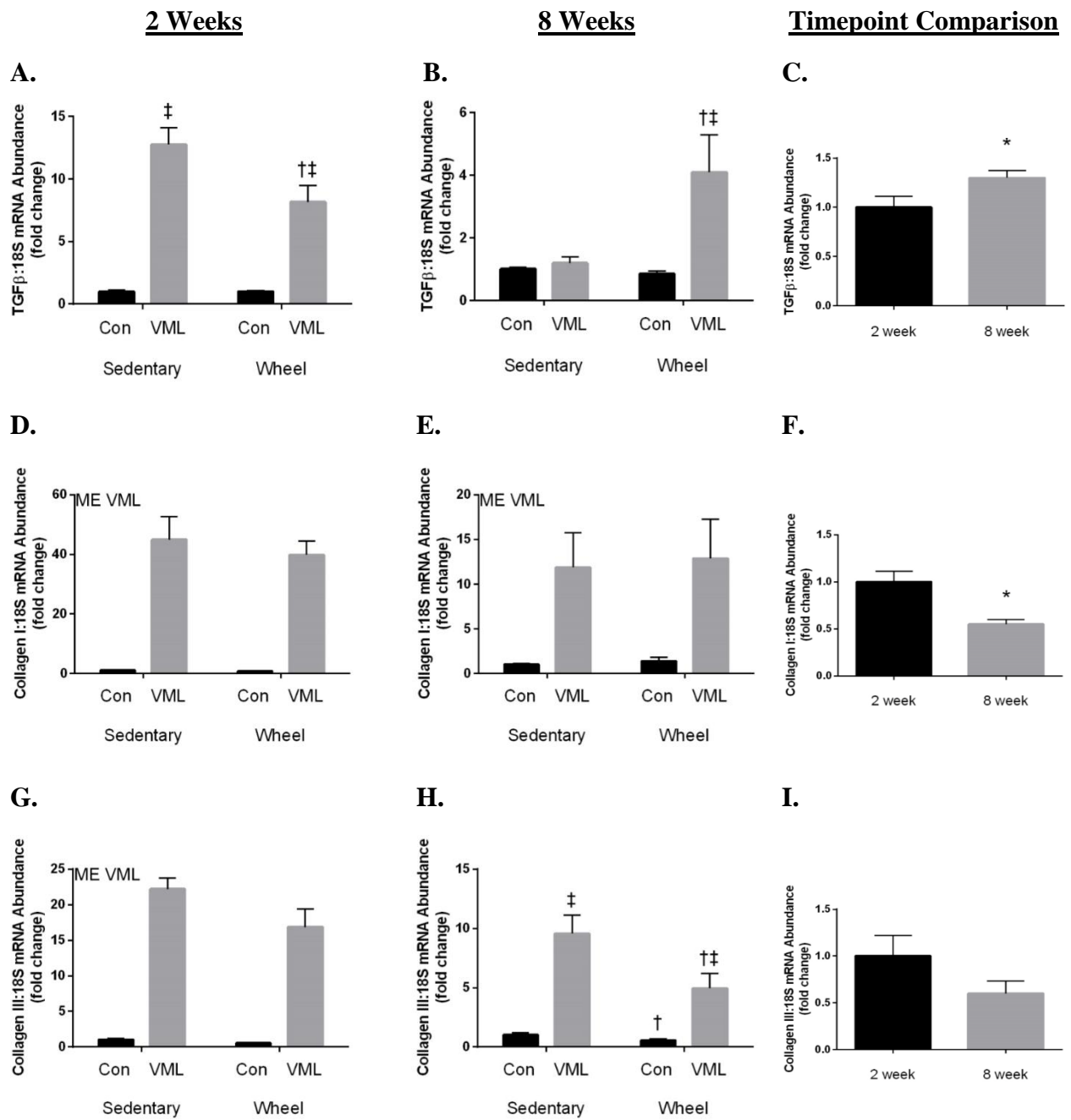
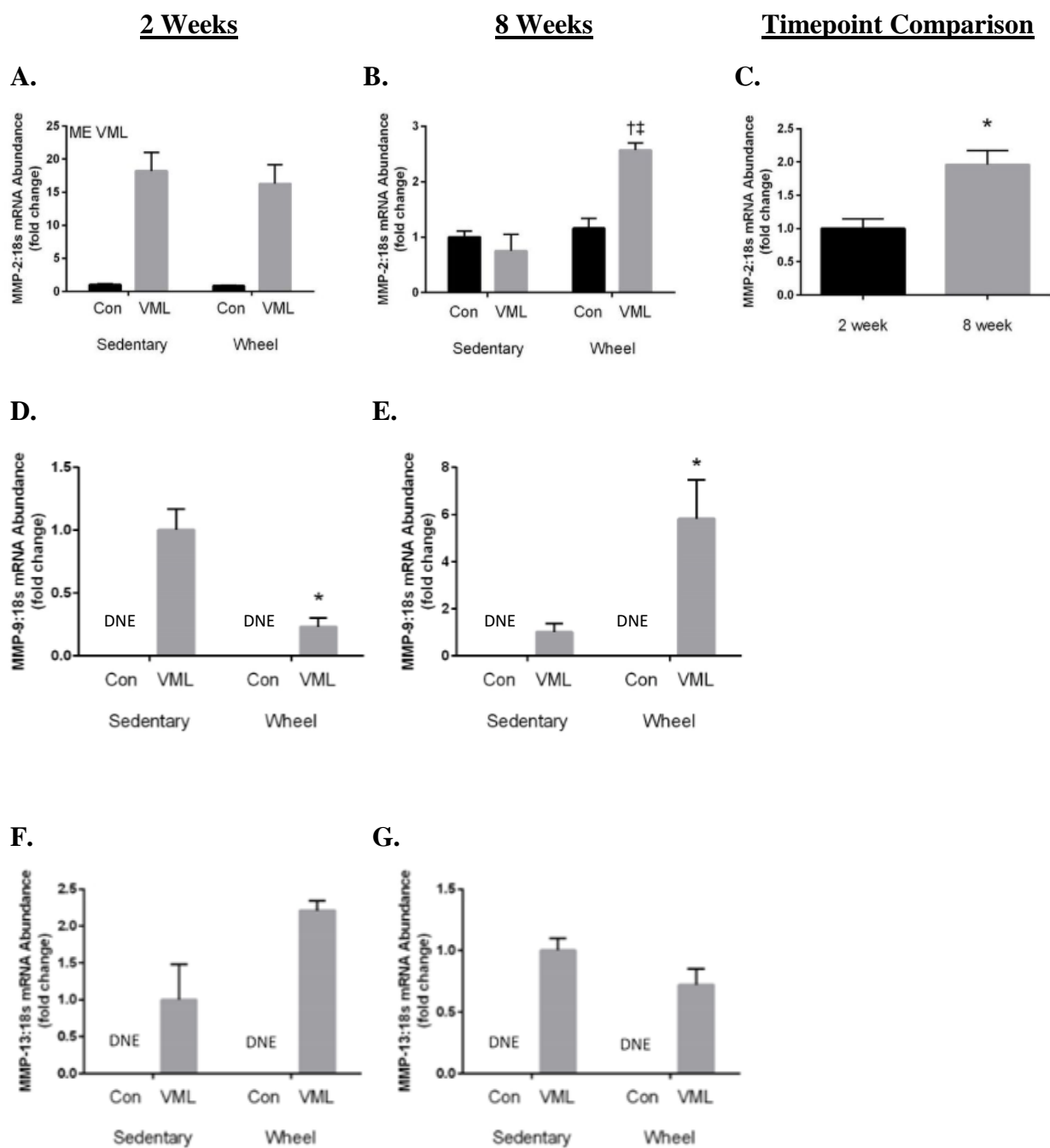


Figure 4



CHAPTER FIVE

AIM 3: VML and Inflammatory Response

ABSTRACT

When damaged, skeletal muscle requires a coordinated response of satellite cell activation and inflammatory response to achieve proper muscle regeneration. Volumetric muscle loss injuries are defined as the loss of tissue with resultant permanent loss of force. A key factor that limits these injuries from complete recovery is the prolonged inflammatory response that limits proper satellite cell activation and also contributes to dysregulated fibrosis. Recent studies have shown benefits to muscle regeneration with the incorporation of physical activity, but little is known about the effect on the inflammatory response. **PURPOSE** Measure the effects of physical activity in a VML model on gene expression of inflammatory cytokines and macrophage markers. **METHODS** 32 male Sprague-Dawley rats had 20% of their LTA removed then replaced to act as autologous repair. Half of the rats utilized wheel running, and at 2 and 8 weeks, the autologous tissue was excised from the LTA from both wheel running and sedentary rats. qRT-PCR was used to measure gene expression of inflammatory cytokines and markers for macrophages. **RESULTS** Wheel running attenuated IL-1 β and TNF α at 2 weeks in the defect tissue but resulted in high expression of IFN γ . At 8 weeks, IL-6, CD68 and iNOS expression was elevated in the wheel running group. At 8 weeks the sedentary group had high expression of IFN γ and Arginase-1 but lower expression of iNOS. **DISCUSSION** Wheel running attenuated pro-inflammatory markers at 2 weeks but showed evidence of an anti-inflammatory environment at 8 weeks post-injury. In comparison, the sedentary group showed evidence of a delayed pro-inflammatory shift from the 2 to 8-week time points. In summary, wheel training promotes an anti-inflammatory environment early on but fails to restrict a pro-inflammatory environment thus

partially allowing for force recovery early but without continual progress after the 2 week time point.

INTRODUCTION

When damaged, skeletal muscle relies on intricately-timed response from the innate immune system in order to undergo effective muscle regeneration. Initially, damaged tissue will release chemo- and cytokines that recruit neutrophils. In turn, neutrophils recruit monocytes that differentiate into macrophages upon entering the tissue. This pro-inflammatory stage is characterized by traditional pro-inflammatory cytokines (TNF α , IL-6, IL-1 β) and the M1 macrophage subtype (Tecchio et al., 2014). The pro-inflammatory stage is beneficial for clearing necrotic tissue, regulating fibrosis and promoting satellite cell activation. Succeeding this phase is the anti-inflammatory environment characterized by anti-inflammatory cytokines (IL-10, TGF β) and the M2 macrophage subtype (Duque and Descoteaux, 2014). The M1 and M2 macrophages are traditionally identified by iNOS and Arginase, respectively. Clearing of this traditional inflammatory response often leads to proper muscle regeneration.

VML studies have consistently observed a chronic, dysregulated inflammatory response in the defect site undergoing muscle regeneration (Corona, Rivera & Greising, 2018, Larouche et al., 2018). This non-traditional response is viewed as a key factor to overcoming inefficient muscle regeneration and subsequent force loss with VML injuries. Consistent observations have been made of a conserved pro-inflammatory response that persist weeks after the initial injury even when a repair strategy has been utilized (Hurtgen et al., 2016, Greising et al., 2017). An asynchronous inflammatory response that contains both pro- and anti-inflammatory factors (cytokines and macrophages from each subset) has also been reported (Garg et al., 2014). Though satellite cell migration into the defect area is limited, immune cell migration is

unhindered; however, these cells are not as active as cells observed in normal, mild muscle damage (Garg et al., 2014). These disjointed reactions result in insufficient signaling for satellite cell activation and muscle regeneration in addition to the unregulated activity of fibroblasts leading to excessive fibrosis.

Exercise, in the case of chronic diseases, has been shown to have advantageous effects in regulating chronic inflammation (Petersen et al., 2005). Though VML is not a progressive disease, recent VML studies using light physical activity (wheel running) have shown promising results in improving repair of the defect area (Aurora et al., 2014; Quarta et al., 2017). Physical activity in a VML model has been shown to promote muscle regeneration in the form of larger CSA, result in more mature NMJs, and reduce fibrosis (Quarta et al., 2017). However, the incorporation and understanding of physical activity in a VML model is still limited. The effect of physical activity on the inflammatory response in a VML model is still not well understood. The purpose of this study is to observe the effects of autologous repair and physical activity (wheel running) on gene expression of macrophage subtypes and pro- and anti-inflammatory cytokines.

METHODS

Animal Care and Use

Animals

All animal care and use within this protocol was approved by the University of Arkansas Institution of Animal Care and Use Committee (protocol #17075) (see Appendix). Male, Sprague-Dawley rats (3-4 months old) were used for this study. Rats were allowed *ad libitum* access to normal chow and water throughout the duration of the study. Rats were individually

caged and kept in a climate-controlled room with automatic 12-12h light/dark cycle. Once rats reached the desired weight of 300g, running wheels were unlocked, and rats were allowed *ad libitum* wheel access for 72 hours to assess baseline running distance. At the conclusion of the 72 hours of wheel access, wheels were locked, and at least seven days were allowed between this time and VML surgery to allow for any activity benefits to rescind. Baseline activity was recorded as the average distance during the last 24 hours of the three-day period of wheel access.

At the end of the one-week wash-out following wheel lock, rats underwent VML surgery. Immediately post-surgery, 24 hours after surgery, and 48 hours after surgery, rats received a .1 cc subcutaneous injection of .3g/1mL buprenorphine to reduce pain-associated distress as conducted in Wu et al. (2012). Additionally, rats were also given Carprofen in the form of either Rodent MD's™ Rimadyl tablets (2mg/tablet) (Bio Serv, MD150-2) or Medigel® CPF packs (ClearH₂O, 74-05-5022) for additional pain management post-surgery. One-week post-surgery, wheels either remained locked (Cage Activity, CA) or unlocked (Wheel Activity, WA) for a period of either one week or seven weeks. Two-weeks post-surgery, tissue harvest was conducted on 16 rats (n=8 CA, n=8 WA). Eight-weeks post-surgery, tissue harvest was conducted on 16 rats (n=8 CA, n=8 WA). Twenty-four hours before tissue harvest, wheels were locked on the WA rats in order to avoid acute variations in exercise between rats.

VML Surgery

Rats were anaesthetized by inhalation of isoflurane (2% in oxygen) during surgery. The lower left hindlimb was shaved and sterilized using three rotations of alcohol and betadine. A 1-2 cm longitudinal incision was made over the belly of the tibialis anterior (TA) cutting through the deep fascia to expose the belly of the TA. A surgical marker was used to draw a line along the length of the medial 1/3 of the TA. Next, a muscle biopsy punch (approximately 8mm x 3mm)

was used to cause a defect equaling approximately 20% of the TA by weight. The weight of the defect was determined using a regression equation based on the rat's body weight as defined by Wu et al. (2012). Once the defect was removed, it was weighed and replaced in the defect site properly aligning with the line made from the surgical marker. Polypropylene sutures were used to anchor the defect to the intact TA tissue using two sutures on both the distal and proximal ends of the defect. Vicryl thread was used to suture the fascia and then the cutaneous layers together to completely close the wound.

Tissue Harvest

The TA, EDL and gastrocnemius were extracted from each leg and weighed. The EDL and gastrocnemius were preserved in their entirety. The left TA (VML) had a complete transverse cut effectively dividing the defect area into two equal halves and subsequently the TA was sectioned into three parts: 1) The distal half of the TA containing half of the defect site (later used for histology), 2) the isolated defect site from the proximal TA, and 3) the remaining proximal TA tissue without the defect. The proximal half of the TA (including the proximal half of the defect) was immediately flash frozen in liquid nitrogen and stored in -80°C . The distal half of the TA (used for histology) was immediately flash frozen in liquid nitrogen-cooled isopentane and stored in -80° . The proximal, isolated defect and proximal TA was used for protein and genetic analyses. Rats were euthanized via either carbon-dioxide asphyxiation or exsanguination by removal of the heart. All collected tissue was stored in -80°C until processed for analysis.

qRT-PCR

RNA was extracted with Trizol reagent (Thermo Fisher Scientific, Waltham, MA, USA). Total RNA was isolated using the Purelink mRNA mini kit (Thermo Fisher Scientific, Waltham, MA, USA). cDNA was reverse transcribed from 1 μg of total RNA using the

Superscript Vilo cDNA synthesis kit (Thermo Fisher Scientific, Waltham, MA, USA) for a final result of a 1:20 ratio of RNA to total volume. This final volume was then brought to a 1:100 dilution factor. Real-time PCR was performed, and results analyzed by using the StepOne Real-Time PCR system (Thermo Fisher Scientific, Waltham, MA, USA). cDNA was amplified in a 25 μ L reaction containing appropriate probes for CD68, Arginase-1, iNOS-1, IL-10, TNF- α , IFN γ , IL-1 β , IL-6 and Taqman Gene Expression Mastermix (Thermo Fisher Scientific). Samples were incubated at 95°C for 4 minutes, followed by 40 cycles of denaturation, annealing and extension at 95°C, 55°C and 72°C, respectively. TaqMan fluorescence was measured at the end of the extension step of each cycle. Cycle Threshold (Ct) was determined, and the Δ Ct value was calculated as the difference between the Ct value and the 18s Ct value. Final quantification of gene expression was calculated using the $\Delta\Delta$ Ct method $Ct = [\Delta Ct(\text{calibrator}) - \Delta Ct(\text{sample})]$. Relative quantification was calculated as $2^{-\Delta\Delta Ct}$.

Statistical Analysis

All data was analyzed using Statistical Package for the Social Sciences (SPSS version 22.0, Armonk, NY). Results were reported as mean \pm SEM. A two-way ANOVA was performed to analyze main effects of physical activity and injury and if there were any interactions between the dependent variables. When a significant interaction was detected, differences among individual means were assessed using Tukey's post-hoc analysis. Statistical significance was set at $p \leq 0.05$.

RESULTS

There was a main effect of VML to increase mRNA abundance of CD68 at 2 weeks post-injury ($p < 0.05$) (Figure 1A). At 8 weeks, there was an interaction of VML and wheel access on the gene expression of CD68. Though no differences were detected within the sedentary group,

CD68 gene expression was ~3.5-fold higher in the VML limb vs the control limb of the wheel access group ($p < 0.05$) (Figure 1B). While the control limbs of the sedentary and wheel access groups were not significantly different, gene expression of CD68 was ~2.2-fold higher in the VML limb of the wheel access group vs the VML limb of the sedentary group ($p < 0.05$). There were no differences in the gene expression of CD68 between the 2-week and 8-week control groups (Figure 1C).

There was a main effect of VML to increase mRNA abundance of Arginase-1 at 2 weeks post-injury ($p < 0.05$) (Figure 1D). At 8 weeks, there was an interaction of VML and wheel access on the gene expression of Arginase-1. Though no differences were detected within the wheel access group, Arginase-1 gene expression was ~4-fold higher in the VML limb vs the control limb of the sedentary group ($p < 0.05$) (Figure 1E). While the control limbs of the sedentary and wheel access groups were not significantly different, gene expression of Arginase-1 was ~4-fold higher in the VML limb of the sedentary group vs the VML limb of the wheel access group ($p < 0.05$) (Figure 1E). There were no differences in the gene expression of Arginase-1 between the 2-week and 8-week control groups (Figure 1F).

At 2 weeks, there was main effect of VML to increase the mRNA abundance of iNOS-1 by ~17-fold ($p < 0.05$) (Figure 1G). At 8 weeks, there was an interaction of injury and wheel activity to alter the mRNA abundance of iNOS-1. In the CA group, iNOS-1 expression in the LTA was 57% of the RTA ($p < 0.05$) (Figure 1H). In the WA group, iNOS-1 expression was 2-fold higher in the LTA compared to the RTA ($p < 0.05$) (Figure 1H). Furthermore, iNOS-1 expression in the WA LTA was ~4-fold higher compared to the CA LTA ($p < 0.05$) (Figure 1H). There were no significant differences in iNOS-1 expression of the control samples between the 2 week and 8 week time points (Figure 1I).

At 2 weeks, there was an interaction of VML and wheel access on the gene expression of IL-1 β . Though no differences were detected within the wheel access group, IL-1 β gene expression was ~4-fold higher in the VML limb vs the control limb of the sedentary group ($p < 0.05$) (Figure 2A). While the control limbs of the sedentary and wheel access groups were not significantly different, gene expression of IL-1 β was ~1.5-fold higher in the VML limb of the sedentary group vs the VML limb of the wheel access group ($p < 0.05$) (Figure 1A). Differences in the gene expression of IL-1 β were not detected at the 8-week time point (Figure 1B). There were no differences in the gene expression of IL-1 β between the 2-week and 8-week control groups (Figure 1C).

At 2 weeks, there was an interaction of VML and wheel access on the gene expression of TNF α . Though no differences were detected within the wheel access group, TNF α gene expression was ~4-fold higher in the VML limb vs the control limb of the sedentary group ($p < 0.05$) (Figure 2D). While the control limbs of the sedentary and wheel access groups were not significantly different, gene expression of TNF α was ~4-fold higher in the VML limb of the sedentary group vs the VML limb of the wheel access group ($p < 0.05$) (Figure 2D). Differences in the gene expression of TNF α were not detected at the 8-week time point (Figure 2E). There were no differences in the gene expression of TNF α between the 2-week and 8-week control groups (Figure 2F).

There was a main effect of VML to increase mRNA abundance of IL-6 at 2 weeks post-injury ($p < 0.05$) (Figure 2G). At 8 weeks, there was an interaction of VML and wheel access on the gene expression of IL-6. Though no differences were detected within the sedentary group, IL-6 gene expression was ~2-fold higher in the VML limb vs the control limb of the wheel access group ($p < 0.05$) (Figure 2H). Differences were not detected between the control limbs or

VML limbs of the sedentary and wheel access groups. Gene expression of IL-6 was ~2-fold higher in the 8-week control group vs the 2-week control group ($p < 0.05$) (Figure 2I).

At 2 weeks there was a main effect of VML to increase mRNA abundance of IL-10 by ~2-fold ($p < 0.05$) (Figure 2J). At 8 weeks, IL-10 expression was 3-fold higher in the LTA of the WA group compared to the LTA of the CA group ($p < 0.05$) (Figure 2K).

At 2 weeks there was a main effect of VML to increase mRNA abundance of IFN γ by ~70-fold ($p < 0.05$) (Figure 2L). At 8 weeks, there was an interaction of injury and wheel activity to alter gene expression of IFN γ . In the CA group, IFN γ expression was 9-fold higher in the LTA vs the RTA ($p < 0.05$) (Figure 2M). In the WA group, IFN γ gene expression was not different between the LTA and RTA. Gene expression of IFN γ was ~3-fold higher in the CA LTA vs the WA RTA ($p < 0.05$) (Figure 2M). Time point comparison revealed a 7-fold increase of IFN γ at 9 weeks compared to the 2-week time point ($p < 0.05$) (Figure 2N).

DISCUSSION

This study supports signs of a non-traditional inflammatory response to both autologous repair and autologous repair with wheel training in VML. Several VML studies have shown irregular responses in both macrophage recruitment and pro- and anti-inflammatory cytokines, but this is the first study to observe changes at an early and late time point (2 weeks and 8 weeks, respectively) with the addition of wheel activity plus autologous repair. Of note, PCR data suggests an inverse timeline of the pro-inflammatory and anti-inflammatory responses dependent upon the addition of wheel activity: At 2 weeks, wheel activity seems to attenuate the pro-inflammatory response observed in the sedentary group; however, at 8 weeks the wheel activity shows suggestive data of a higher pro-inflammatory environment compared to the wheel activity group.

VML is a severe injury, and these types of injuries have been reported to have chronic inflammatory conditions (Corona, Rivera, Griesing, 2018). Chronic inflammation has been shown to reduce proper muscle regeneration and even induce muscle loss (Perandini et al., 2018). Access to wheel training appeared to attenuate the pro-inflammatory response at 2 weeks post-surgery as indicated by a reduction in pro-inflammatory cytokines such as TNF α and IL-1 β , and these early modifications to the inflammatory response may partially explain the early progress of force recovery in the wheel activity group.

However, our data seem to support an asynchronous immune response as has also been previously observed in VML models (Garg et al., 2014). Cytokines share a complex feedback response with macrophages as cytokines can induce macrophage recruitment and also be secreted by macrophages (Cavaillon, 1994). Regardless, certain pro-inflammatory cytokines, such as IFN γ , are associated with M1 macrophage recruitment and activity (Martinez et al., 2008). Therefore, IFN γ expression should coincide with reduced expression of Arginase-1 (traditional M2 marker) and high expression of iNOS-1 (traditional M1 marker). However, at 8 weeks, the sedentary LTA defect tissue expresses high levels of both IFN γ and Arginase-1 while simultaneously expressing low levels of iNOS-1. This asynchronous response may be explained when considering another prominent cell that secretes IFN γ , T-regulatory cells, which have shown to have an important role of the adaptive immune system in muscle regeneration (Shiaffino et al., 2017). Specifically, these cells have been observed to positively benefit muscle regeneration (Deyhle et al., 2018). T-regulatory cells have also been shown to induce the M1-M2 transition during muscle regeneration, and IFN γ secretion from these cells has been shown to promote the regenerative process as well as limit fibrosis (Cheng et al., 2008). Considering these markers for M1/M2 macrophages and IFN γ , it is possible that the sedentary group undergoes a

delayed pro-inflammatory to anti-inflammatory shift which may account for the delayed force recovery with autologous repair.

In conclusion, autologous repair alone appears to delay the inflammatory shift as evidenced by early high expression of pro-inflammatory cytokines coupled with the reduction of these cytokines plus an apparent M1 to M2 transition at the 8-week time point. Simultaneously, wheel activity attenuates the pro-inflammatory response early but appears susceptible to a pro-inflammatory environment at the late time point as evidenced by high expression of iNOS-1 and IL-6 8 weeks post-surgery. This reverse shift between groups may partially explain why force recovery in the LTA of the wheel activity group is significant early on but appears to plateau by 8 weeks. Contrast to the wheel activity group, the delayed pro- to ant-inflammatory shift in the sedentary group may account for why force recovery is not evident at the early time point but is then similar to the wheel activity group by 8 weeks. Future studies should incorporate an intervention to help continue attenuate the pro-inflammatory response in the wheel activity group. Also, future VML studies should consider the importance of the adaptive immune system in addition to the innate.

Figure Legend

Figure 1 Macrophage Markers. A) mRNA abundance of CD68 at 2 weeks. B) mRNA abundance of CD68 at 8 weeks. C) Time point comparison of CD68 mRNA abundance. D) mRNA abundance of Arginase-1 at 2 weeks. E) mRNA abundance of Arginase-1 at 8 weeks. F) Time point comparison of Arginase-1 mRNA abundance. G) mRNA abundance of iNOS-1 at 2 weeks. H) mRNA abundance of iNOS-1 at 8 weeks. I) Time point comparison of iNOS-1 mRNA abundance. ME = Main Effect. † indicates significant difference between RTA and LTA of same group. ‡ indicates significant difference from same limb of opposing group. * indicates significant difference between groups. Significance was set at $p < 0.05$.

Figure 2 Inflammatory Cytokines. A) mRNA abundance of IL-1 β at 2 weeks. B) mRNA abundance of IL-1 β at 8 weeks. C) Time point comparison of IL-1 β mRNA abundance. D) mRNA abundance of TNF α at 2 weeks. E) mRNA abundance of TNF α at 8 weeks. F) Time point comparison of TNF α mRNA abundance. G) mRNA abundance of IL-6 at 2 weeks. H) mRNA abundance of IL-6 at 8 weeks. I) Time point comparison of IL-6 mRNA abundance. J) mRNA abundance of IL-10 at 2 weeks. K) mRNA abundance of IL-10 at 8 weeks. L) mRNA abundance of IFN γ at 2 weeks. M) mRNA abundance of IFN γ at 8 weeks. N) Time point comparison of IFN γ mRNA abundance. DNE = Did Not Express. ME = Main Effect. † indicates significant difference between RTA and LTA of the same group. ‡ indicates significant difference from same limb of opposing group. * indicates significant difference between groups. Significance was set at $p < 0.05$.

Figure 1

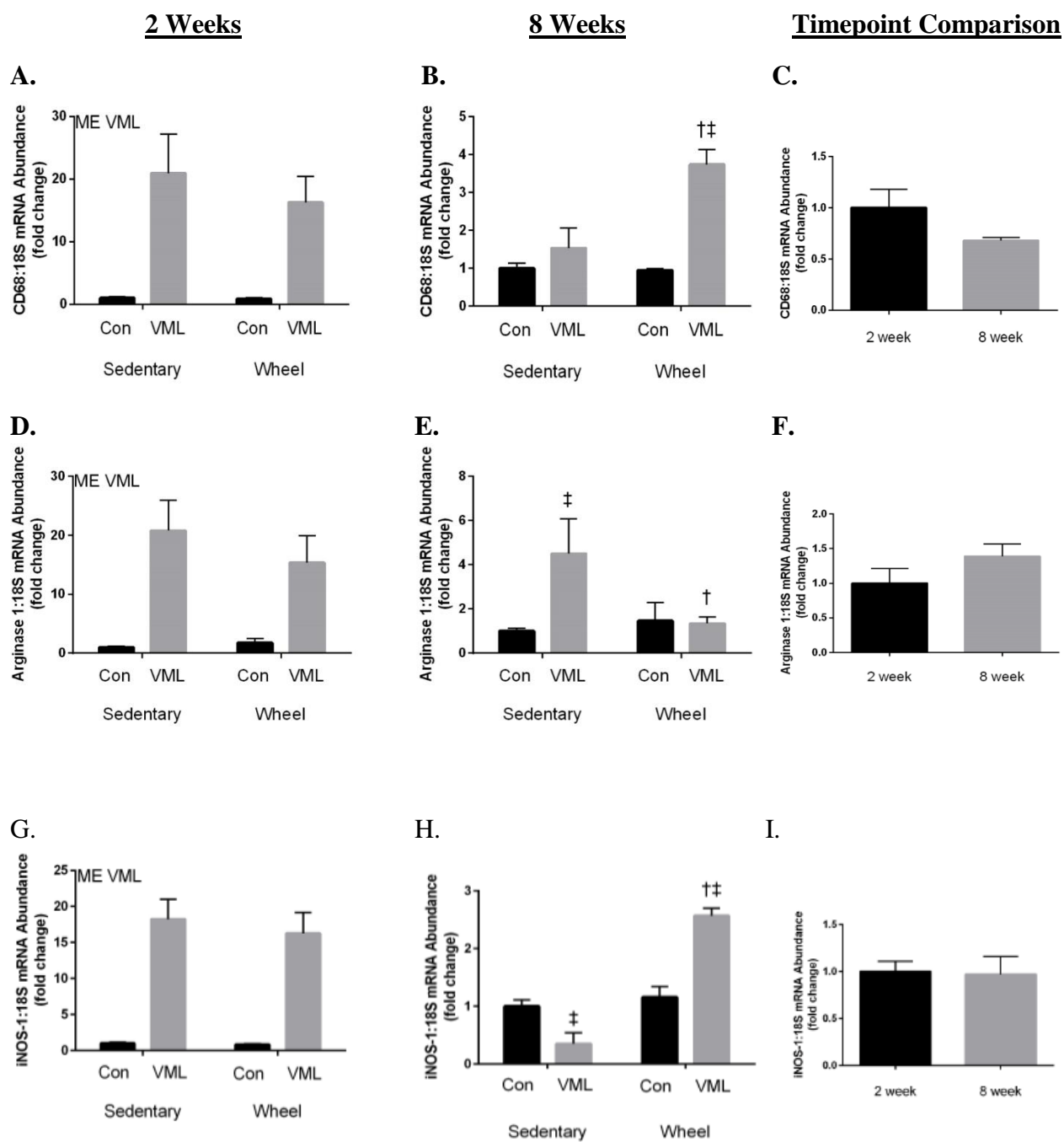
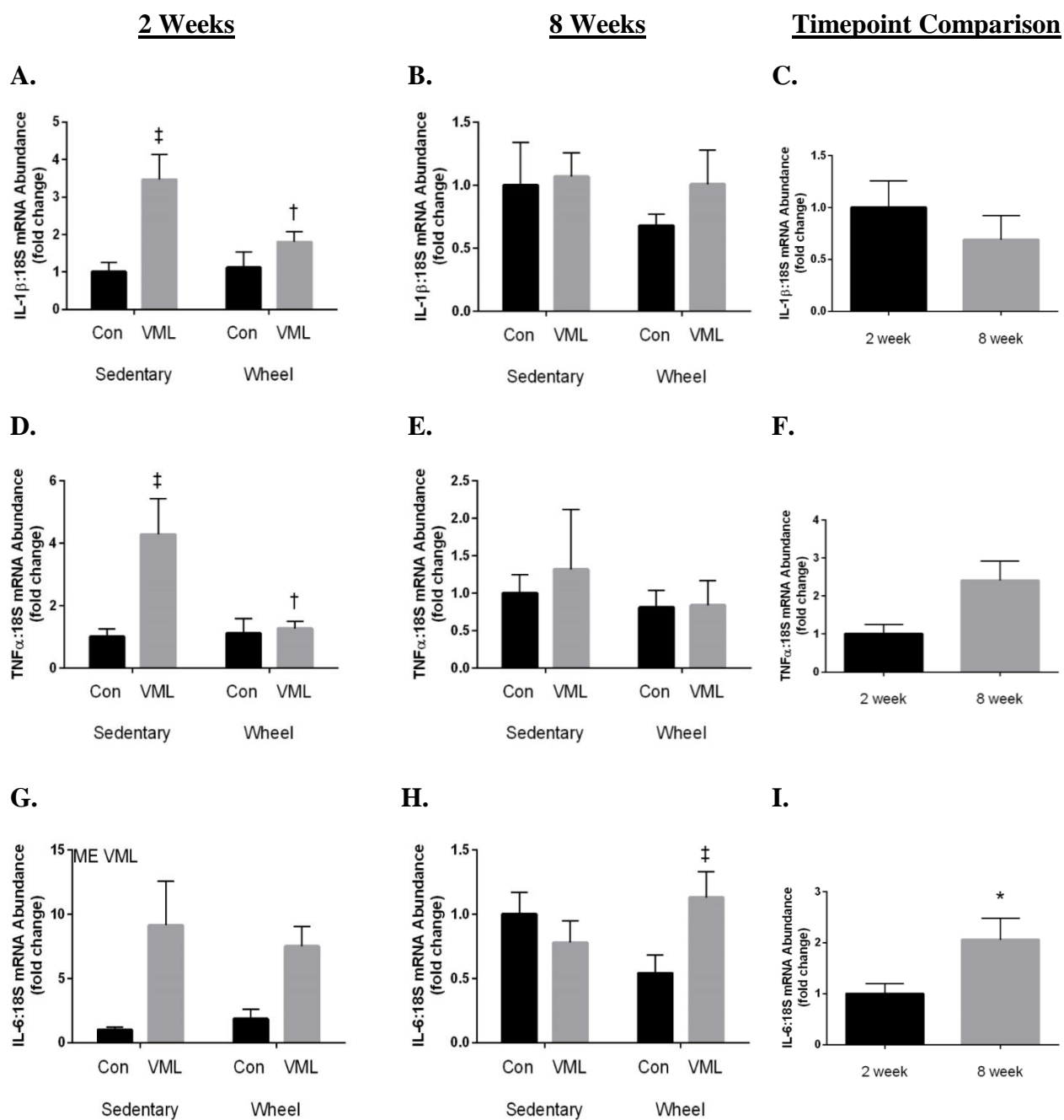
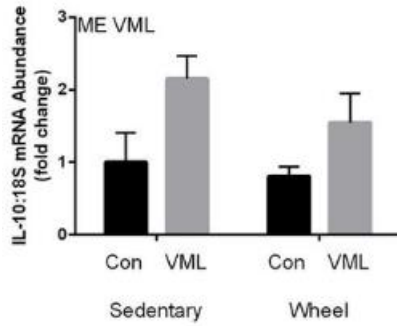


Figure 2

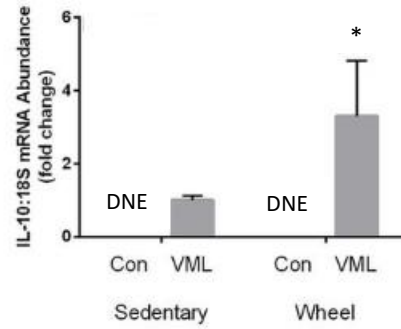


2 Weeks8 WeeksTimepoint Comparison

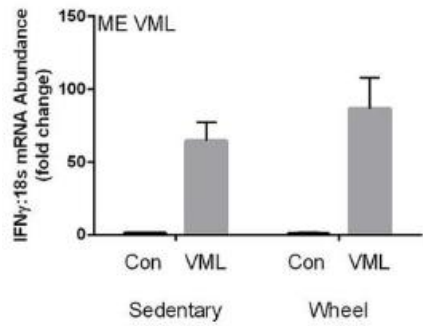
J.



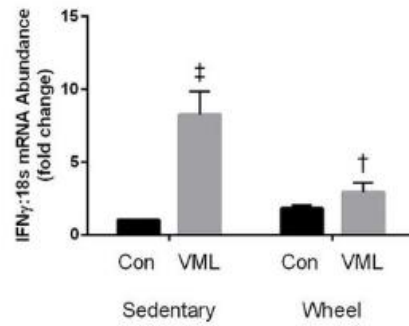
K.



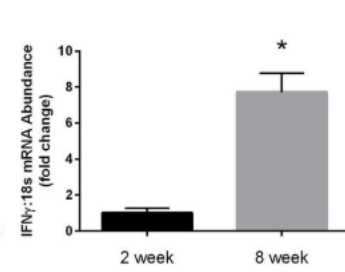
L.



M.



N.



OVERALL CONCLUSION

Since volumetric muscle loss is defined as an injury resulting in permanent functional loss, measurement of force recovery is the key data point of interest for many VML studies. Most early studies that focused on unrepaired VML injuries show VML-injured muscles to be 40-50% of the contralateral limb even months following the injury. We had similar findings at 2 weeks post-surgery when only autologous repair was used. When physical activity is incorporated however, force production rises to ~70% of the contralateral limb just 2 weeks following the injury. At 8 weeks post-injury, two unexpected findings were observed 1) Force production of wheel activity group did not change at all and 2) Force production of the sedentary group was equivalent to the wheel activity group. Regardless of the group, these findings indicate that neither autologous repair nor autologous repair with physical activity are effective interventions to recover force production to clinically effective limits. However, 8 weeks is still an early time point, and investigation into later time points using the same interventions may reveal continued progress in one or both groups.

If future studies are to be conducted using these same interventions, two prominent questions should be asked when completing the experimental design: 1) What caused the immediate promotion and subsequent cessation of force recovery in the wheel activity group and 2) What caused the sedentary group to quickly undergo force recovery from 2 to 8 weeks to a degree that matched the force production of the wheel activity group. There are many factors that were not examined within the confines of this study (i.e. satellite cell migration, vascularization, innervation, role of adaptive immunity, etc.), but the following items of data may answer the previous questions.

Early force recovery in the wheel activity group

Both the sedentary and wheel activity groups showed increased expression of myogenic markers, so it is unlikely that satellite mechanics were vastly different between groups. However, CSA in the LTA tissue adjacent to the defect area was larger in the wheel activity group at 2 weeks potentially allowing greater force output by default compared to the sedentary group. Collagen 3/1 ratio was increased in the defect area (main effect of exercise) and adjacent LTA tissue. This has several implications the likely of which is either force transmission, rather force production, could potentially be the reason for the force differences between wheel activity and sedentary groups early on. Also, the difference in collagen content could allow for more efficient satellite cell migration which could also explain why CSA was larger in the wheel activity group at 2 weeks. Additionally, TGF β and MMP9 gene expression was lower in the wheel activity group. If gene expression is representative of activity, then the function of MMP9 can be narrowed; however, TGF β is a multifunctional protein whose roles could be of importance in many roles outside of regulating ECM remodeling (i.e. anti-inflammatory, cell survival, protein synthesis, etc.). Finally wheel running appeared to attenuate pro-inflammatory cytokines early on. These important findings may suggest that physical activity, even when using a propulsive muscle, benefits force recovery including modulation of the inflammatory response and extracellular remodeling among other possible factors not researched within this study,

Cessation of force recovery after 2 weeks post-injury.

For many of the previously listed data points for the wheel activity group at 2 weeks, by 8 weeks, those same factors were reduced to control levels. In other words, the factors that may have been key to promoting force recovery early on were not able to maintain the same high expression after the 2 week time point. Additionally, many differences in these morphological

and genetic factors followed a contradictory pattern to the sedentary group at 8 weeks. Thus, the factors that may have been allowing the sedentary group to recover force during the late time point were not present in the wheel activity group. Notably, the wheel activity group had high levels of CD68. Coupled with the Arginase-1, iNOS and IL-6 data, this would suggest that the wheel activity group shifted from an anti- to pro-inflammatory environment.

Furthermore, MMP2, MMP9 and TGF β gene expression, factors thought to be associated with early force recovery, were high expressing at 8 weeks when at 2 weeks they were similar to control levels. Consistent with the patterns of these genes and collagen deposition, the higher expression of MMP9 and TGF β had similar inverse correlations with the collagen 3/1 ratio at 8 weeks.

Late-onset force recovery in the sedentary group

Many of the patterns of interest to help identify force recovery and subsequent cessation of recovery in the wheel activity group are also key markers used to identify the late-onset of force recovery in the sedentary group. Contrast to the wheel activity group showing signs of a pro-inflammatory environment by 8 weeks, the sedentary group expressed markers of anti-inflammation (normal levels of CD68 and iNOS, and elevated levels of Arginase-1). Other key factors in the sedentary group showed contrasting effects of that of the wheel activity group. MMP2, MMP9 and TGF β gene expression was all low expressing compared to the wheel activity group at 8 weeks.

The commonalities between force recovery/cessation and the inflammatory and ECM markers implicate that in a VML model using autologous repair, ECM remodeling and modulation of the inflammatory response may be of higher importance than satellite cell mechanics. In other words, myogenic markers are highly expressed in both groups at the early

time points, but proper satellite activation, migration, proliferation, differentiation and incorporation may not be permitted if ECM remodeling and inflammation is dysregulated.

Future studies should focus on obtaining better understanding of not only the inflammatory environment but also the interplay between inflammation and ECM remodeling. Furthermore, wheel activity promoted differential changes that led to early force recovery. Apparently, this continued stimulus was not sufficient to further promote force recovery. Therefore, future studies should also incorporate progressive exercise training as a means to alter the stimulus.

This is not the first study to utilize wheel activity for a model of VML that uses the tibialis anterior as the injured muscle. Benefits have been observed in multiple studies with this similar model of VML and physical activity when physical activity has been initiated at an early time point following injury. It might be important to utilize an exercise that does not target the injured muscle as the prime mover so that physical activity/rehab can be implemented early on. As has been shown in this study, this is a beneficial approach for early force recovery, and choosing an exercise that uses the injured muscle early on may exacerbate functional loss due to over-stressing the local environment. However, when progressing exercise, it may be advantageous to incorporate treadmill exercise, eccentric contraction, or some form of resistance training to see continual development of force production in the injured limb.

REFERENCES

- Allen, D. L., Harrison, B. C., Maass, A., Bell, M. L., Byrnes, W. C., & Leinwand, L. A. (2001). Cardiac and skeletal muscle adaptations to voluntary wheel running in the mouse. *Journal of applied physiology*, *90*(5), 1900-1908.
- Acharyya, S., Sharma, S. M., Cheng, A. S., Ladner, K. J., He, W., Kline, W., ... & Guttridge, D. C. (2010). TNF inhibits Notch-1 in skeletal muscle cells by Ezh2 and DNA methylation mediated repression: implications in duchenne muscular dystrophy. *PLoS one*, *5*(8), e12479.
- Akimoto, T., Pohnert, S. C., Li, P., Zhang, M., Gumbs, C., Rosenberg, P. B., ... & Yan, Z. (2005). Exercise stimulates Pgc-1 α transcription in skeletal muscle through activation of the p38 MAPK pathway. *Journal of Biological Chemistry*, *280*(20), 19587-19593.
- Archile-Contreras, A. C., Mandell, I. B., & Purslow, P. P. (2010). Phenotypic differences in matrix metalloproteinase 2 activity between fibroblasts from 3 bovine muscles. *Journal of animal science*, *88*(12), 4006-4015.
- Allen, R. E., Sheehan, S. M., Taylor, R. G., Kendall, T. L., & Rice, G. M. (1995). Hepatocyte growth factor activates quiescent skeletal muscle satellite cells in vitro. *Journal of cellular physiology*, *165*(2), 307-312.
- Aurora, A., Corona, B. T., Garg, K., & Walters, T. J. (2014). Physical rehabilitation improves muscle function following volumetric muscle loss injury. *BMC sports science, medicine and rehabilitation*, *6*(1), 41.
- Aurora, A., Corona, B. T., & Walters, T. J. (2016). A Porcine Urinary Bladder Matrix Does Not Recapitulate the Spatiotemporal Macrophage Response of Muscle Regeneration after Volumetric Muscle Loss Injury. *Cells Tissues Organs*, *202*(3-4), 189-201.
- Bazgir, B., Fathi, R., Valojerdi, M. R., Mozdziaik, P., & Asgari, A. (2017). Satellite cells contribution to exercise mediated muscle hypertrophy and repair. *Cell Journal (Yakhteh)*, *18*(4), 473.
- Beach, R. L., Rao, J. S., & Festoff, B. W. (1985). Extracellular-matrix synthesis by skeletal muscle in culture. Major secreted collagenous proteins of clonal myoblasts. *Biochemical Journal*, *225*(3), 619-627.
- Beauchamp, J. R., Heslop, L., David, S. W., Tajbakhsh, S., Kelly, R. G., Wernig, A., ... & Zammit, P. S. (2000). Expression of CD34 and Myf5 defines the majority of quiescent adult skeletal muscle satellite cells. *The Journal of cell biology*, *151*(6), 1221-1234.
- Bodine, S. C., Stitt, T. N., Gonzalez, M., Kline, W. O., Stover, G. L., Bauerlein, R., ... & Yancopoulos, G. D. (2001). Akt/mTOR pathway is a crucial regulator of skeletal muscle hypertrophy and can prevent muscle atrophy in vivo. *Nature cell biology*, *3*(11), 1014-1019.
- Brack, A. S., Conboy, I. M., Conboy, M. J., Shen, J., & Rando, T. A. (2008). A temporal switch from notch to Wnt signaling in muscle stem cells is necessary for normal adult myogenesis. *Cell stem cell*, *2*(1), 50-59.
- Brigitte, M., Schilte, C., Plonquet, A., Baba-Amer, Y., Henri, A., Charlier, C., ... & Chrétien, F. (2010).

- Muscle resident macrophages control the immune cell reaction in a mouse model of notexin-induced myoinjury. *Arthritis & Rheumatology*, 62(1), 268-279.
- Cadot, B., Gache, V., Vasyutina, E., Falcone, S., Birchmeier, C., & Gomes, E. R. (2012). Nuclear movement during myotube formation is microtubule and dynein dependent and is regulated by Cdc42, Par6 and Par3. *EMBO reports*, 13(8), 741-749.
- Cadot, B., Gache, V., & Gomes, E. R. (2015). Moving and positioning the nucleus in skeletal muscle—one step at a time. *Nucleus*, 6(5), 373-381.
- Chazaud, B., Brigitte, M., Yacoub-Youssef, H., Arnold, L., Gherardi, R., Sonnet, C., ... & Chretien, F. (2009). Dual and beneficial roles of macrophages during skeletal muscle regeneration. *Exercise and sport sciences reviews*, 37(1), 18-22.
- Chen, S. E., Jin, B., & Li, Y. P. (2007). TNF- α regulates myogenesis and muscle regeneration by activating p38 MAPK. *American Journal of Physiology-Cell Physiology*, 292(5), C1660-C1671.
- Cheng, M., Nguyen, M. H., Fantuzzi, G., & Koh, T. J. (2008). Endogenous interferon- γ is required for efficient skeletal muscle regeneration. *American Journal of Physiology-Cell Physiology*, 2
- Chin, E. R., Olson, E. N., Richardson, J. A., Yang, Q., Humphries, C., Shelton, J. M., ... & Williams, R. S. (1998). A calcineurin-dependent transcriptional pathway controls skeletal muscle fiber type. *Genes & development*, 12(16), 2499-2509.
- Ciciliot, S., & Schiaffino, S. (2010). Regeneration of mammalian skeletal muscle: basic mechanisms and clinical implications. *Current pharmaceutical design*, 16(8), 906-914.
- Conboy, I. M., & Rando, T. A. (2005). Aging, stem cells and tissue regeneration: lessons from muscle. *Cell cycle*, 4(3), 407-410.
- Cooper, R. N., Tajbakhsh, S., Mouly, V., Cossu, G., Buckingham, M., & Butler-Browne, G. S. (1999). In vivo satellite cell activation via Myf5 and MyoD in regenerating mouse skeletal muscle. *J Cell Sci*, 112(17), 2895-2901.
- Cornelison, D. D. W., & Wold, B. J. (1997). Single-cell analysis of regulatory gene expression in quiescent and activated mouse skeletal muscle satellite cells. *Developmental biology*, 191(2), 270-283.
- Corona, B. T., Henderson, B. E., Ward, C. L., & Greising, S. M. (2017). Contribution of minced muscle graft progenitor cells to muscle fiber formation after volumetric muscle loss injury in wild-type and immune deficient mice. *Physiological reports*, 5(7), e13249.
- Corona, B. T., Machingal, M. A., Criswell, T., Vadhavkar, M., Dannahower, A. C., Bergman, C., ... & Christ, G. J. (2012). Further development of a tissue engineered muscle repair construct in vitro for enhanced functional recovery following implantation in vivo in a murine model of volumetric muscle loss injury. *Tissue Engineering Part A*, 18(11-12), 1213-1228.
- Corona, B. T., Wu, X., Ward, C. L., McDaniel, J. S., Rathbone, C. R., & Walters, T. J. (2013). The promotion of a functional fibrosis in skeletal muscle with volumetric muscle loss injury following the transplantation of muscle-ECM. *Biomaterials*, 34(13), 3324-3335.

- Corona, B. T., Ward, C. L., Baker, H. B., Walters, T. J., & Christ, G. J. (2013). Implantation of in vitro tissue engineered muscle repair constructs and bladder acellular matrices partially restore in vivo skeletal muscle function in a rat model of volumetric muscle loss injury. *Tissue Engineering Part A*, 20(3-4), 705-715.
- Corona, B. T., Rivera, J. C., & Greising, S. M. (2017). Inflammatory and Physiological Consequences of Debridement of Fibrous Tissue after Volumetric Muscle Loss Injury. *Clinical and translational science*.
- Cornelison, D. D. W., & Wold, B. J. (1997). Single-cell analysis of regulatory gene expression in quiescent and activated mouse skeletal muscle satellite cells. *Developmental biology*, 191(2), 270-283.
- Corona, B. T., Rivera, J. C., & Greising, S. M. (2018). Inflammatory and Physiological consequences of debridement of fibrous tissue after volumetric muscle loss injury. *Clinical and translational science*, 11(2), 208-217.
- Duque, A. G., & Descoteaux, A. (2014). Macrophage cytokines: involvement in immunity and infectious diseases. *Frontiers in immunology*, 5, 491.
- Dziki, Jenna, Stephen Badylak, Mohammad Yabroudi, Brian Sicari, Fabrisia Ambrosio, Kristen Stearns, Neill Turner et al. "An acellular biologic scaffold treatment for volumetric muscle loss: results of a 13-patient cohort study." *npj Regenerative Medicine* 1 (2016): 16008.
- Eikelboom, R., & Mills, R. (1988). A microanalysis of wheel running in male and female rats. *Physiology & Behavior*, 43(5), 625-630.
- El Fahime, E., Torrente, Y., Caron, N. J., Bresolin, M. D., & Tremblay, J. P. (2000). In vivo migration of transplanted myoblasts requires matrix metalloproteinase activity. *Experimental cell research*, 258(2), 279-287.
- Folker, E., & Baylies, M. (2013). Nuclear positioning in muscle development and disease. *Frontiers in physiology*, 4, 363.
- Fu, X., Wang, H., & Hu, P. (2015). Stem cell activation in skeletal muscle regeneration. *Cellular and molecular life sciences*, 72(9), 1663-1677.
- Fujimaki, S., Hidaka, R., Asashima, M., Takemasa, T., & Kuwabara, T. (2014). Wnt protein-mediated satellite cell conversion in adult and aged mice following voluntary wheel running. *Journal of Biological Chemistry*, 289(11), 7399-7412.
- Fukushima, K., Nakamura, A., Ueda, H., Yuasa, K., Yoshida, K., Takeda, S., & Ikeda, S. (2007). Activation and localization of matrix metalloproteinase-2 and -9 in the skeletal muscle of the muscular dystrophy dog (CXMD₁). *BMC Musculoskeletal Disorders*, 8, 54. <http://doi.org/10.1186/1471-2474-8-54>
- Garg, K., Ward, C. L., & Corona, B. T. (2014). Asynchronous inflammation and myogenic cell migration limit muscle tissue regeneration mediated by a cellular scaffolds. *Inflammation and cell signaling*, 1(4).

- Garg, K., Ward, C. L., Rathbone, C. R., & Corona, B. T. (2014). Transplantation of devitalized muscle scaffolds is insufficient for appreciable de novo muscle fiber regeneration after volumetric muscle loss injury. *Cell and tissue research*, 358(3), 857-873.
- Garg, K., Corona, B. T., & Walters, T. J. (2014). Losartan administration reduces fibrosis but hinders functional recovery after volumetric muscle loss injury. *Journal of Applied Physiology*, 117(10), 1120-1131.
- Garg, K., Corona, B. T., & Walters, T. J. (2015). Therapeutic strategies for preventing skeletal muscle fibrosis after injury. *Frontiers in pharmacology*, 6.
- Gillies, A. R., & Lieber, R. L. (2011). Structure and function of the skeletal muscle extracellular matrix. *Muscle & nerve*, 44(3), 318-331.
- Goodyear, L. J., Chang, P. Y., Sherwood, D. J., Dufresne, S. D., & Moller, D. E. (1996). Effects of exercise and insulin on mitogen-activated protein kinase signaling pathways in rat skeletal muscle. *American Journal of Physiology-Endocrinology And Metabolism*, 271(2), E403-E408.
- Gosselin, L. E., Adams, C., Cotter, T. A., McCormick, R. J., & Thomas, D. P. (1998). Effect of exercise training on passive stiffness in locomotor skeletal muscle: role of extracellular matrix. *Journal of applied physiology*, 85(3), 1011-1016.
- Greising, S. M., Corona, B. T., Warren, G. L., & Call, J. A. (2017). Early Rehabilitation and Volumetric Muscle Loss Injury Adapts the Genetic Response of the Remaining Muscle Mass. *The FASEB Journal*, 31(1 Supplement), 1083-10.
- Greising, S. M., Rivera, J. C., Goldman, S. M., Watts, A., Aguilar, C. A., & Corona, B. T. (2017). Unwavering Pathobiology of volumetric muscle loss injury. *Scientific Reports*, 7(1), 13179.
- Heinemeier, K. M., Bjerrum, S. S., Schjerling, P., & Kjaer, M. (2013). Expression of extracellular matrix components and related growth factors in human tendon and muscle after acute exercise. *Scandinavian journal of medicine & science in sports*, 23(3).
- Hill, M., Wernig, A., & Goldspink, G. (2003). Muscle satellite (stem) cell activation during local tissue injury and repair. *Journal of anatomy*, 203(1), 89-99.
- Hjorth, M., Norheim, F., Meen, A. J., Pourteymour, S., Lee, S., Holen, T., ... & Eckardt, K. (2015). The effect of acute and long-term physical activity on extracellular matrix and serglycin in human skeletal muscle. *Physiological reports*, 3(8), e12473.
- Honda, H., Kimura, H., & Rostami, A. (1990). Demonstration and phenotypic characterization of resident macrophages in rat skeletal muscle. *Immunology*, 70(2), 272.
- Humphrey, J. D., Dufresne, E. R., & Schwartz, M. A. (2014). Mechanotransduction and extracellular matrix homeostasis. *Nature reviews Molecular cell biology*, 15(12), 802-8127.
- Hurtgen, B. J., Ward, C. L., Garg, K., Pollot, B. E., Goldman, S. M., Mckinley, T. O., ... & Corona, B. T. (2016). Severe muscle trauma triggers heightened and prolonged local musculoskeletal inflammation and impairs adjacent tibia fracture healing. *Journal of musculoskeletal & neuronal interactions*, 16(2), 122.

- Irintchev, A., & Wernig, A. (1987). Muscle damage and repair in voluntarily running mice: strain and muscle differences. *Cell and tissue research*, 249(3), 509-521.
- Kasukonis, B., Kim, J., Brown, L., Jones, J., Ahmadi, S., Washington, T., & Wolchok, J. (2016). Codelivery of infusion decellularized skeletal muscle with minced muscle autografts improved recovery from volumetric muscle loss injury in a rat model. *Tissue Engineering Part A*, 22(19-20), 1151-1163.
- Kherif, S., Lafuma, C., Dehaupas, M., Lachkar, S., Fournier, J. G., Verdière-Sahuqué, M., ... & Alameddine, H. S. (1999). Expression of Matrix Metalloproteinases 2 and 9 in Regenerating Skeletal Muscle: A Study in Experimentally Injured andmdxMuscles. *Developmental biology*, 205(1), 158-170.
- Kim, J. T., Kasukonis, B. M., Brown, L. A., Washington, T. A., & Wolchok, J. C. (2016). Recovery from volumetric muscle loss injury: A comparison between young and aged rats. *Experimental gerontology*, 83, 37-46.
- Kjær, M., Magnusson, P., Krogsgaard, M., Møller, J. B., Olesen, J., Heinemeier, K., ... & Langberg, H. (2006). Extracellular matrix
- Koskinen, S. O., Heinemeier, K. M., Olesen, J. L., Langberg, H., & Kjaer, M. (2004). Physical exercise can influence local levels of matrix metalloproteinases and their inhibitors in tendon-related connective tissue. *Journal of applied physiology*, 96(3), 861-864.
- Kühl, U., Timpl, R., & von der Mark, K. (1982). Synthesis of type IV collagen and laminin in cultures of skeletal muscle cells and their assembly on the surface of myotubes. *Developmental biology*, 93(2), 344-354.
- Kurosaka, M., Naito, H., Ogura, Y., Kojima, A., Goto, K., & Katamoto, S. (2009). Effects of voluntary wheel running on satellite cells in the rat plantaris muscle. *Journal of sports science & medicine*, 8(1), 51.
- Kurosaka, M., & Machida, S. (2013). Interleukin-6-induced satellite cell proliferation is regulated by induction of the JAK2/STAT3 signalling pathway through cyclin D1 targeting. *Cell proliferation*, 46(4), 365-373.
- Larouche, J., Greising, S. M., Corona, B. T., & Aguilar, C. A. (2018). Robust inflammatory and fibrotic signaling following volumetric muscle loss: a barrier to muscle regeneration. *Cell death & disease*, 9(3), 409.
- Leask, A., & Abraham, D. J. (2004). TGF- β signaling and the fibrotic response. *The FASEB Journal*, 18(7), 816-827.
- Legerlotz, K., Elliott, B., Guillemin, B., & Smith, H. K. (2008). Voluntary resistance running wheel activity pattern and skeletal muscle growth in rats. *Experimental physiology*, 93(6), 754-762.
- Light, N., & Champion, A. E. (1984). Characterization of muscle epimysium, perimysium and endomysium collagens. *Biochemical Journal*, 219(3), 1017-1026.
- Machingal, M. A., Corona, B. T., Walters, T. J., Kesireddy, V., Koval, C. N., Dannahower, A., ... &

- Christ, G. J. (2011). A tissue-engineered muscle repair construct for functional restoration of an irrecoverable muscle injury in a murine model. *Tissue engineering Part A*, 17(17-18), 2291-2303.
- Mackey, A. L., Kjaer, M., Charifi, N., Henriksson, J., Bojsen-Moller, J., Holm, L., & Kadi, F. (2009). Assessment of satellite cell number and activity status in human skeletal muscle biopsies. *Muscle & nerve*, 40(3), 455-465.
- Mase, V. J., Hsu, J. R., Wolf, S. E., Wenke, J. C., Baer, D. G., Owens, J., ... & Walters, T. J. (2010). Clinical application of an acellular biologic scaffold for surgical repair of a large, traumatic quadriceps femoris muscle defect. *Orthopedics*, 33(7).
- McKinsey, T. A., Zhang, C. L., Lu, J., & Olson, E. N. (2000). Signal-dependent nuclear export of a histone deacetylase regulates muscle differentiation. *Nature*, 408(6808), 106-111.
- Mendias, C. L., Gumucio, J. P., Davis, M. E., Bromley, C. W., Davis, C. S., & Brooks, S. V. (2012). Transforming growth factor-beta induces skeletal muscle atrophy and fibrosis through the induction of atrogen-1 and scleraxis. *Muscle & nerve*, 45(1), 55-59.
- Mintz, E. L., Passipieri, J. A., Lovell, D. Y., & Christ, G. J. (2016). Applications of In Vivo Functional Testing of the Rat Tibialis Anterior for Evaluating Tissue Engineered Skeletal Muscle Repair. *Journal of visualized experiments: JoVE*, (116).
- Nuutila, K., Sakthivel, D., Kruse, C., Tran, P., Giatsidis, G., & Sinha, I. (2017). Gene expression profiling of skeletal muscle after volumetric muscle loss. *Wound Repair and Regeneration*.
- Olguin, H. C., & Olwin, B. B. (2004). Pax-7 up-regulation inhibits myogenesis and cell cycle progression in satellite cells: a potential mechanism for self-renewal. *Developmental biology*
- Olguin, H. C., Yang, Z., Tapscott, S. J., & Olwin, B. B. (2007). Reciprocal inhibition between Pax7 and muscle regulatory factors modulates myogenic cell fate determination. *J Cell Biol*, 177(5), 769-779.
- Otto, A., Schmidt, C., Luke, G., Allen, S., Valasek, P., Muntoni, F., ... & Patel, K. (2008). Canonical Wnt signalling induces satellite-cell proliferation during adult skeletal muscle regeneration. *Journal of cell science*, 121(17), 2939-2950.
- Palacios, D., Mozzetta, C., Consalvi, S., Caretti, G., Saccone, V., Proserpio, V., ... & Sartorelli, V. (2010). TNF/p38 α /polycomb signaling to Pax7 locus in satellite cells links inflammation to the epigenetic control of muscle regeneration. *Cell stem cell*, 7(4), 455-469.
- Pisconti, A., Brunelli, S., Di Padova, M., De Palma, C., Deponti, D., Baesso, S., ... & Clementi, E. (2006). Follistatin induction by nitric oxide through cyclic GMP: a tightly regulated signaling pathway that controls myoblast fusion. *J Cell Biol*, 172(2), 233-244.
- Podhorska-Okolow, M., Sandri, M., Zampieri, S., Brun, B., Rossini, K., & Carraro, U. (1998). Apoptosis of myofibres and satellite cells: exercise-induced damage in skeletal muscle of the mouse. *Neuropathology and applied neurobiology*, 24(6), 518-531.
- Quarta, M., Cromie, M., Chacon, R., Blonigan, J., Garcia, V., Akimenko, I., ... & Rando, T. A. (2017). Bioengineered constructs combined with exercise enhance stem cell-mediated treatment of volumetric muscle loss. *Nature Communications*, 8, 15613.

- Rantanen, J., Hurme, T., Lukka, R., Heino, J., & Kalimo, H. (1995). Satellite cell proliferation and the expression of myogenin and desmin in regenerating skeletal muscle: evidence for two different populations of satellite cells. *Laboratory investigation; a journal of technical methods and pathology*, 72(3), 341-347.
- Sanes, J. R. (2003). The basement membrane/basal lamina of skeletal muscle. *Journal of Biological Chemistry*, 278(15), 12601-12604.
- Sarasa-Renedo, A., & Chiquet, M. (2005). Mechanical signals regulating extracellular matrix gene expression in fibroblasts. *Scandinavian journal of medicine & science in sports*, 15(4), 223-230.
- Seale, P., Sabourin, L. A., Girgis-Gabardo, A., Mansouri, A., Gruss, P., & Rudnicki, M. A. (2000). Pax7 is required for the specification of myogenic satellite cells. *Cell*, 102(6), 777-786.
- Serrano, A. L., Baeza-Raja, B., Perdiguero, E., Jardí, M., & Muñoz-Cánoves, P. (2008). Interleukin-6 is an essential regulator of satellite cell-mediated skeletal muscle hypertrophy. *Cell metabolism*, 7(1), 33-44.
- Schultz, E., Gibson, M. C., & Champion, T. (1978). Satellite cells are mitotically quiescent in mature mouse muscle: an EM and radioautographic study. *Journal of Experimental Zoology Part A: Ecological Genetics and Physiology*, 206(3), 451-456.
- Sicari, B. M., Agrawal, V., Siu, B. F., Medberry, C. J., Dearth, C. L., Turner, N. J., & Badylak, S. F. (2012). A murine model of volumetric muscle loss and a regenerative medicine approach for tissue replacement. *Tissue engineering Part A*, 18(19-20), 1941-1948.
- Singh, A., Nelson-Moon, Z. L., Thomas, G. J., Hunt, N. P., & Lewis, M. P. (2000). Identification of matrix metalloproteinases and their tissue inhibitors type 1 and 2 in human masseter muscle. *Archives of Oral Biology*, 45(6), 431-440.
- Skapek, S. X., Rhee, J., Spicer, D. B., & Lassar, A. B. (1995). Inhibition of myogenic differentiation in proliferating myoblasts by cyclin D1-dependent kinase. *Science*, 267(5200), 1022.
- Slater, C. R., & Schiaffino, S. (2008). Innervation of regenerating muscle. *Skeletal muscle repair and regeneration*, 303-334.
- Smith, C., Janney, M. J., & Allen, R. E. (1994). Temporal expression of myogenic regulatory genes during activation, proliferation, and differentiation of rat skeletal muscle satellite cells. *Journal of cellular physiology*, 159(2), 379-385.
- Song, T., Lee, K., & Farrar, R. (2015). Enhanced Muscle Mass and Contractile Function Recovery via Resistance Training after VML Injury. *The FASEB Journal*, 29(1 Supplement), 677-22.
- Tamaki, T., Akatsuka, A., Yoshimura, S., Roy, R. R., & Edgerton, V. R. (2002). New fiber formation in the interstitial spaces of rat skeletal muscle during postnatal growth. *Journal of Histochemistry & Cytochemistry*, 50(8), 1097-1111.
- Tatsumi, R., Anderson, J. E., Nevoret, C. J., Halevy, O., & Allen, R. E. (1998). HGF/SF is present in normal adult skeletal muscle and is capable of activating satellite cells. *Developmental biology*, 194(1), 114-128.

- Tecchio, C., Micheletti, A., & Cassatella, M. A. (2014). Neutrophil-derived cytokines: facts beyond expression. *Frontiers in immunology*, 5.
- Tidball, J. G. (2008). Inflammation in skeletal muscle regeneration. In *Skeletal Muscle Repair and Regeneration*(pp. 243-268). Springer Netherlands.
- Tidball, J. G., & Villalta, S. A. (2010). Regulatory interactions between muscle and the immune system during muscle regeneration. *American Journal of Physiology-Regulatory, Integrative and Comparative Physiology*, 298(5), R1173-R1187.
- Tidball, J. G. (2017). Regulation of muscle growth and regeneration by the immune system. *Nature Reviews Immunology*, 17(3), 165-178.
- Timmons, J. A., Jansson, E., Fischer, H., Gustafsson, T., Greenhaff, P. L., Riddén, J., ... & Sundberg, C. J. (2005). Modulation of extracellular matrix genes reflects the magnitude of physiological adaptation to aerobic exercise training in humans
- Toth, M., Sohail, A., & Fridman, R. (2012). Assessment of gelatinases (MMP-2 and MMP-9) by gelatin zymography. *Metastasis Research Protocols*, 121-135.
- Turner, N. J., & Badylak, S. F. (2012). Regeneration of skeletal muscle. *Cell and tissue research*, 347(3), 759-774.
- Valentin, J. E., Turner, N. J., Gilbert, T. W., & Badylak, S. F. (2010). Functional skeletal muscle formation with a biologic scaffold. *Biomaterials*, 31(29), 7475-7484.
- Villalta, S. A., Nguyen, H. X., Deng, B., Gotoh, T., & Tidball, J. G. (2008). Shifts in macrophage phenotypes and macrophage competition for arginine metabolism affect the severity of muscle pathology in muscular dystrophy. *Human molecular genetics*, 18(3), 482-496.
- Vincent, B., Windelinckx, A., Nielens, H., Ramaekers, M., Van Leemputte, M., Hespel, P., & Thomis, M. A. (2010). Protective role of α -actinin-3 in the response to an acute eccentric exercise bout. *Journal of applied Physiology*, 109(2), 564-573.
- Wang, W., Pan, H., Murray, K., Jefferson, B. S., & Li, Y. (2009). Matrix metalloproteinase-1 promotes muscle cell migration and differentiation. *The American journal of pathology*, 174(2), 541-549.
- Washington, T. A., White, J. P., Davis, J. M., Wilson, L. B., Lowe, L. L., Sato, S., & Carson, J. A. (2011). Skeletal muscle mass recovery from atrophy in IL-6 knockout mice. *Acta Physiologica*, 202(4), 657-669.
- Whalen, R. G., Harris, J. B., Butler-Browne, G. S., & Sesodia, S. (1990). Expression of myosin isoforms during notexin-induced regeneration of rat soleus muscles. *Developmental biology*, 141(1), 24-40.
- Wozniak, A. C., & Anderson, J. E. (2007). Nitric oxide-dependence of satellite stem cell activation and quiescence on normal skeletal muscle fibers. *Developmental Dynamics*, 236(1), 240-250.
- Wu, N., Jansen, E. D., & Davidson, J. M. (2003). Comparison of mouse matrix metalloproteinase 13 expression in free-electron laser and scalpel incisions during wound healing. *Journal of investigative dermatology*, 121(4), 926-932.
- Wu, X., Corona, B. T., Chen, X., & Walters, T. J. (2012). A standardized rat model of volumetric muscle

- loss injury for the development of tissue engineering therapies. *BioResearch open access*, 1(6), 280-290.
- Yang, W., Zhang, Y., Li, Y., Wu, Z., & Zhu, D. (2007). Myostatin induces cyclin D1 degradation to cause cell cycle arrest through a phosphatidylinositol 3-kinase/AKT/GSK-3 β pathway and is antagonized by insulin-like growth factor 1. *Journal of biological chemistry*, 282(6), 3799-3808.
- Yin, H., Price, F., & Rudnicki, M. A. (2013). Satellite cells and the muscle stem cell niche. *Physiological reviews*, 93(1), 23-67.

APPENDIX

5/18/2017

vpredevb.usrk.edu/iacuc-webapp/mods/letter2.php



Office of Research Compliance

To: Jeffrey Wolchok
Fr: Craig Coon
Date: May 18th, 2017
Subject: IACUC Approval
Expiration Date: May 17th, 2020

The Institutional Animal Care and Use Committee (IACUC) has APPROVED your personnel addition(s) of Wesley Haynie and Richard Perry Jr. to protocol # 17075: *Rehabilitation Strategies for Volumetric Muscle Loss Injuries*.

In granting its approval, the IACUC has approved only the information provided. Should there be any further changes to the protocol during the research, please notify the IACUC in writing (via the Modification form) prior to initiating the changes. If the study period is expected to extend beyond May 17th, 2020 you must submit a newly drafted protocol prior to that date to avoid any interruption. By policy the IACUC cannot approve a study for more than 3 years at a time.

The IACUC appreciates your cooperation in complying with University and Federal guidelines involving animal subjects.

CNC/aem